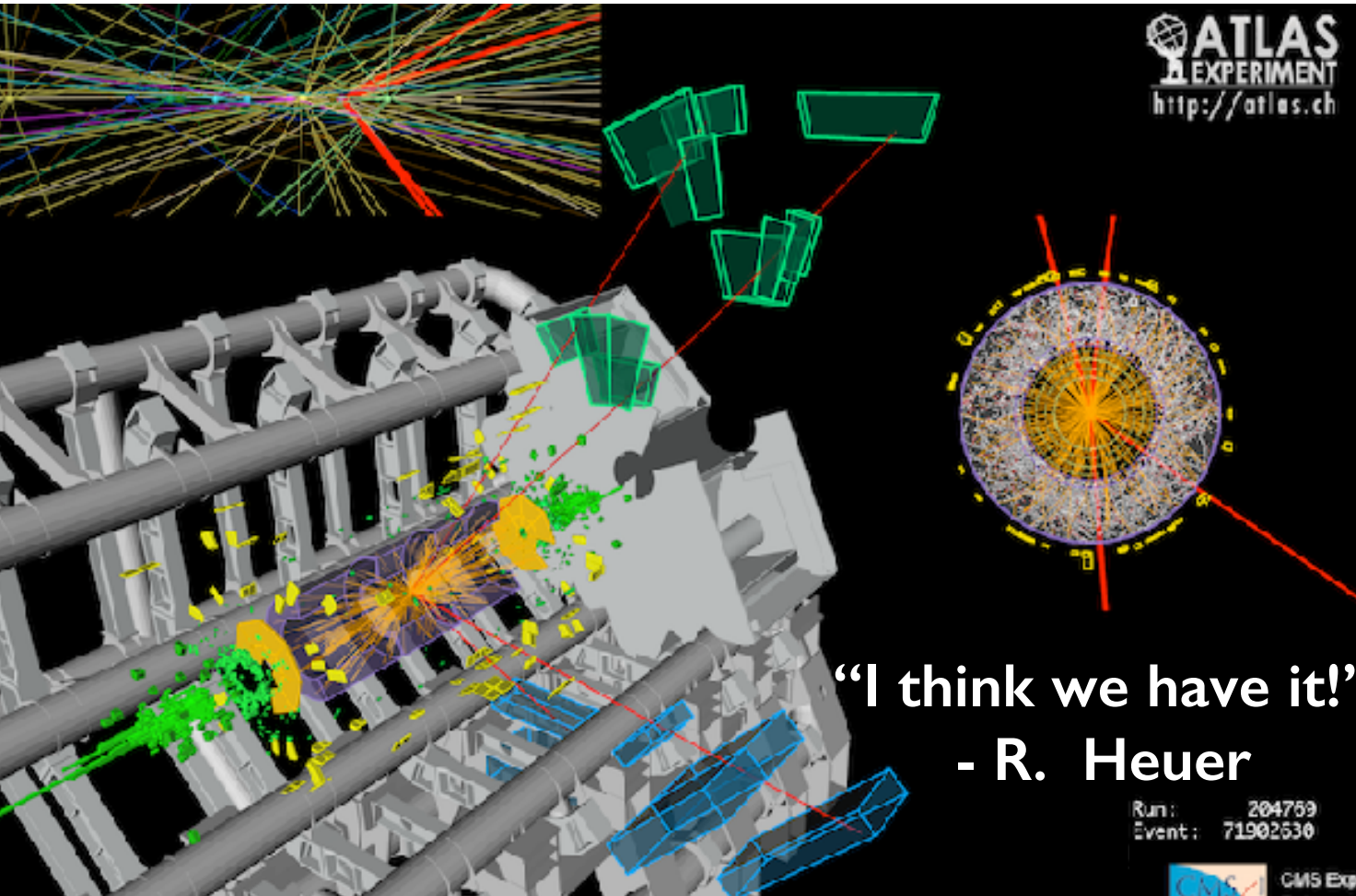
A 3D visualization of the CMS particle detector. The central part shows a yellow cone representing a Higgs boson decay into two photons, each shown as a yellow line. The detector's structure is visible as red and blue wireframes. A green track enters from the top left and interacts with the detector. The background is black with some green and blue noise-like patterns.

BSM Higgs with Photons at the CMS Experiment

Rafael Teixeira de Lima (Northeastern University)

2012: YEAR OF THE HIGGS



ATLAS
EXPERIMENT
<http://atlas.ch>

Run: 204759
Event: 71902530

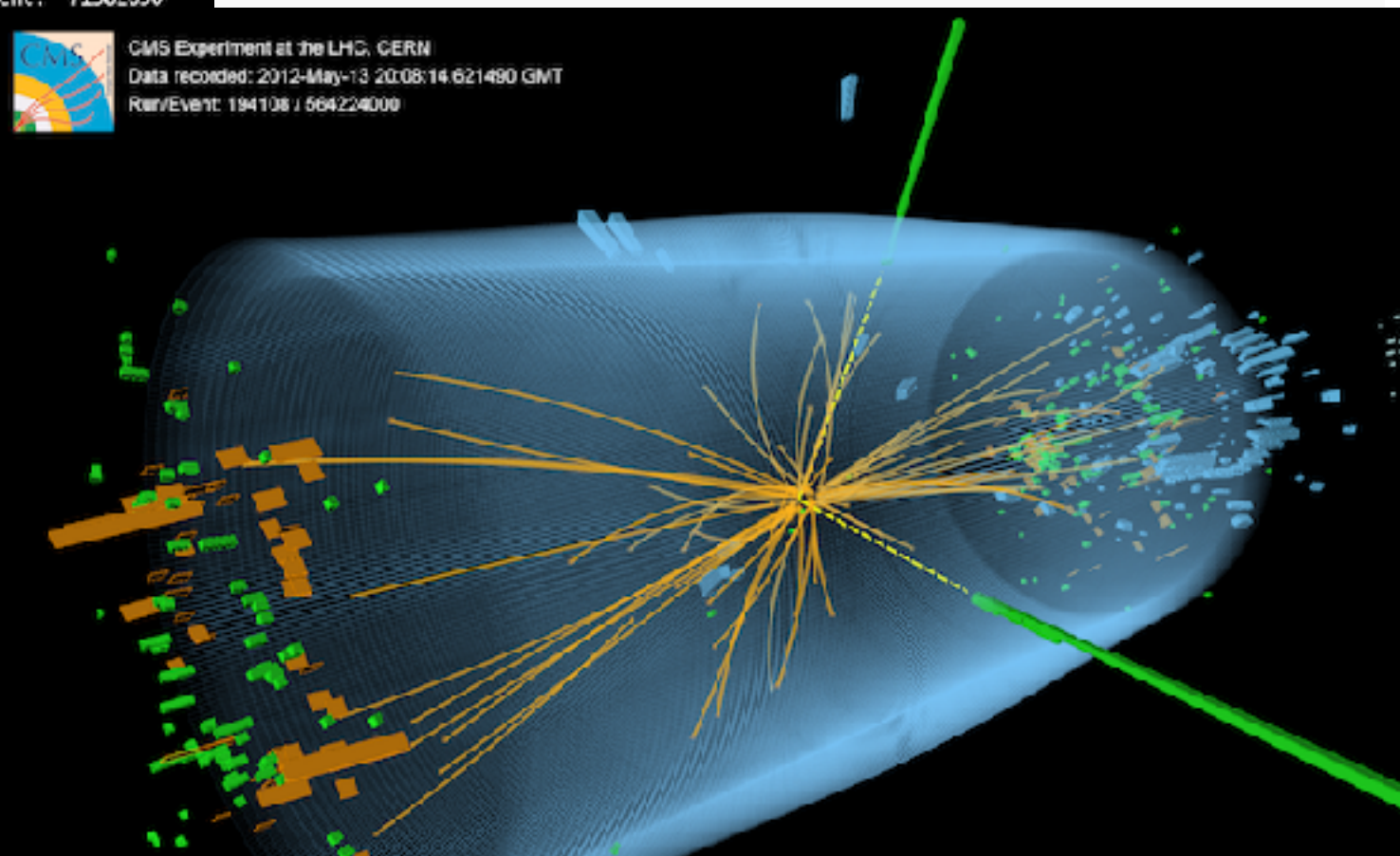


CMS Experiment at the LHC, CERN
Data recorded: 2012-May-13 20:08:14 621490 GMT
Run/Event: 194108 / 564224000

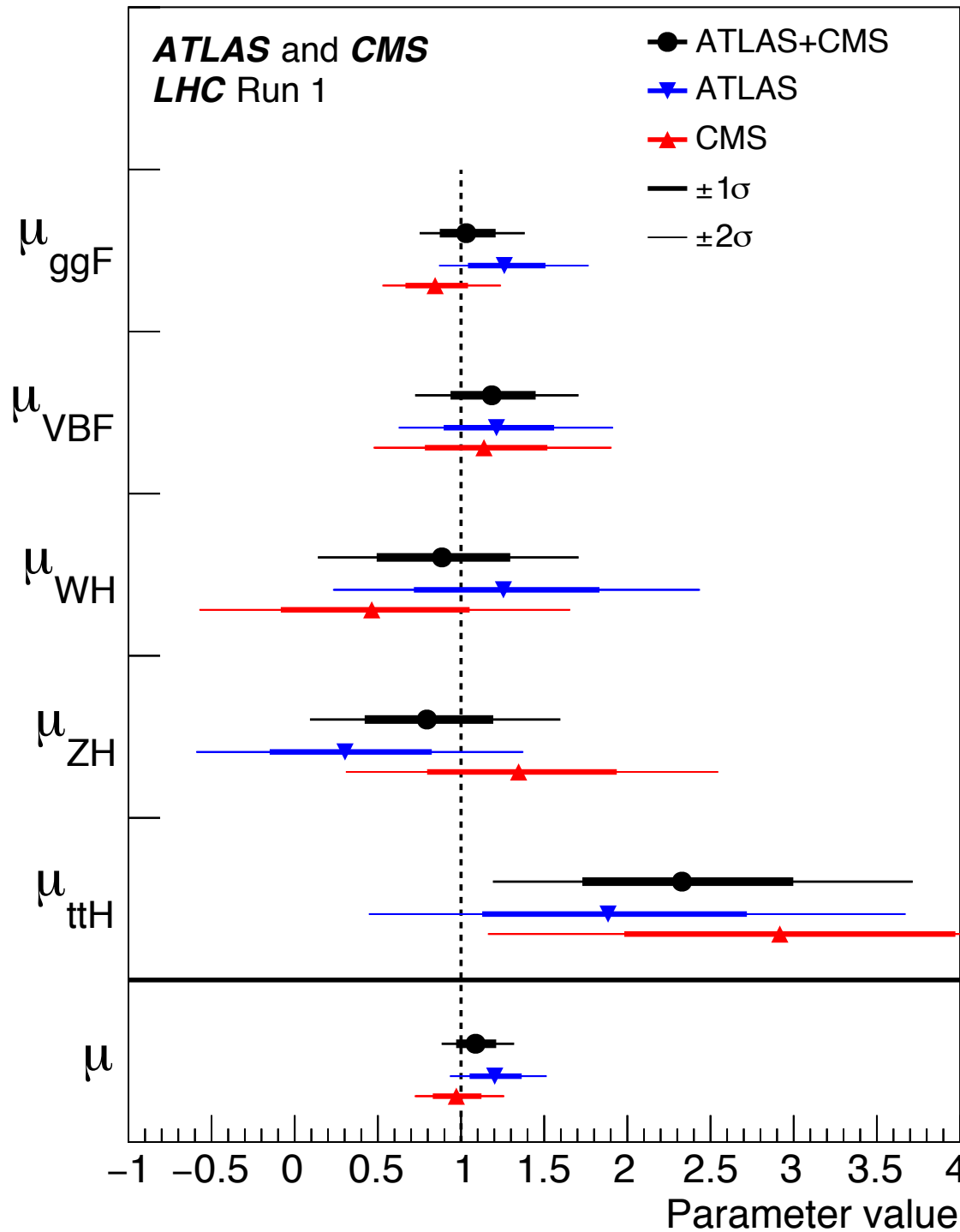


Should The Higgs Boson be TIME's Person of the Year 2012?

19.74% Definitely 80.26% No Way

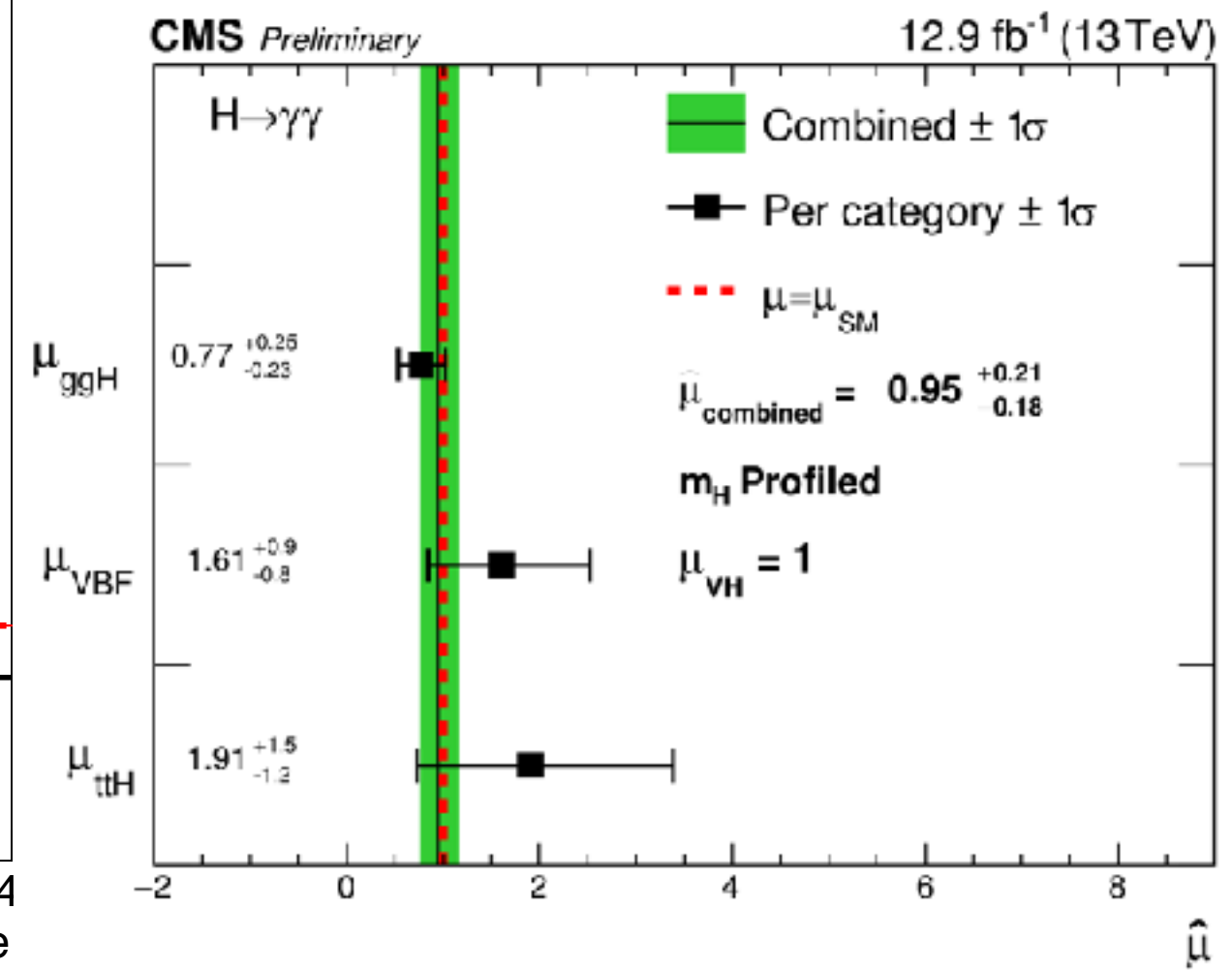


WHAT DO WE HAVE HERE?



Run 1 and Run 2 results seem to show
Higgs signal strength
consistent with SM expectations

the Higgs appears to be The (SM) Higgs



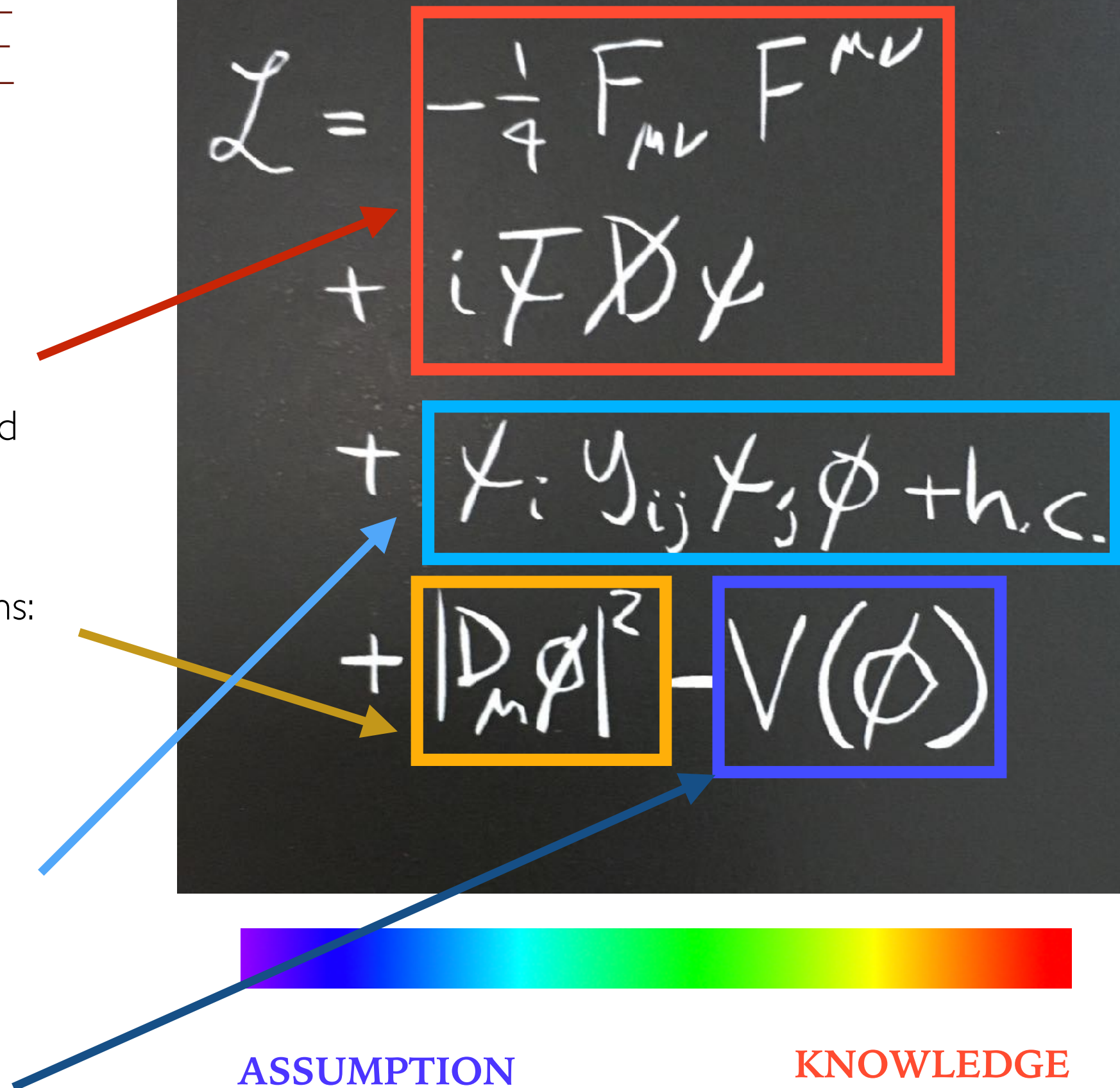
WHERE ARE WE?

Well tested base of SM:
before LHC, LHC and beyond

Higgs couplings to EWK bosons:
LHC Run I and beyond

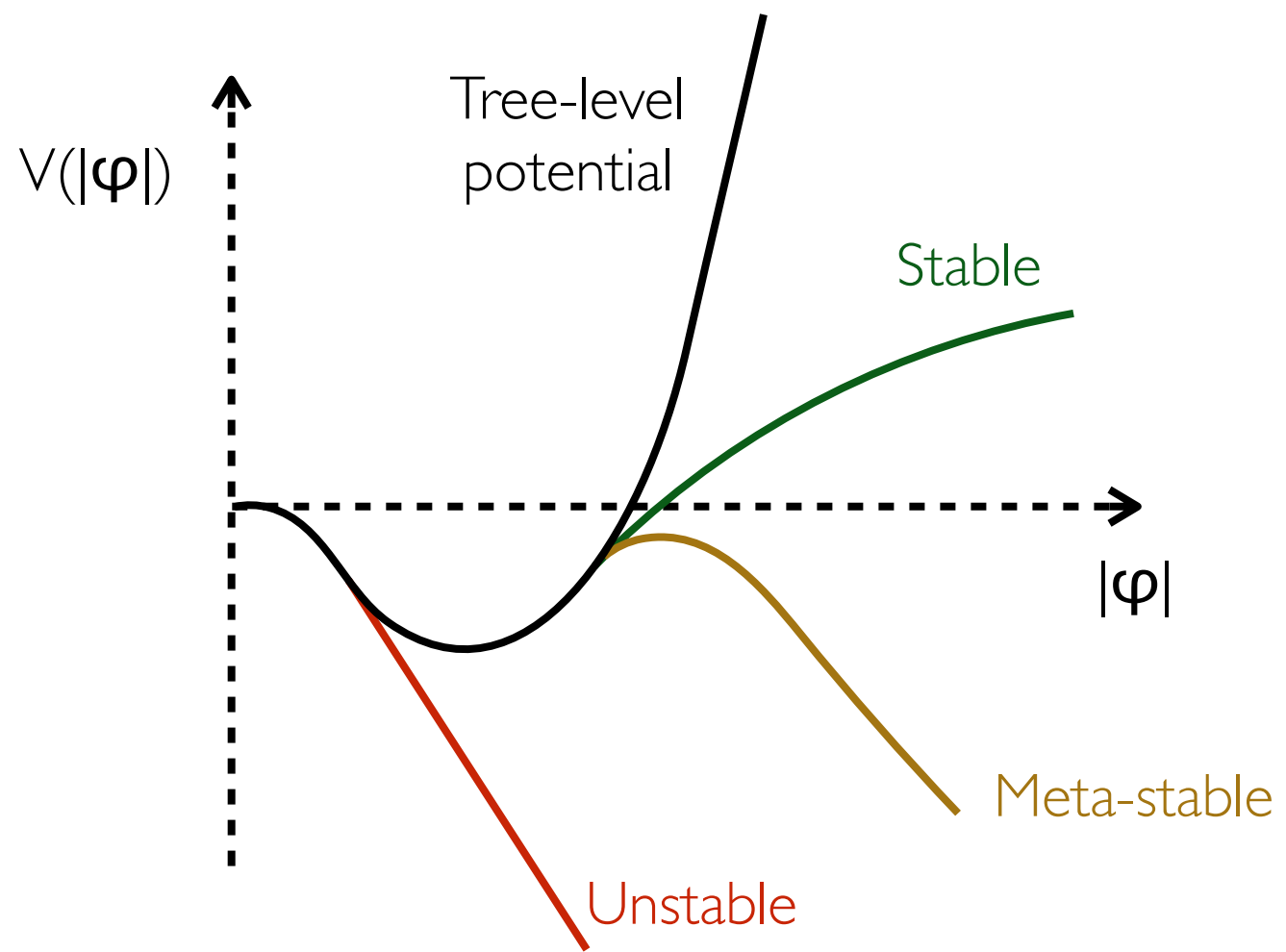
Higgs couplings to fermions:
LHC Run 2 and beyond

Higgs potential:
Higgs mass: done!
Self-coupling: HL-LHC and beyond



THE HIGGS POTENTIAL

Tree level potential suffers radiative corrections

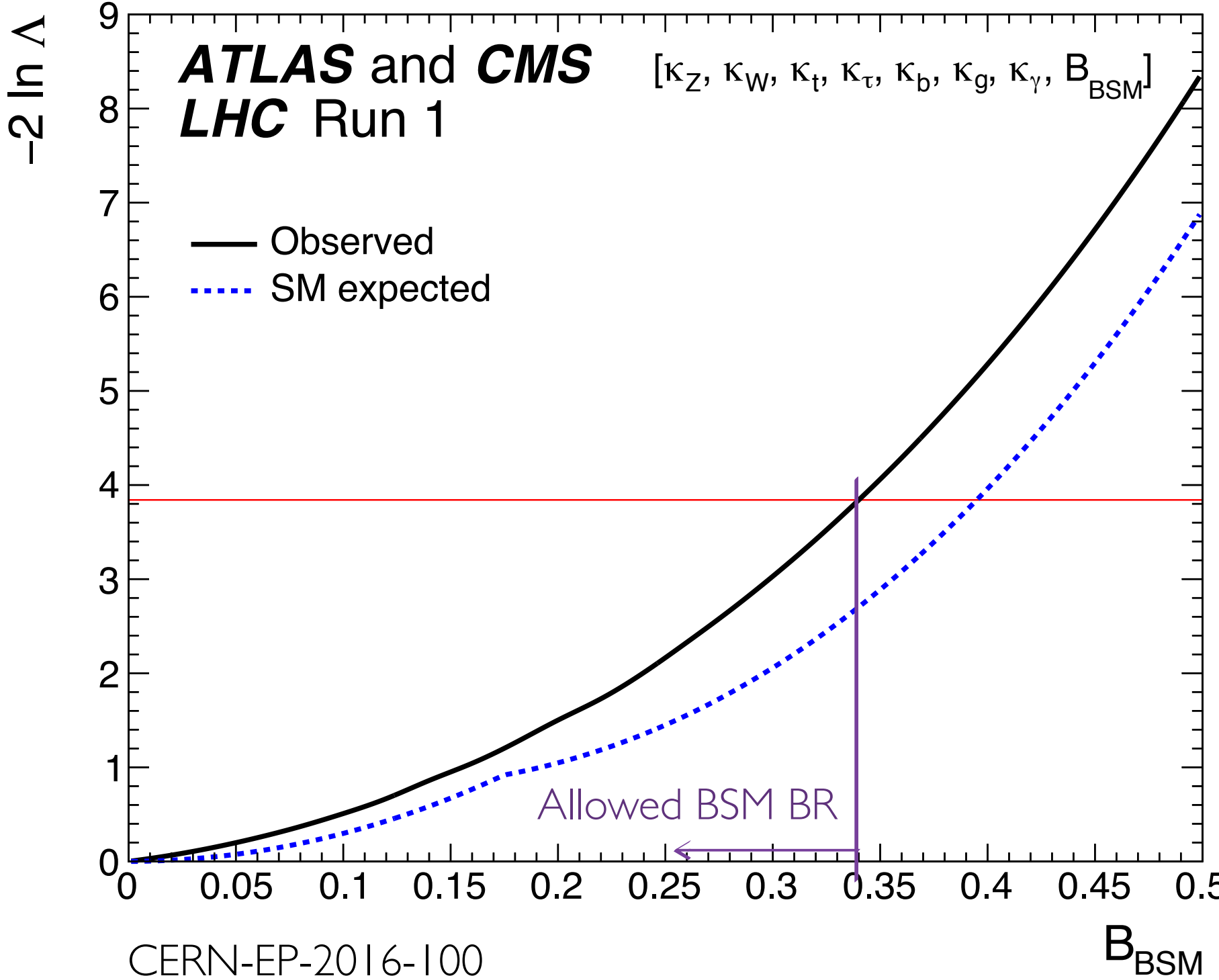


Current measurements of Higgs and Top mass seem to indicate that the Higgs potential is meta-stable at high energy scales

However, low energy modifications of the Higgs potential (such as an extended Higgs sector) can potentially change this picture

HIGGS EXOTIC DECAYS

Assumes $B_{\text{BSM}} \geq 0$, $|\kappa_Z| \leq 1$, $|\kappa_W| \leq 1$ and $\kappa_Z/|\kappa_Z| = \kappa_W/|\kappa_W|$



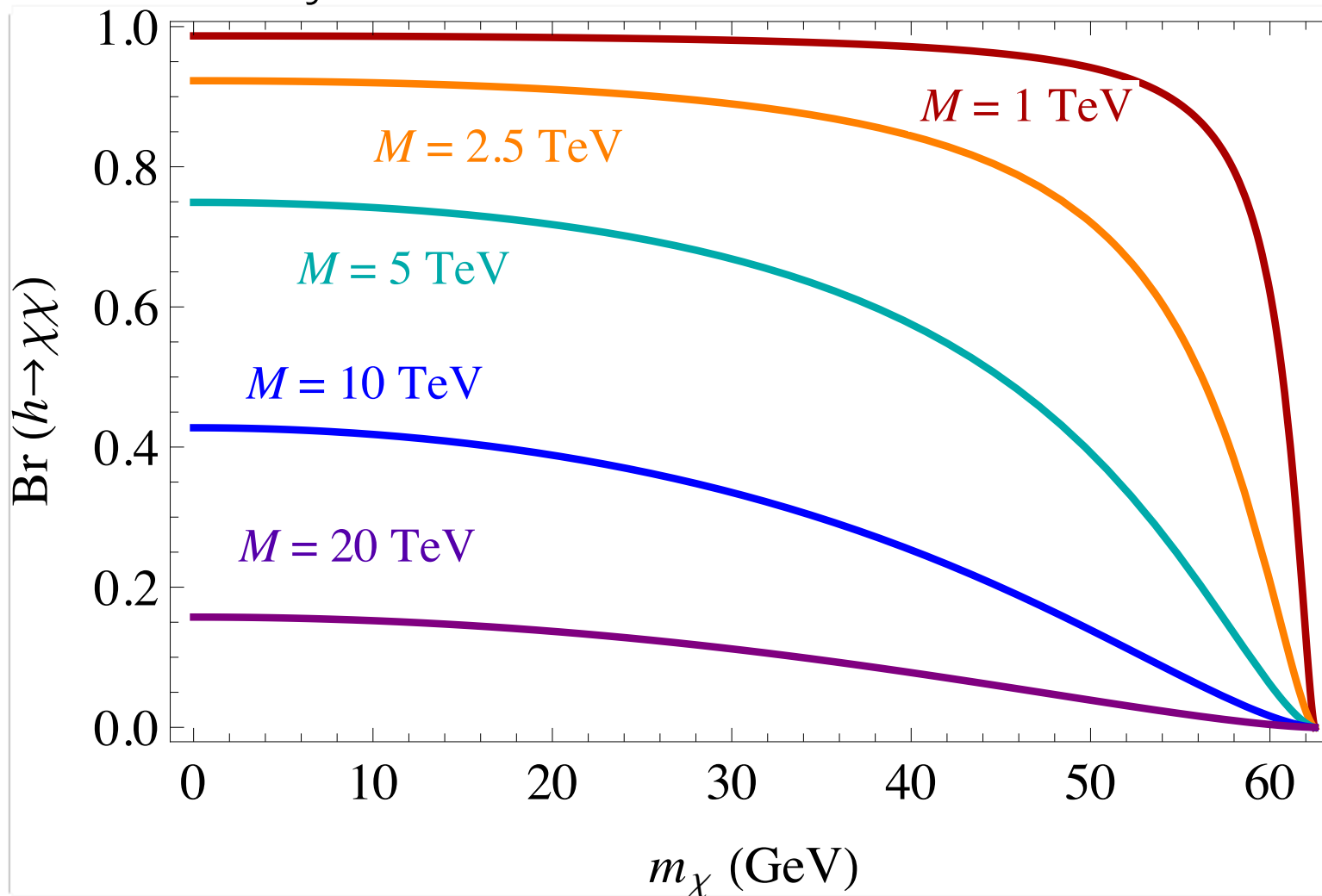
Large open phase space
for BSM Higgs decays:
 $B_{\text{BSM}} \leq 34\%$

From theory:
Cataloging exotic decays
Survey of Exotic Higgs
Decays

Experimental point of view:
1) Constrain B_{BSM} indirectly
(precision Higgs physics)
2) **Directly look for Higgs
exotic decays**

WHY HIGGS DECAYS?

From J. Shelton



If BSM state is light and weakly coupled to SM: hard to see over LHC background

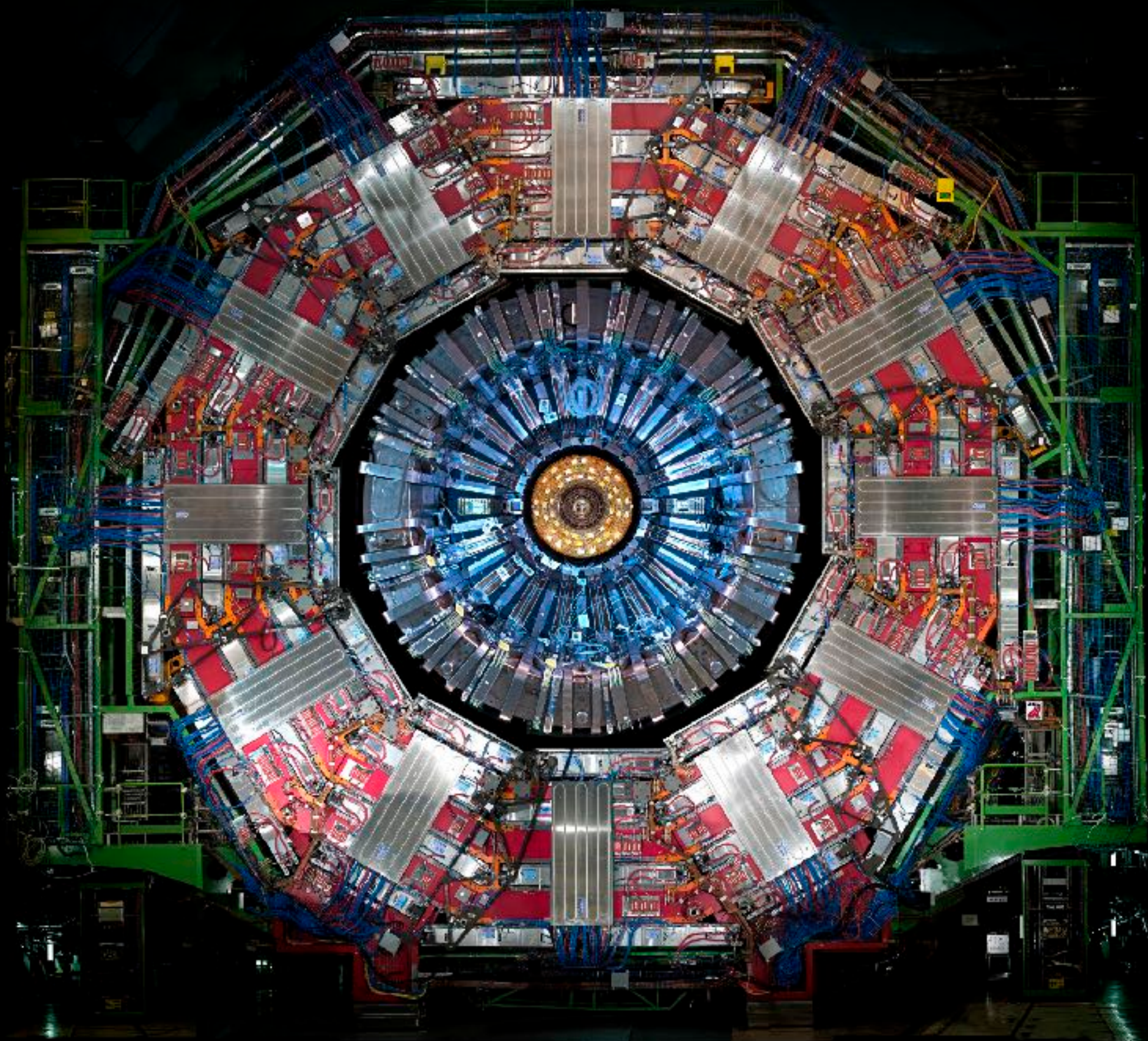
If BSM is light, weakly coupled and couples to Higgs:

- 1) Higgs-tag to mitigate background
- 2) SM-Higgs couplings are also weak, so **Br(H → BSM)** can be large even with weak BSM-Higgs coupling

Assuming a simple H-fermion-fermion dim-5 coupling:

$$\Delta \mathcal{L} = \frac{1}{M} \bar{\psi} \psi |H|^2$$

Large Higgs cross section allows exploration of small branching ratios

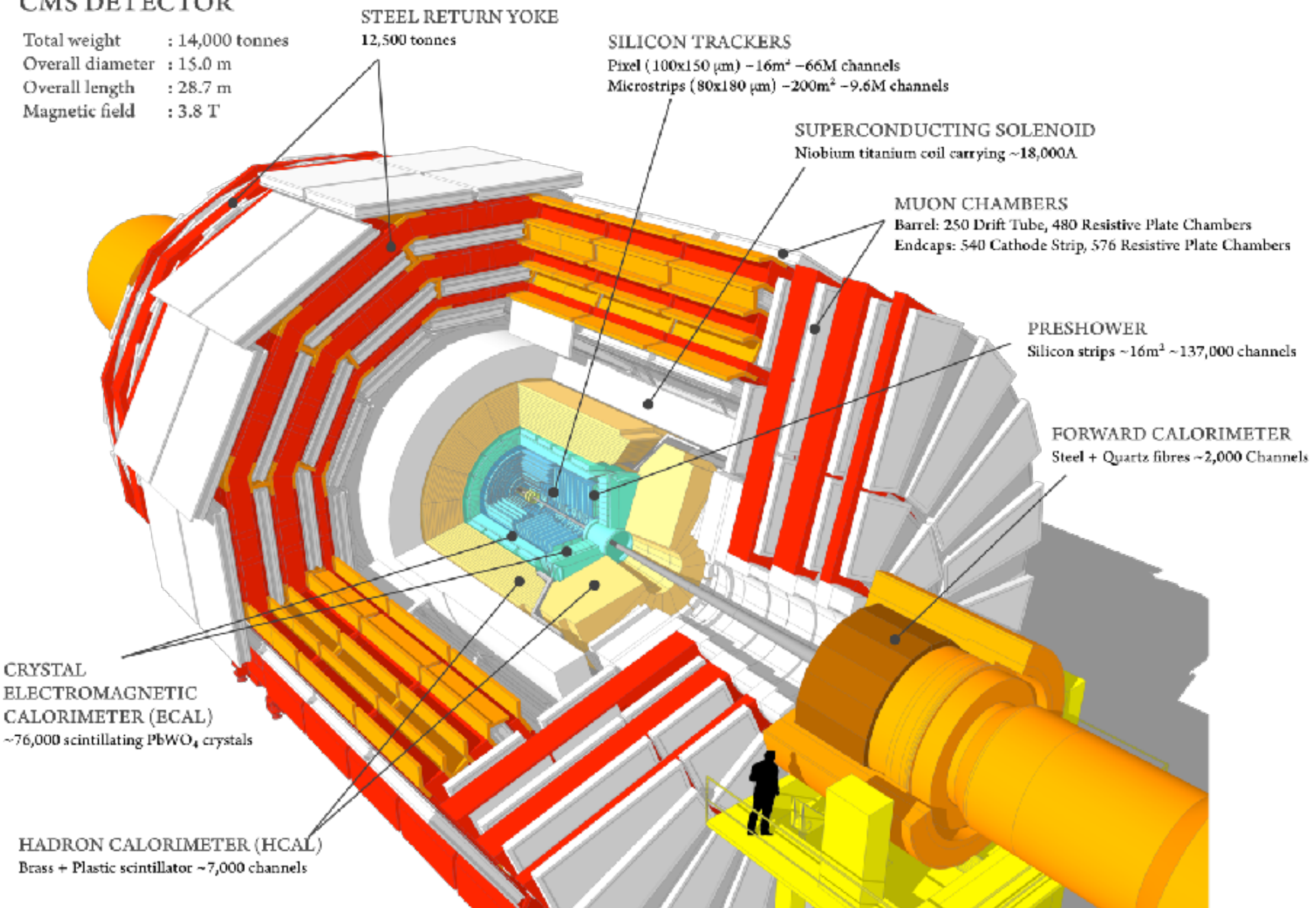


The CMS Experiment

THE CMS EXPERIMENT

CMS DETECTOR

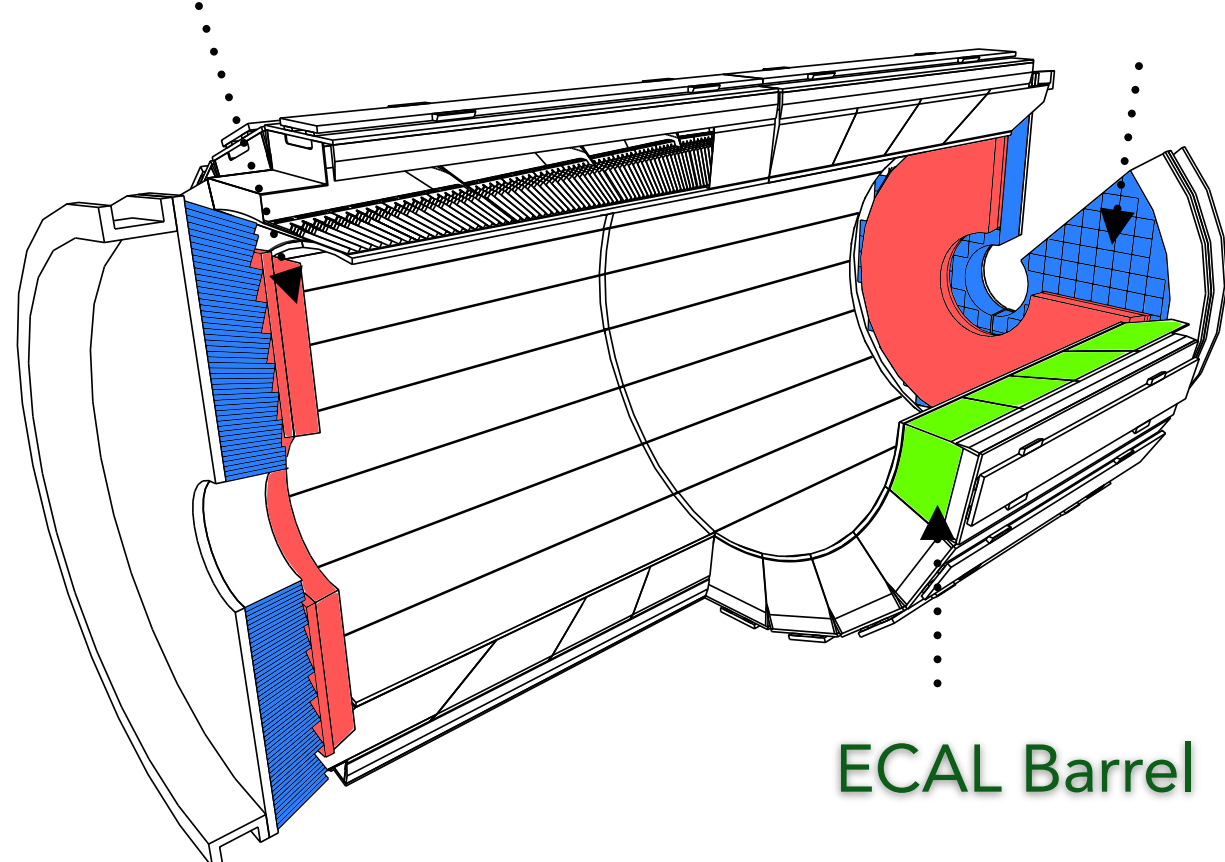
Total weight : 14,000 tonnes
Overall diameter : 15.0 m
Overall length : 28.7 m
Magnetic field : 3.8 T



THE CMS ECAL

Preshower

ECAL Endcap



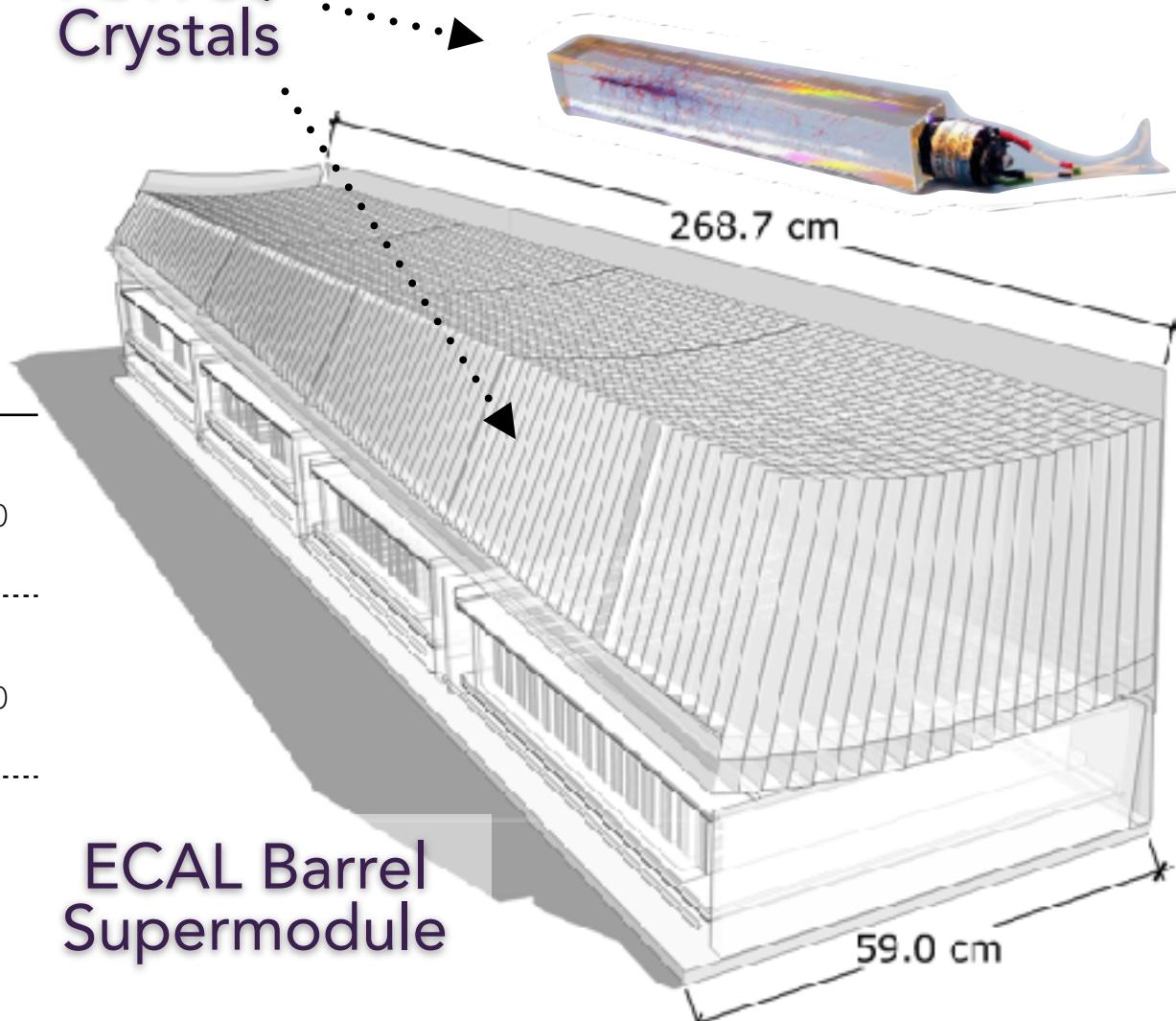
ECAL Characteristics

Barrel (EB)	$ \eta < 1.48$	61200 ($2.2 \times 2.2 \times 23 \text{ cm}^3$) PbWO ₄ Crystals	$\sim 26X_0$
Endcap (EE)	$1.48 < \eta < 3.0$	14648 ($2.9 \times 2.9 \times 22 \text{ cm}^3$) PbWO ₄ Crystals	$\sim 25X_0$
Preshower	$1.65 < \eta < 2.6$	137200 ($6.3 \times 6.3 \text{ cm}^2$) Pb/ Si strips	$\sim 3X_0$

CMS ECAL Must Provide:

- Good energy reconstruction resolution
- Good position resolution for reconstructed deposits
- Fast and efficient readout for online selection (DAQ & Trigger)

PbWO₄
Crystals

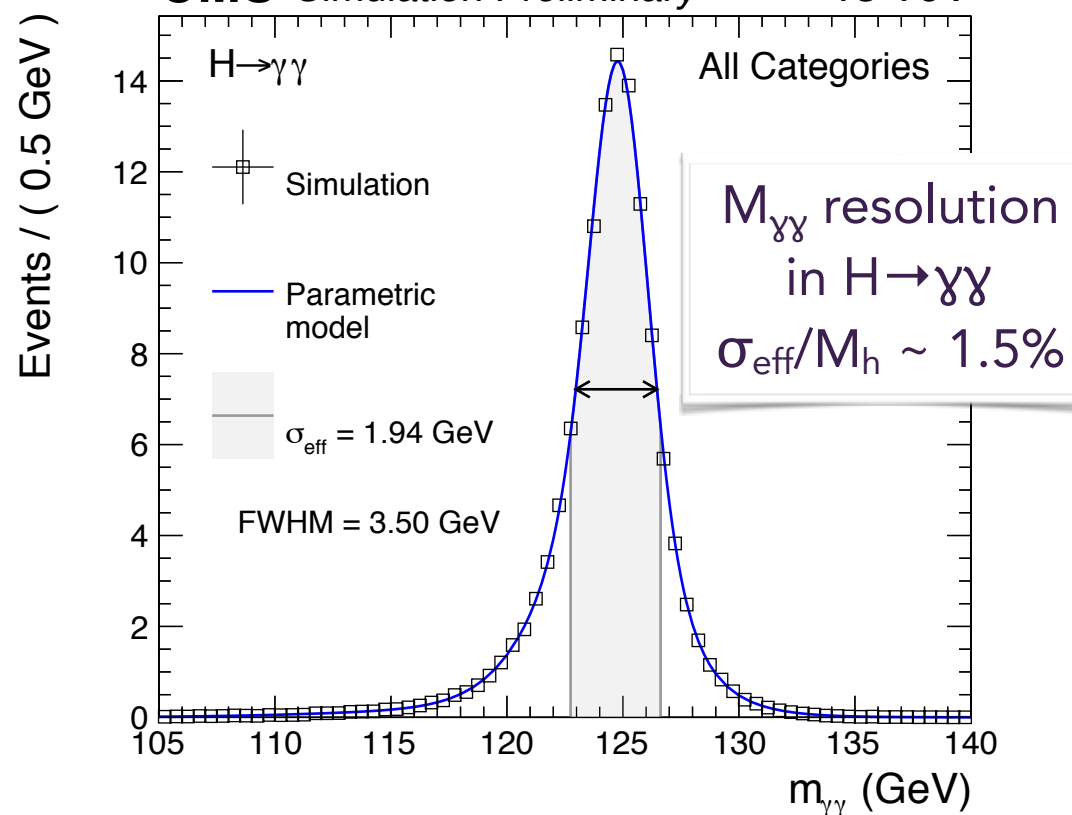


ECAL Barrel
Supermodule

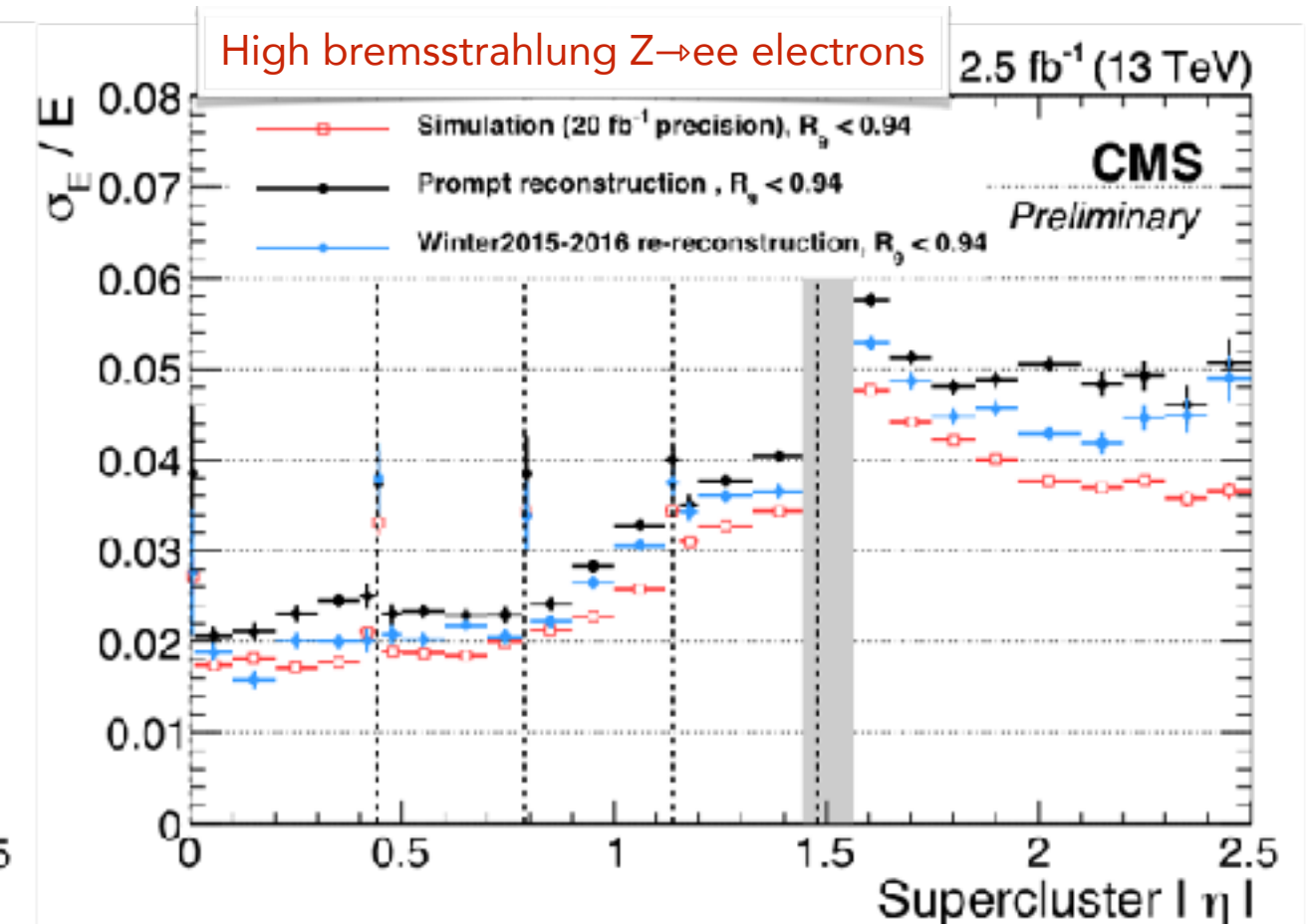
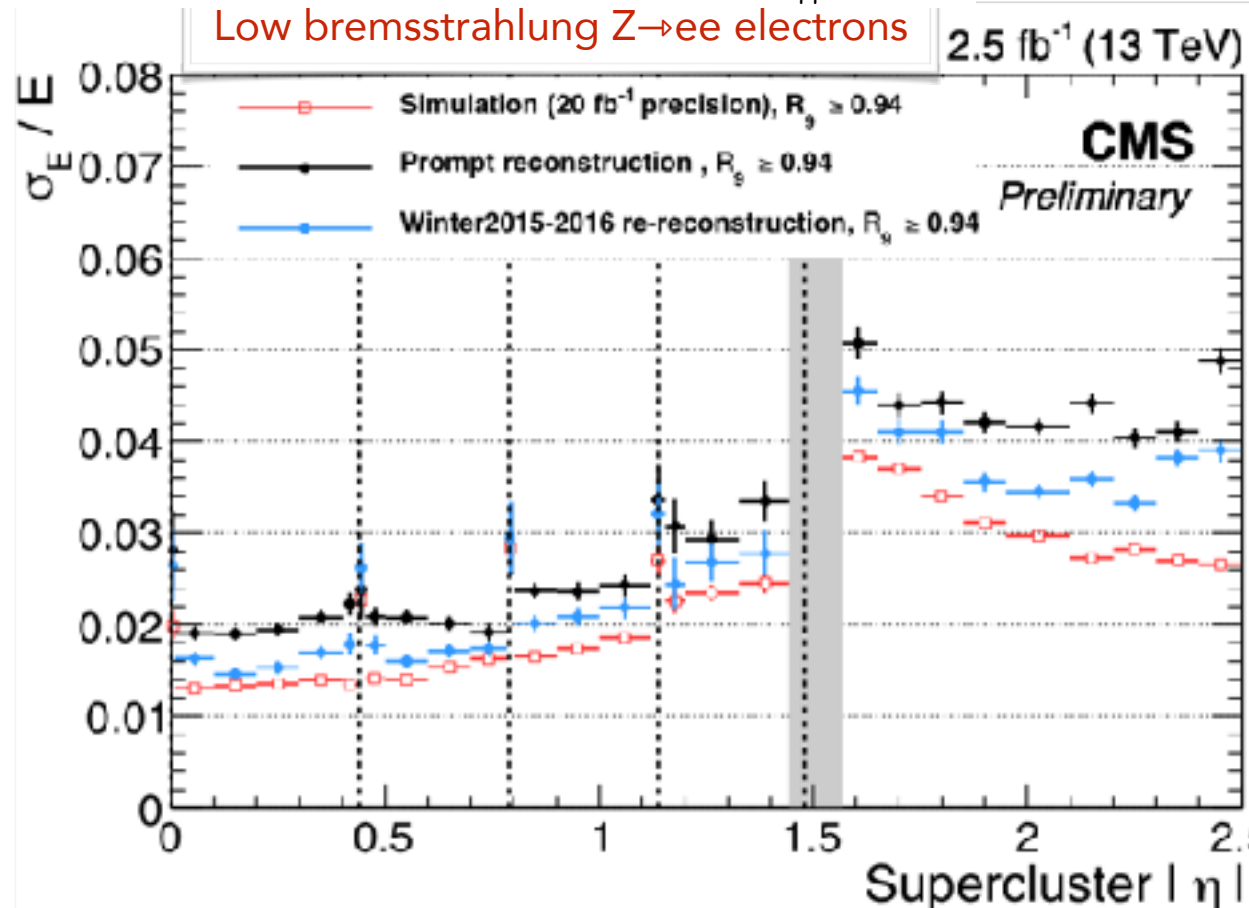
ECAL PERFORMANCE W/2015 DATA

CMS Simulation Preliminary

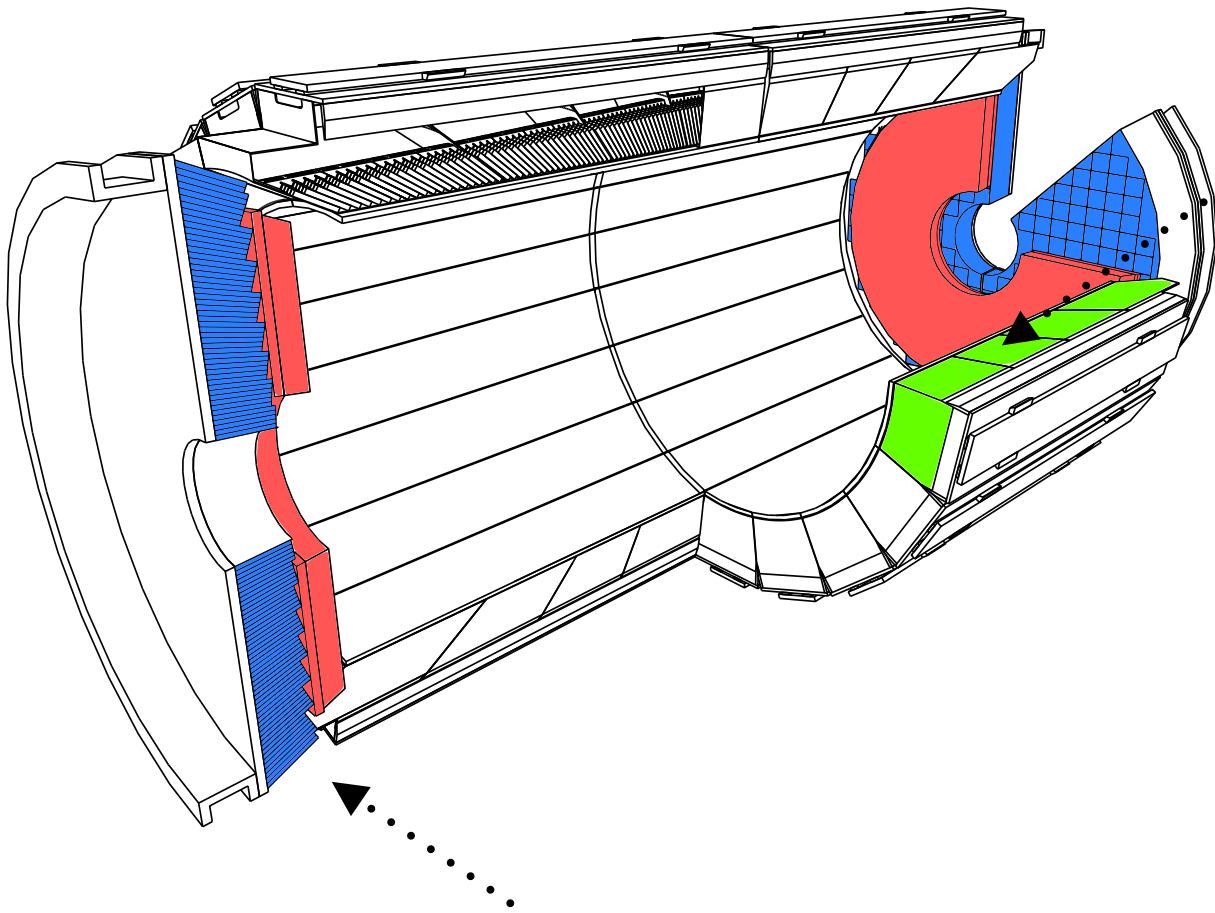
13 TeV



- ECAL relative energy resolution better than 2% for low bremsstrahlung $Z \rightarrow ee$ electrons in the central barrel with 2015 calibration
- Calibration precision statistically constrained with 2.5 fb⁻¹, particularly at high $|\eta|$
- For more details on ECAL calibration and performance, see my talk at [CALOR 2016 \(Daegu, SK\)](#)



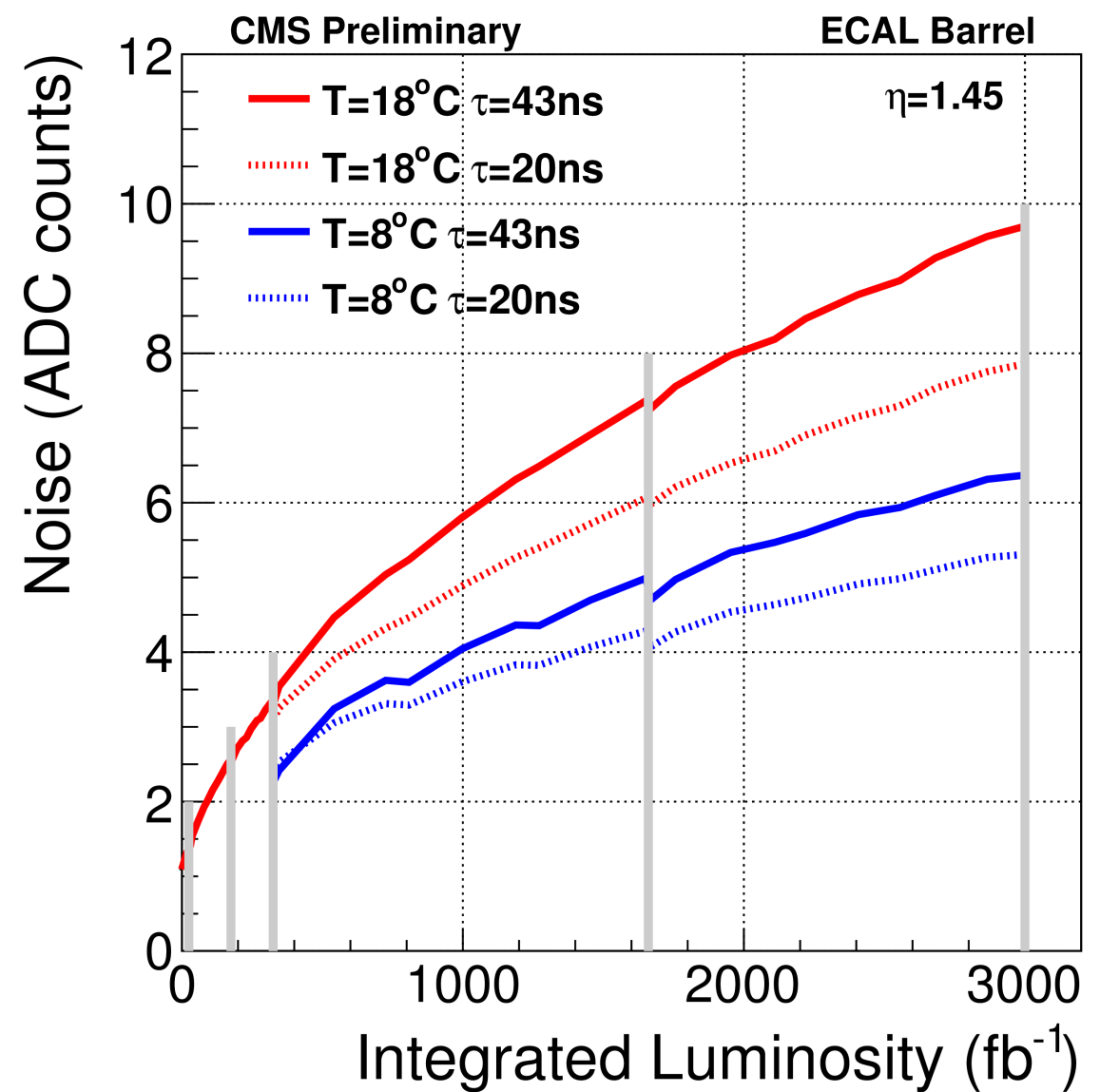
HL-LHC AND ECAL



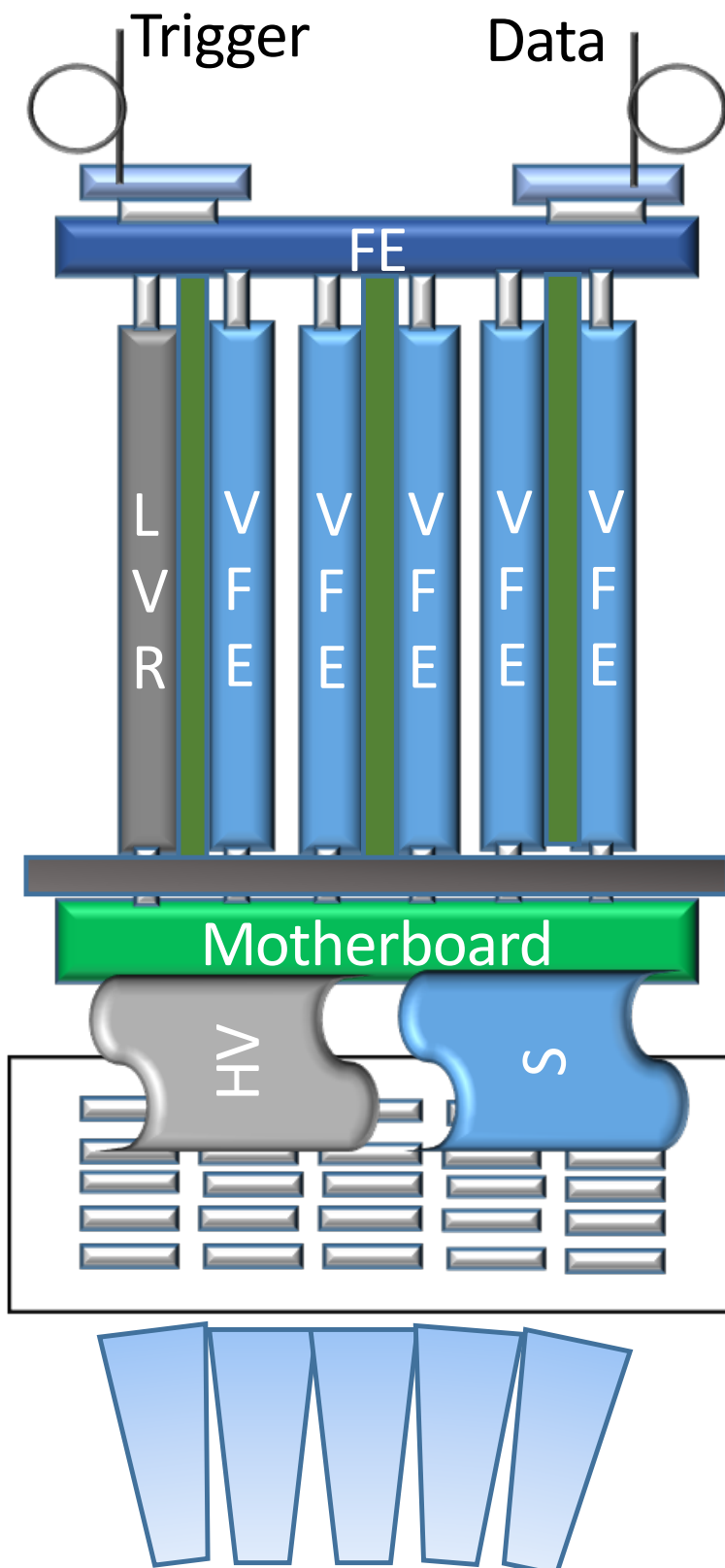
Under the harsh HL-LHC environment,
the ECAL **endcap crystals** would lose
~100% of their transparency

CMS will replace the endcap calorimeters
(EE, ES and HE) by a **silicon based**
sampling endcap calorimeter (HGCal)

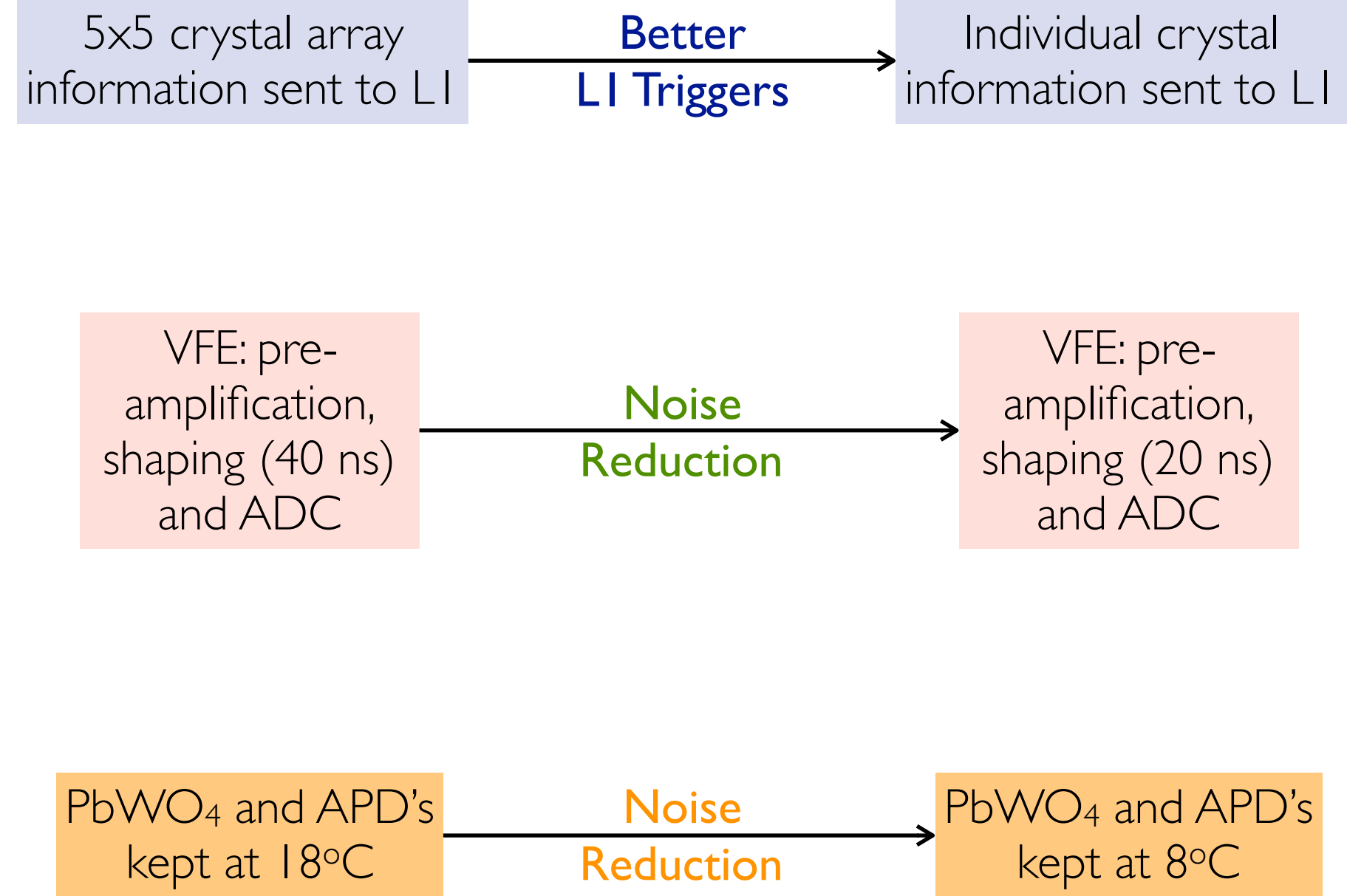
The ECAL barrel crystals will be able to cope with HL-LHC radiation flux, but increase in APD's dark current (**noise**) needs to be mitigated by electronics upgrades



THE ECAL PHASE II UPGRADE



Upgrades focused on lowering the expected VFE/FE noise and optimizing LI triggering

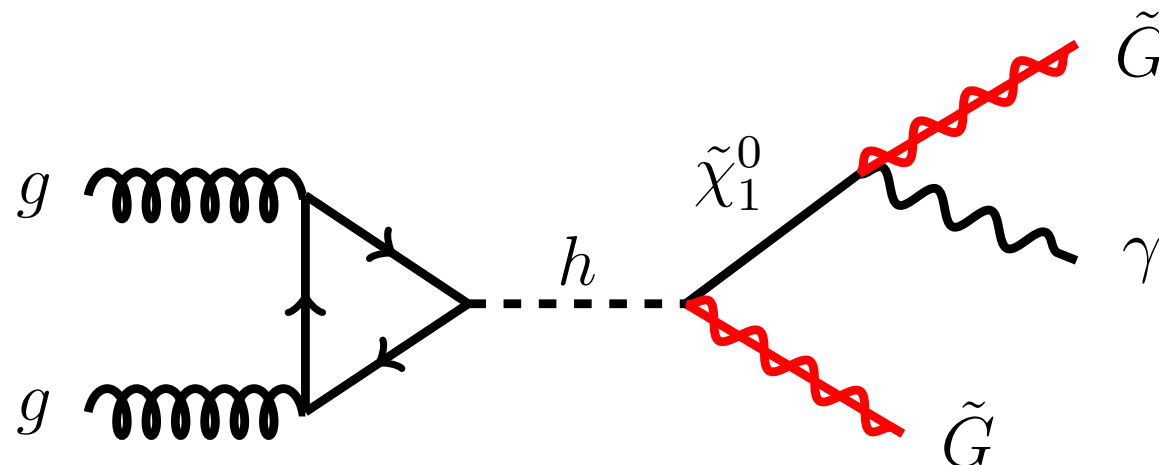




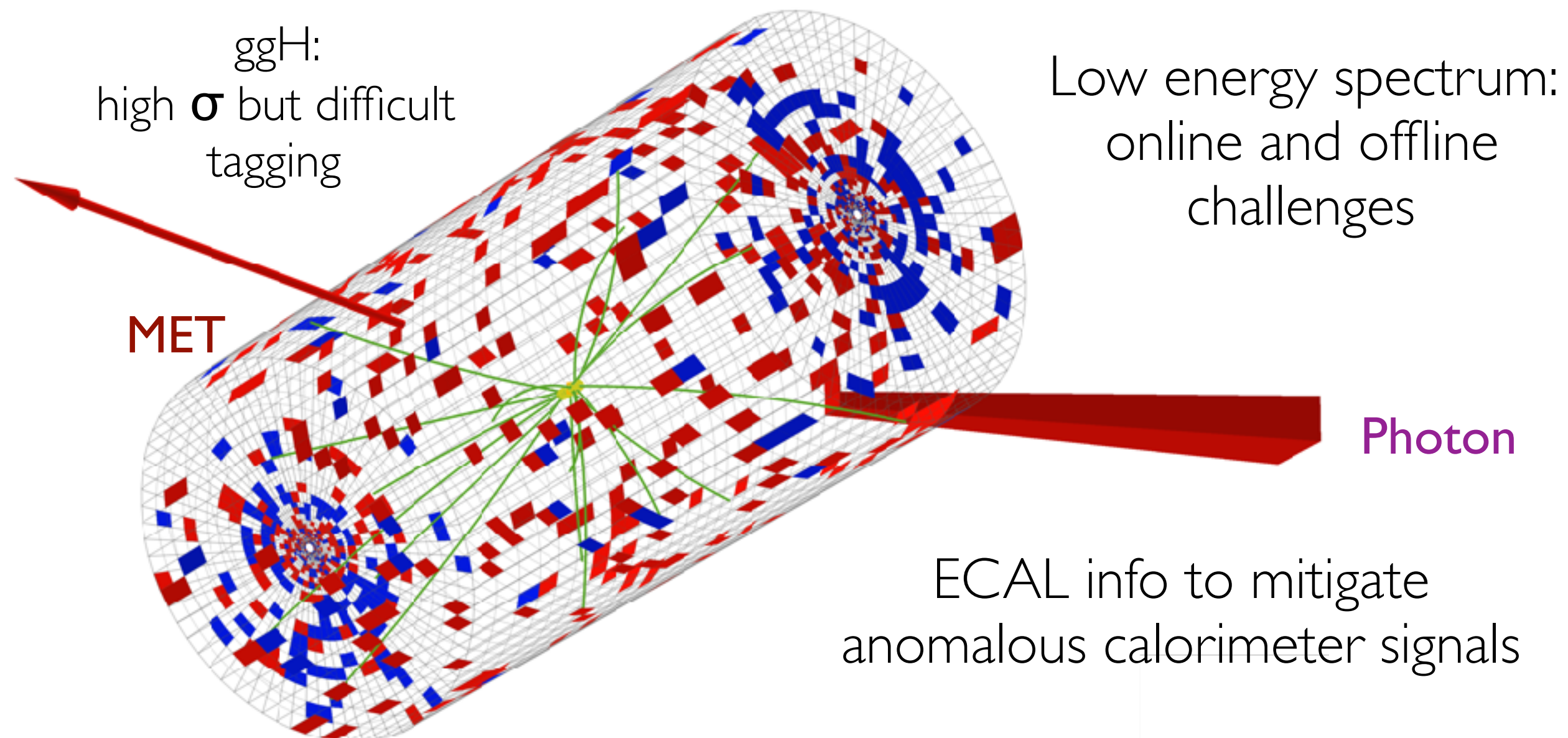
A 3D simulation visualization of particle collisions and detector components. The scene features a central yellow cone representing a Higgs boson decay, surrounded by various colored tracks (yellow, green, blue) representing different particle types. In the background, there are red wireframe structures representing the ATLAS detector's inner calorimeter and muon chambers. A large blue rectangular region at the bottom right represents the missing transverse energy (MET) detector. The overall atmosphere is dark, with the particles and detector components highlighted in bright colors.

HIGGS EXOTIC DECAYS WITH PHOTONS AND MET

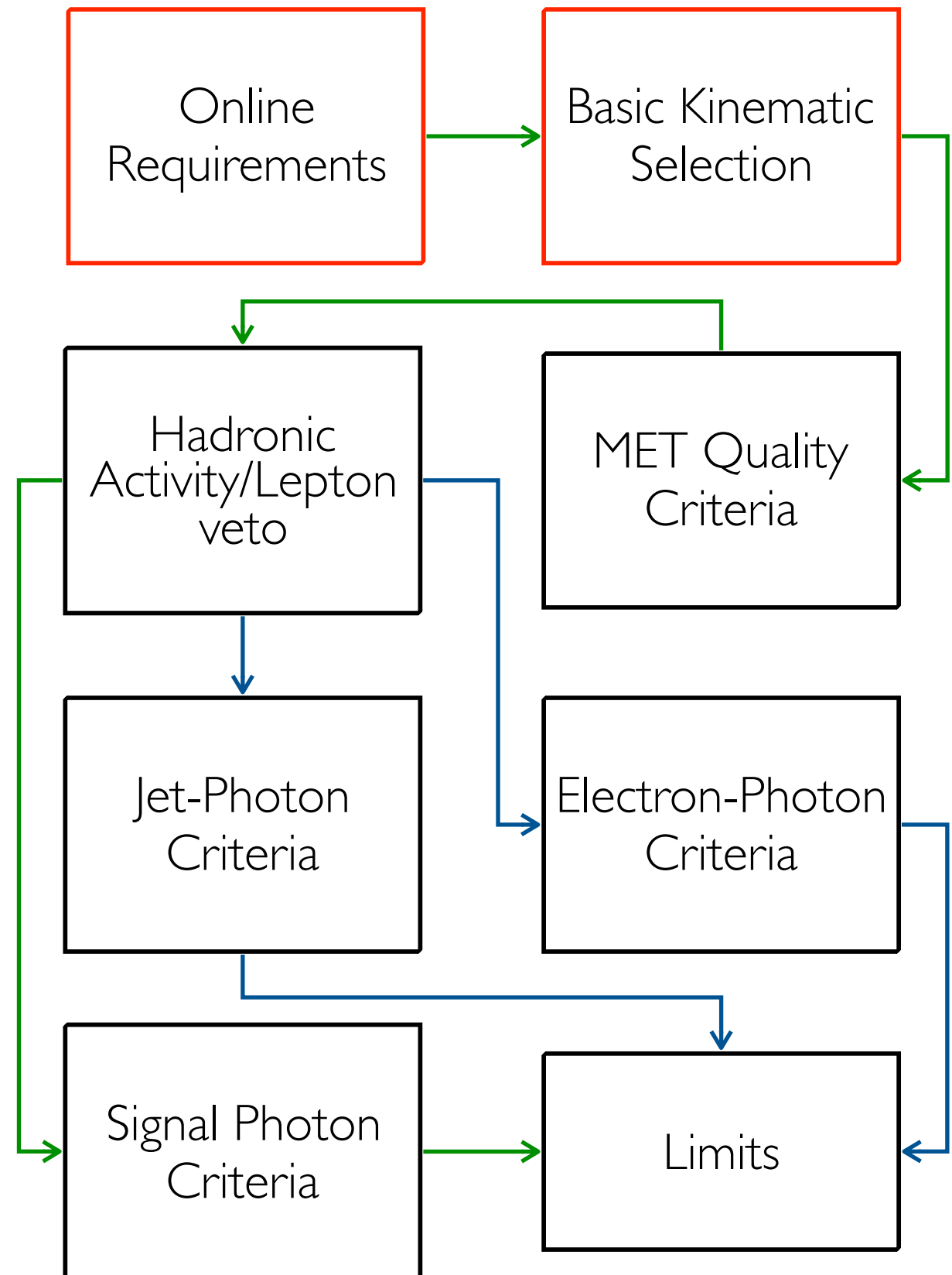
HIGGS, PHOTONS AND MET



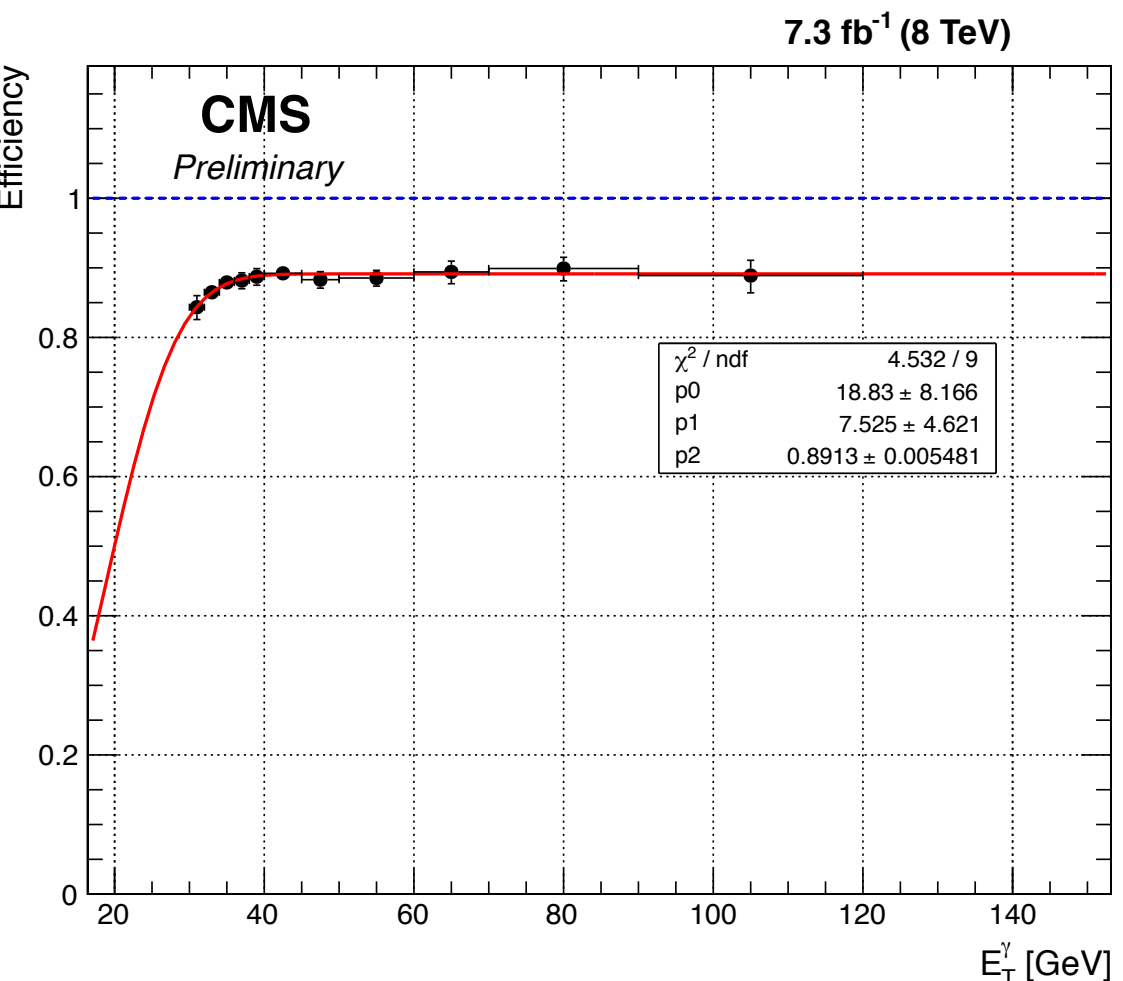
Gauge-mediated SUSY
breaking scenarios with
 $\sqrt{f} \sim \text{TeV}$



STRATEGY

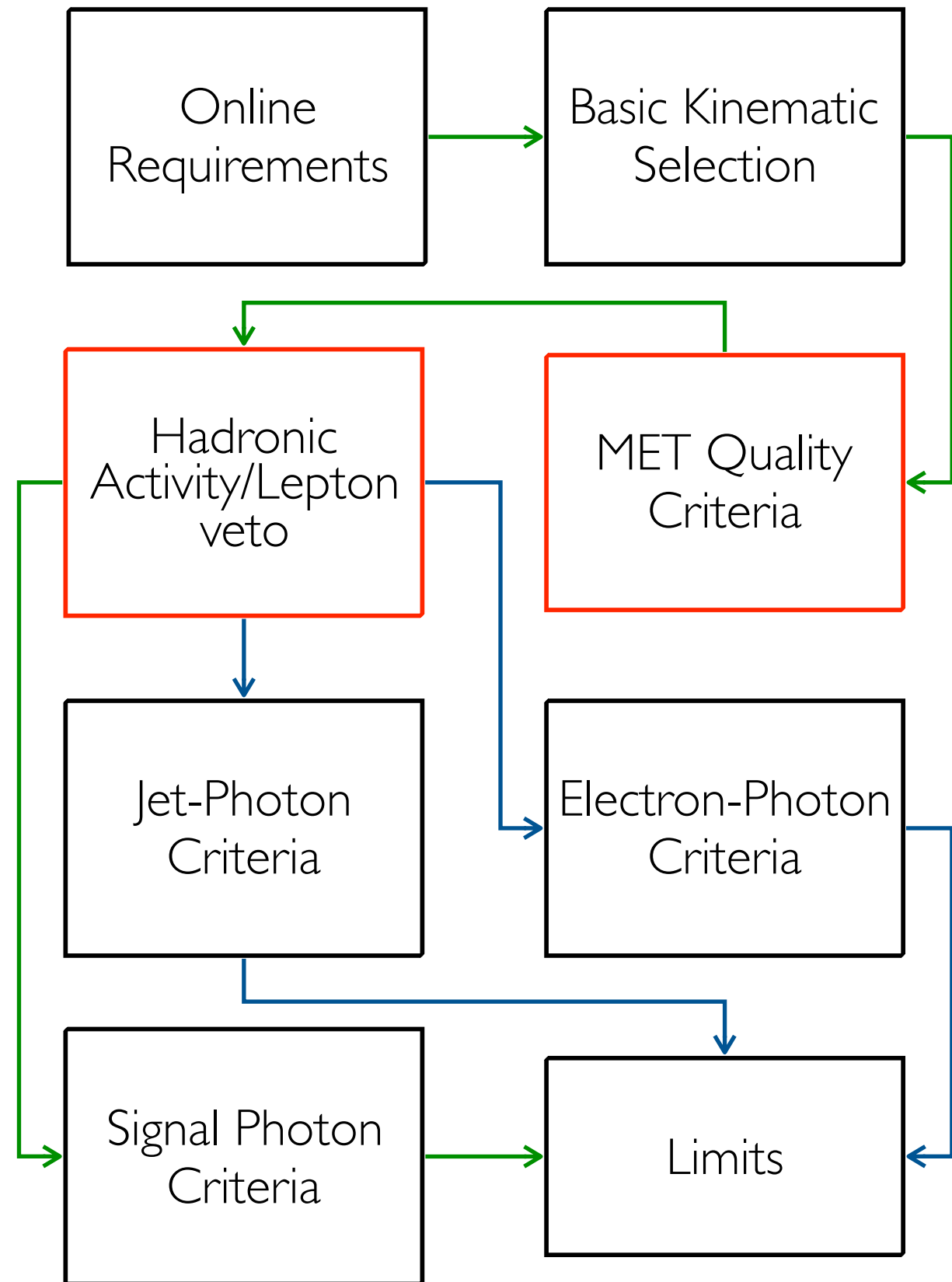


Triggering based on calorimetry:
 γ +CALO MET Trigger

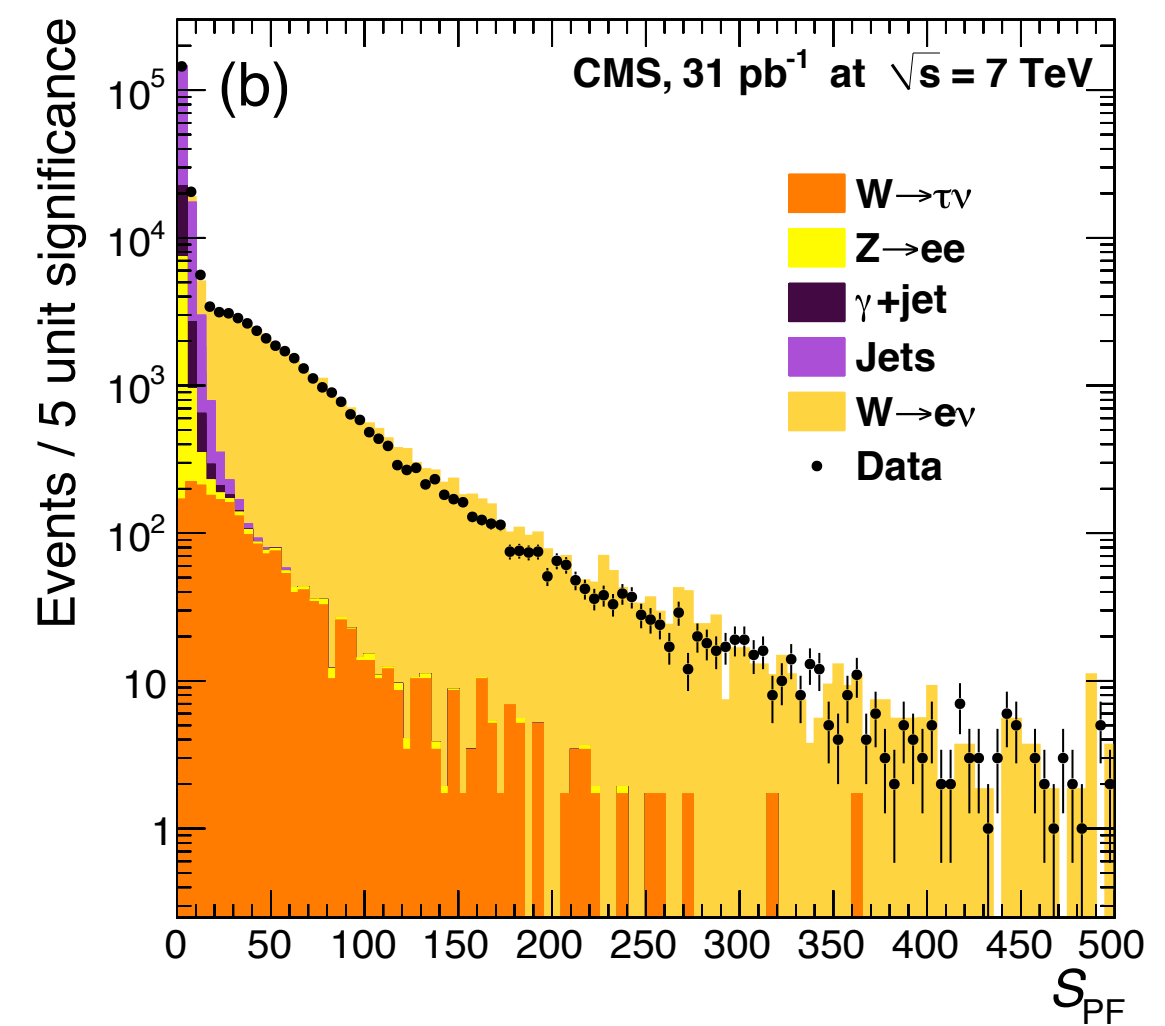


Online: barrel γ with $E_T(\gamma) > 30 + \text{quality}$,
calo MET > 25

STRATEGY

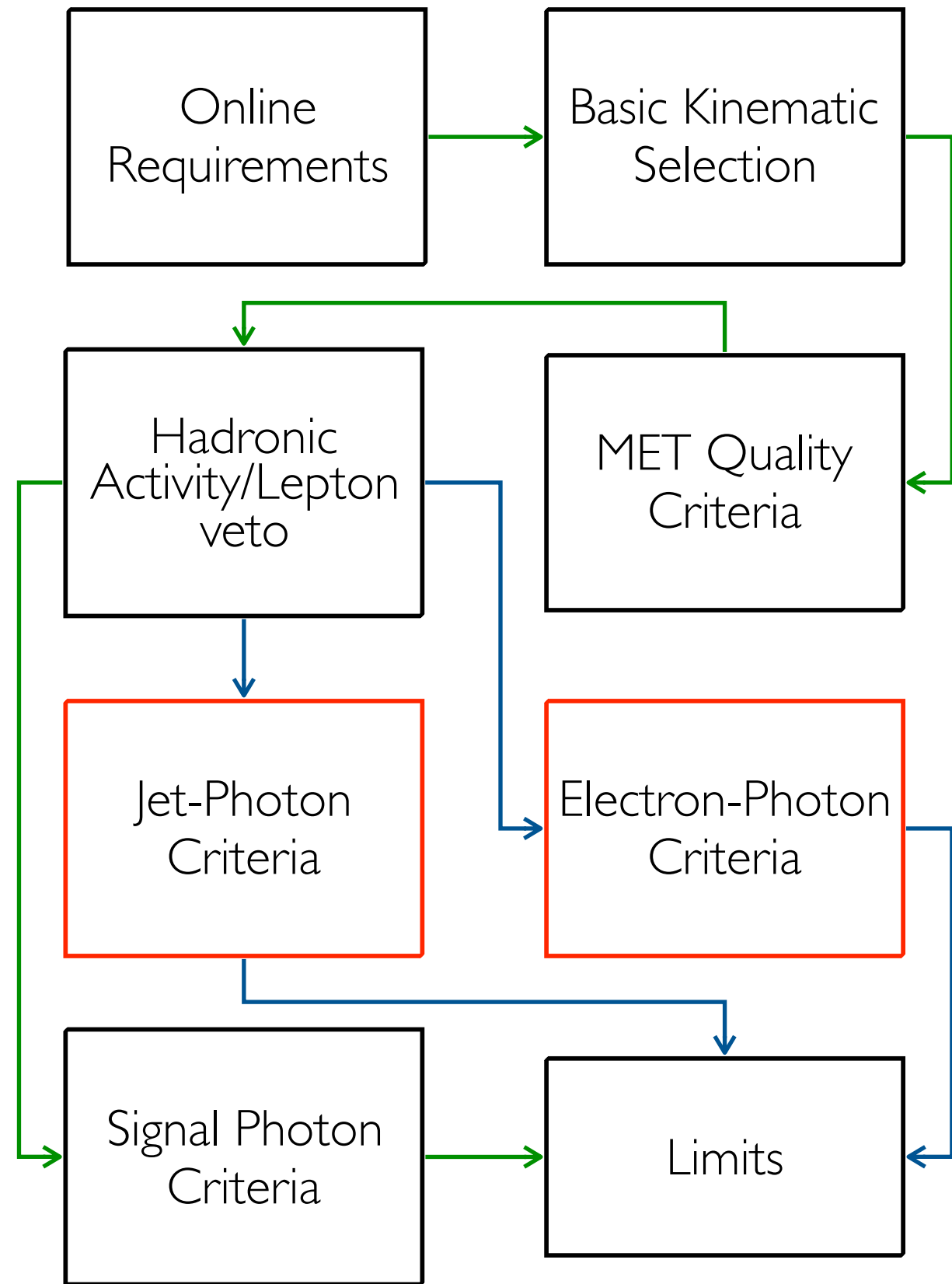


MET Significance and quality requirements to reduce pure QCD contamination

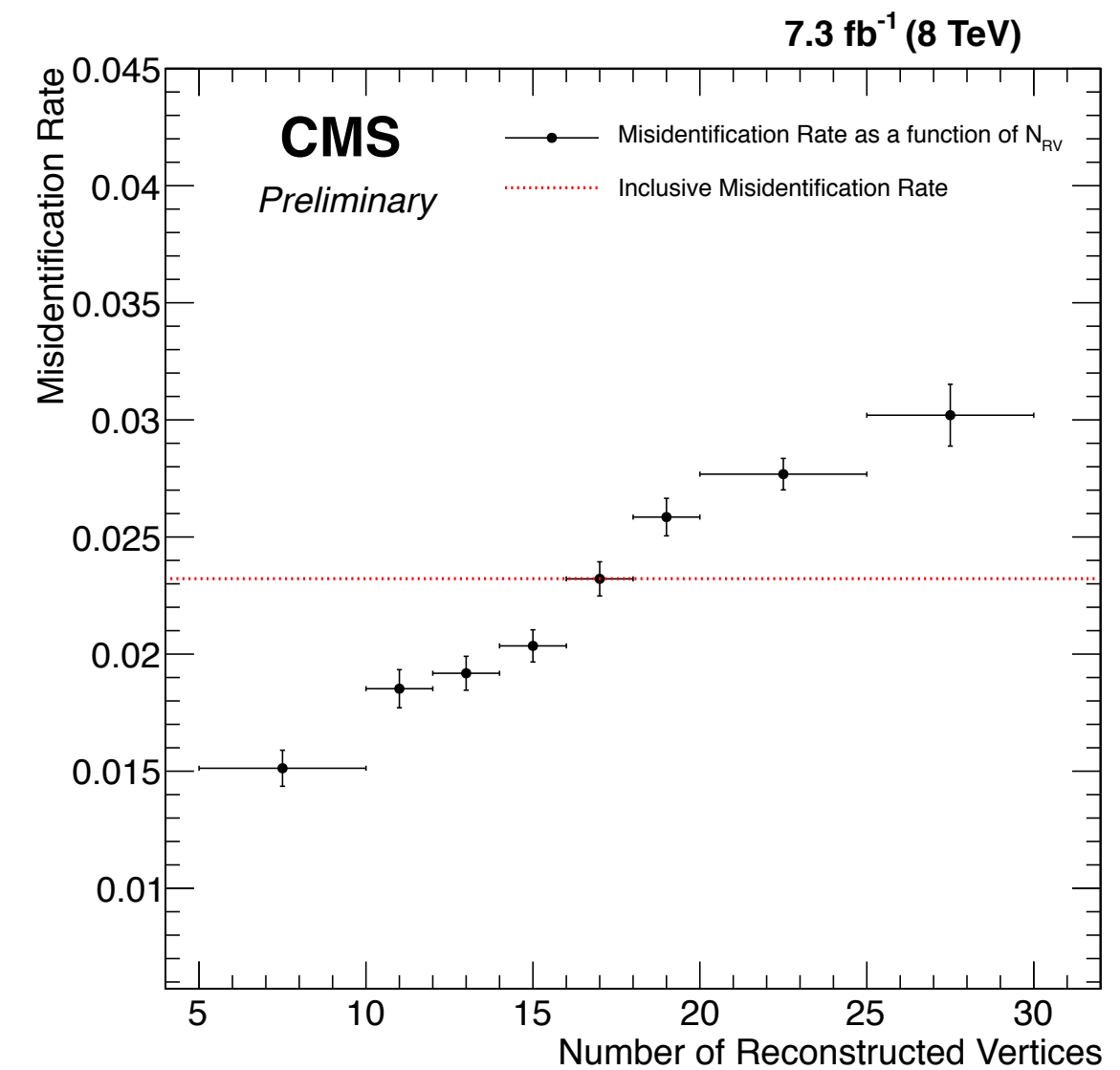


MET performance
of the CMS detector
arXiv:1106.5048

STRATEGY

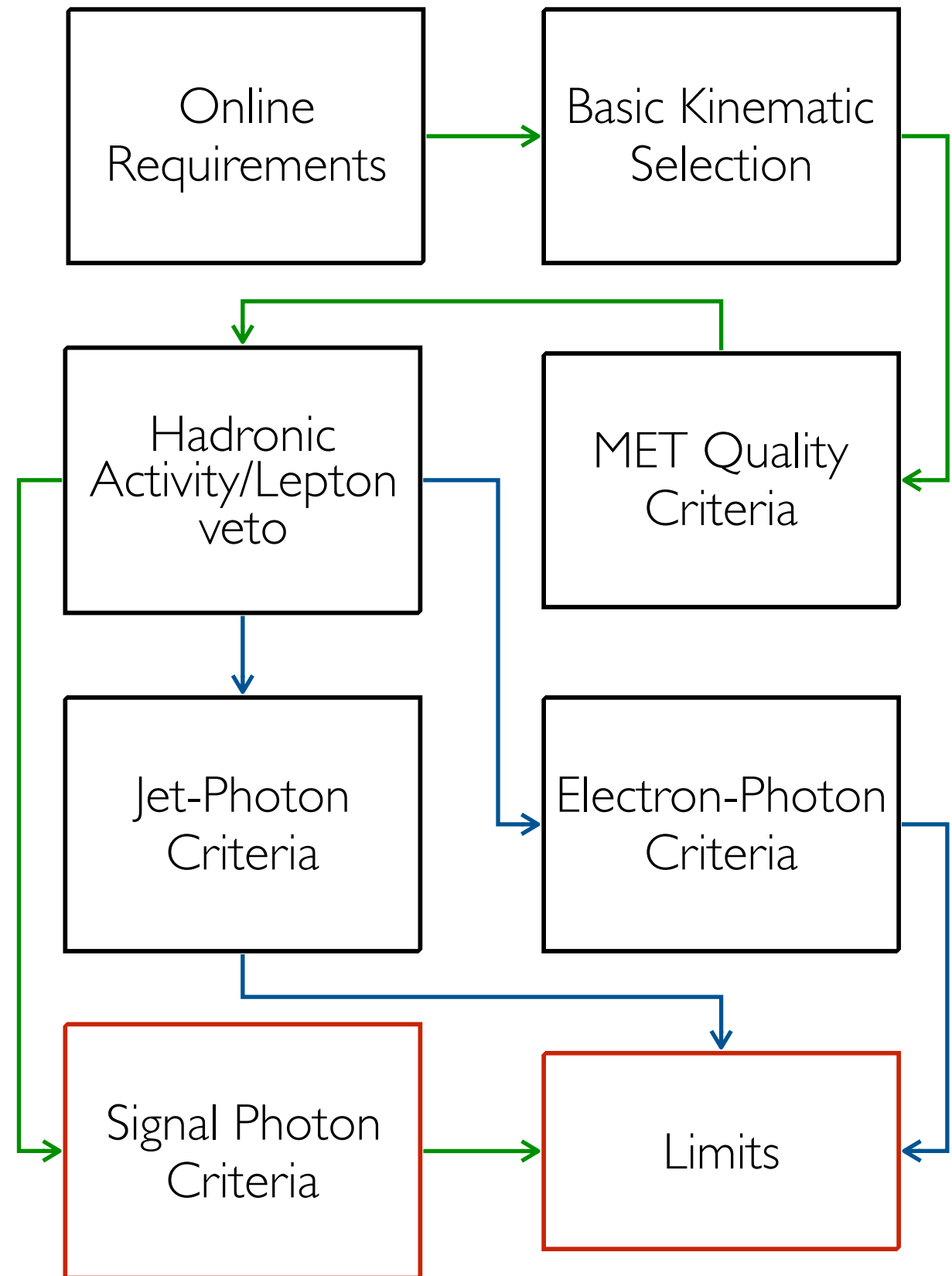


Largest backgrounds from misidentified photons (jets and electrons) are estimated from data



Electron to photon mis-identification rate

STRATEGY



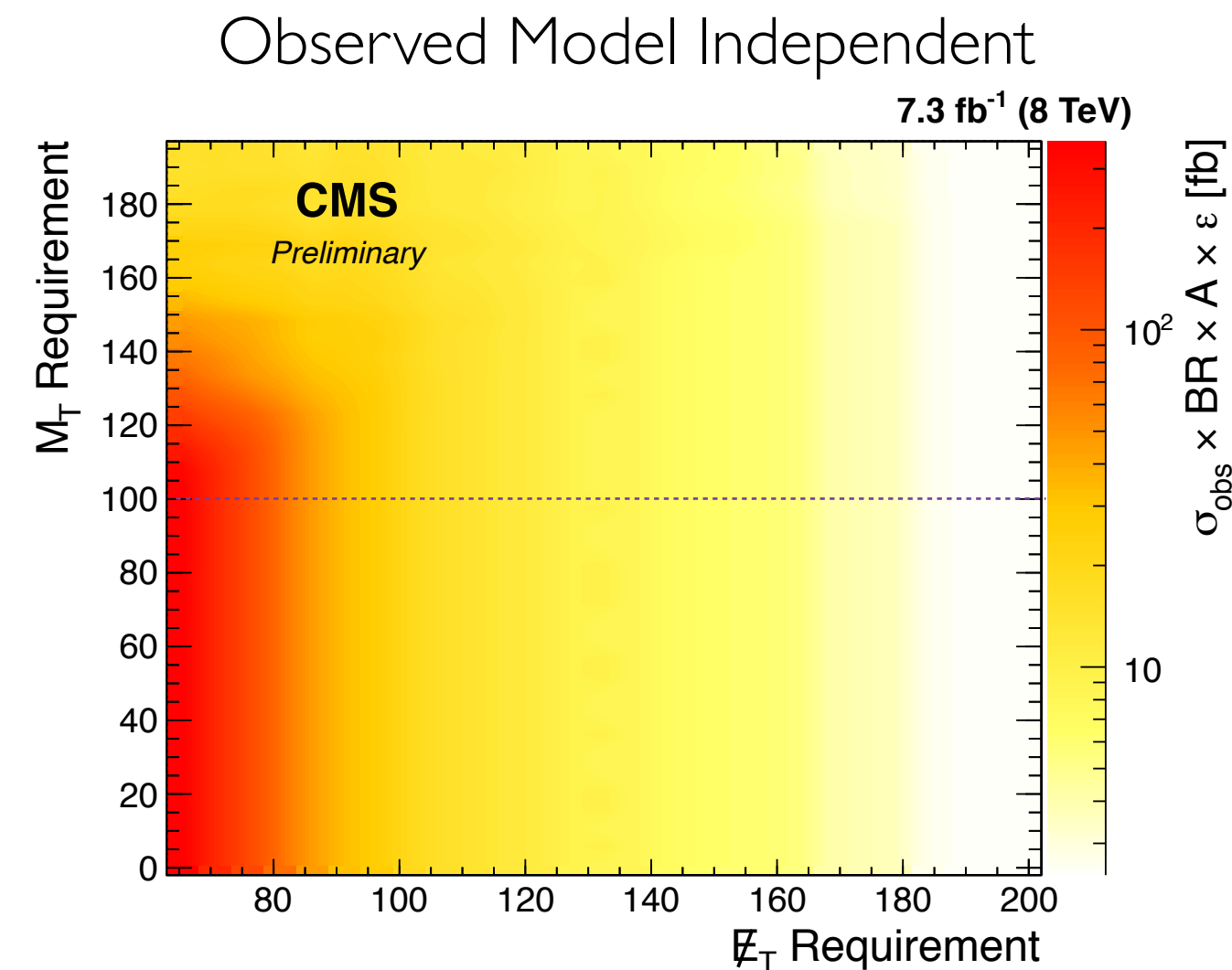
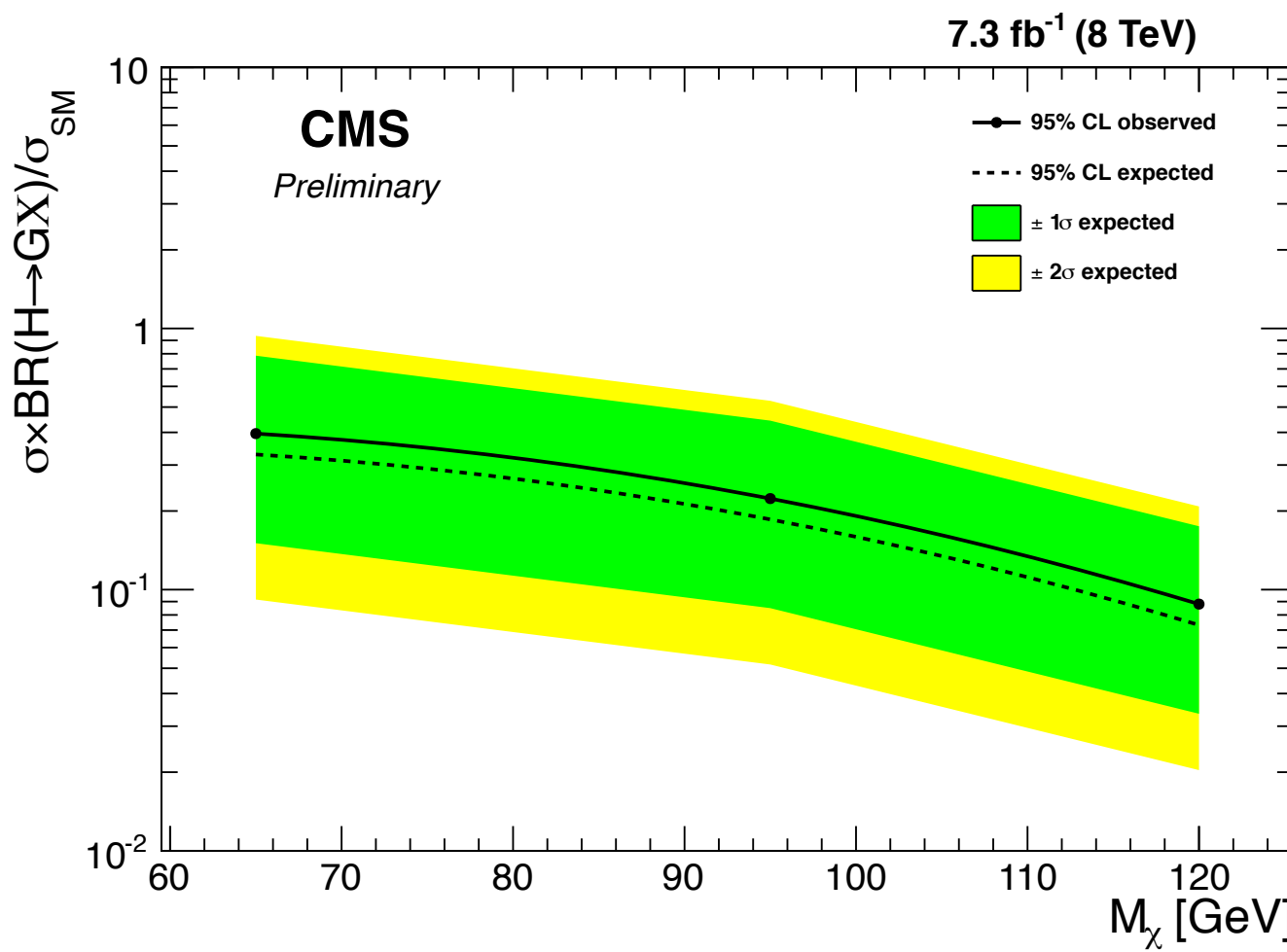
After full selection, $W \rightarrow e\nu$
 (with electron faking a photon) is the **analysis largest background but with sub-leading uncertainty**

Process	Estimate
$\gamma + \text{jets}$	179 ± 28
$\text{jet} \rightarrow \gamma$	269 ± 94
$e \rightarrow \gamma$	355 ± 28
$W(\rightarrow \ell\nu) + \gamma$	154 ± 15
$Z(\rightarrow \nu\bar{\nu}) + \gamma$	182 ± 13
Other	91 ± 10
Total background	1232 ± 188
Data	1296
$M_{\tilde{\chi}_1^0} = 65 \text{ GeV}$	653.0 ± 77
$M_{\tilde{\chi}_1^0} = 95 \text{ GeV}$	1158.1 ± 137
$M_{\tilde{\chi}_1^0} = 120 \text{ GeV}$	2935.0 ± 349

Signal yields assuming 100% branching ratio

RESULTS

CMS-PAS-HIG-14-024

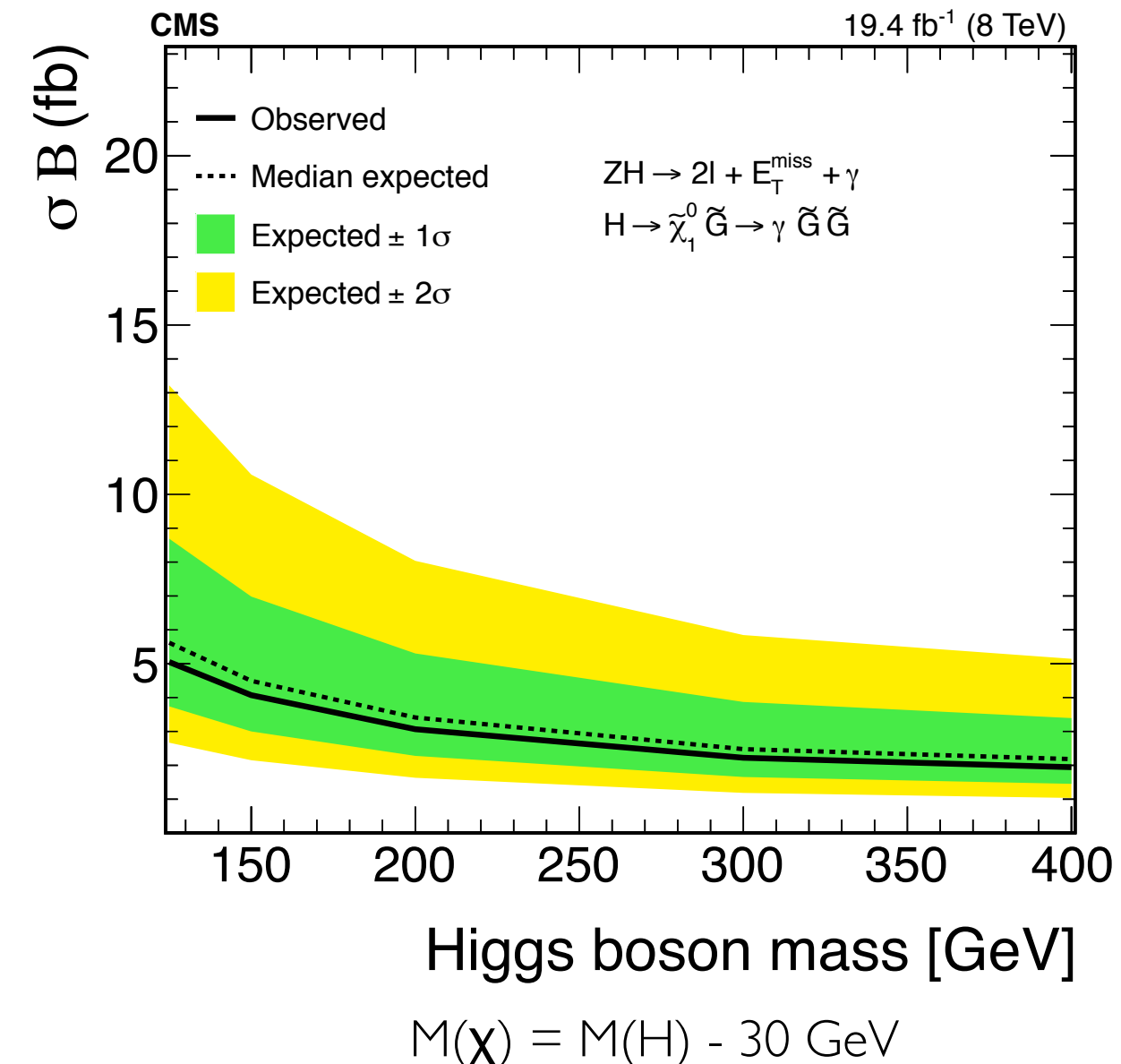
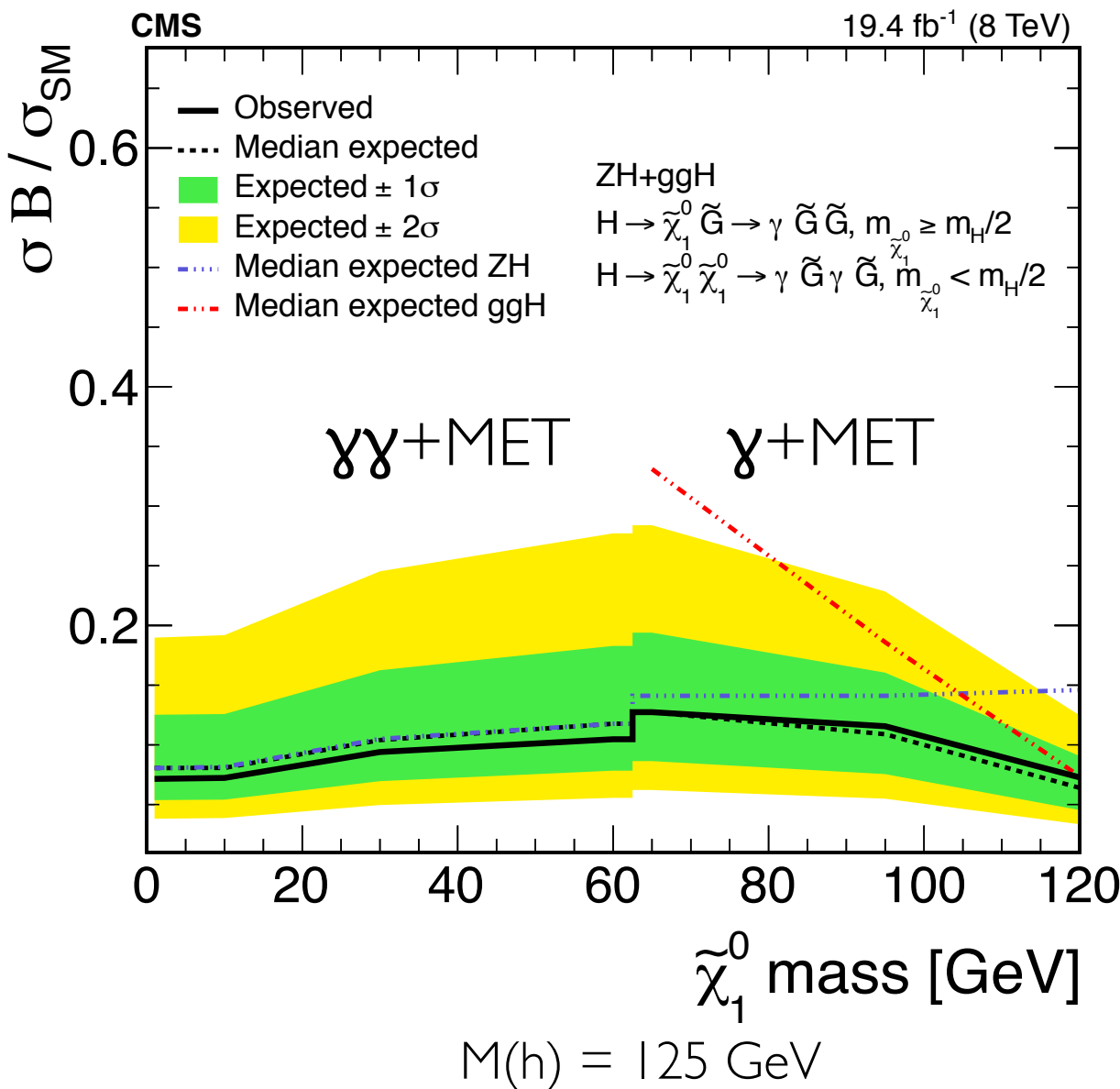


- Limits set assuming prompt decays
- Also set limits on model independent search for low energy monophoton final state

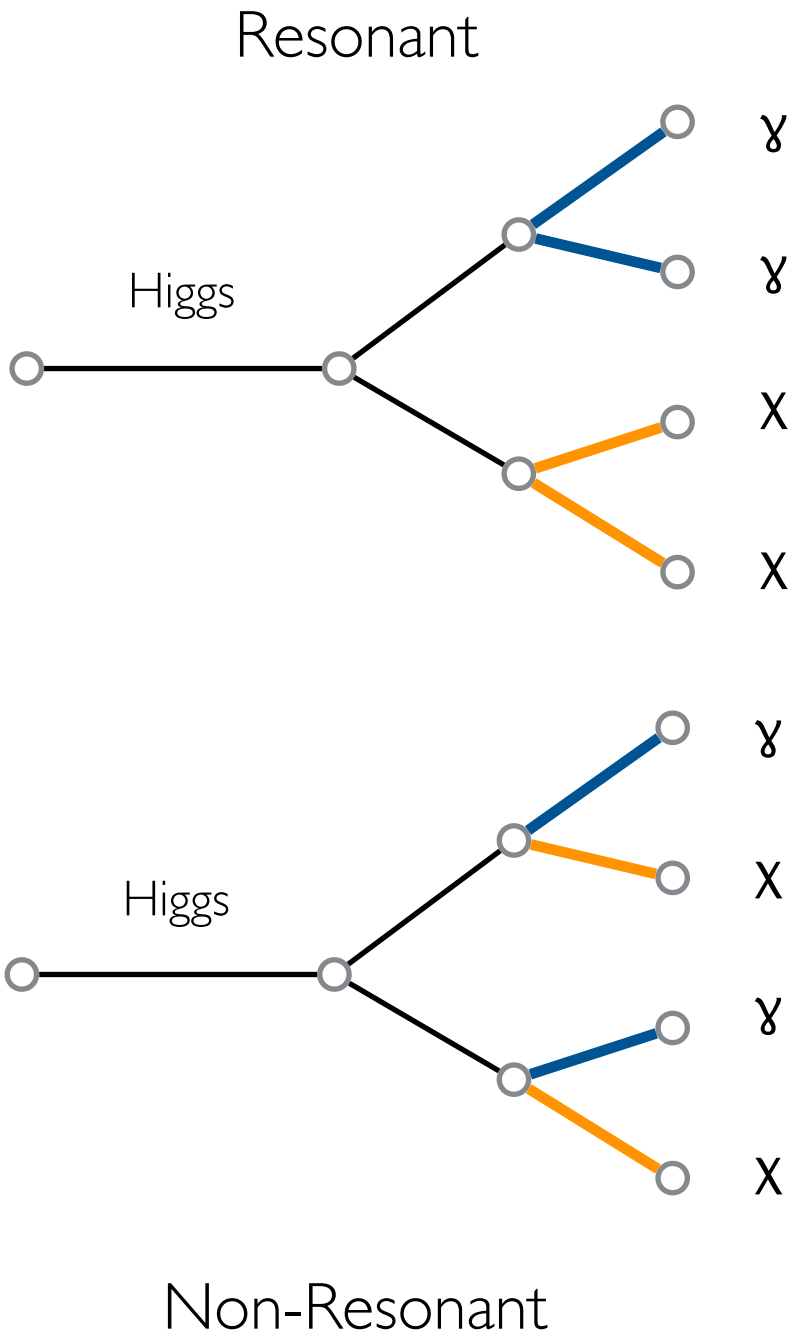
COMBINATION

Phys.Lett. B753 (2016) 363-388

Gluon fusion channel combined with $Z(\rightarrow \ell\ell)H(\rightarrow \gamma + \text{MET})$ production mechanism

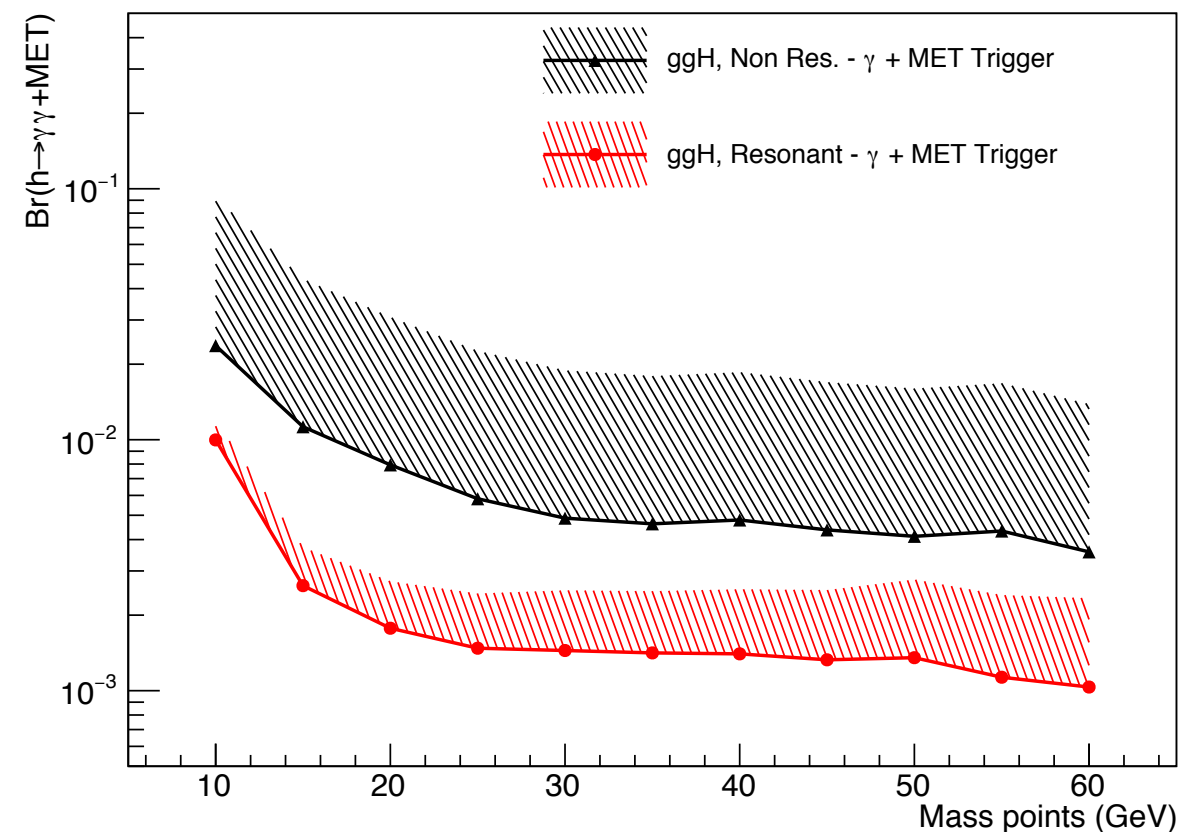


FUTURE STUDIES



- Analysis sensitivity with **100 fb $^{-1}$ at 14 TeV**
Focus on $h \rightarrow \gamma\gamma + \text{MET}$ final state
- Delphes-level study for **Yellow Report 4**
- Branching ratio for 5σ significance < 10% (1%)
for non-resonant (resonant) decay

Br. for 5σ significance + 10% syst. uncertainty



Gluon fusion $\rightarrow H(125) \rightarrow \gamma\gamma + \text{MET}$



A 3D simulation visualization of particle collisions and detector components. The scene features a central yellow starburst-like collision point from which numerous yellow lines radiate outwards, representing particle tracks. A red wireframe rectangular structure is positioned in the upper left, while a blue wireframe structure is on the right. Green and blue dashed lines form a grid-like pattern across the background. In the lower left, there is a cluster of green and blue rectangular blocks.

PROBING THE HIGGS POTENTIAL: $HH \rightarrow bb\gamma\gamma$

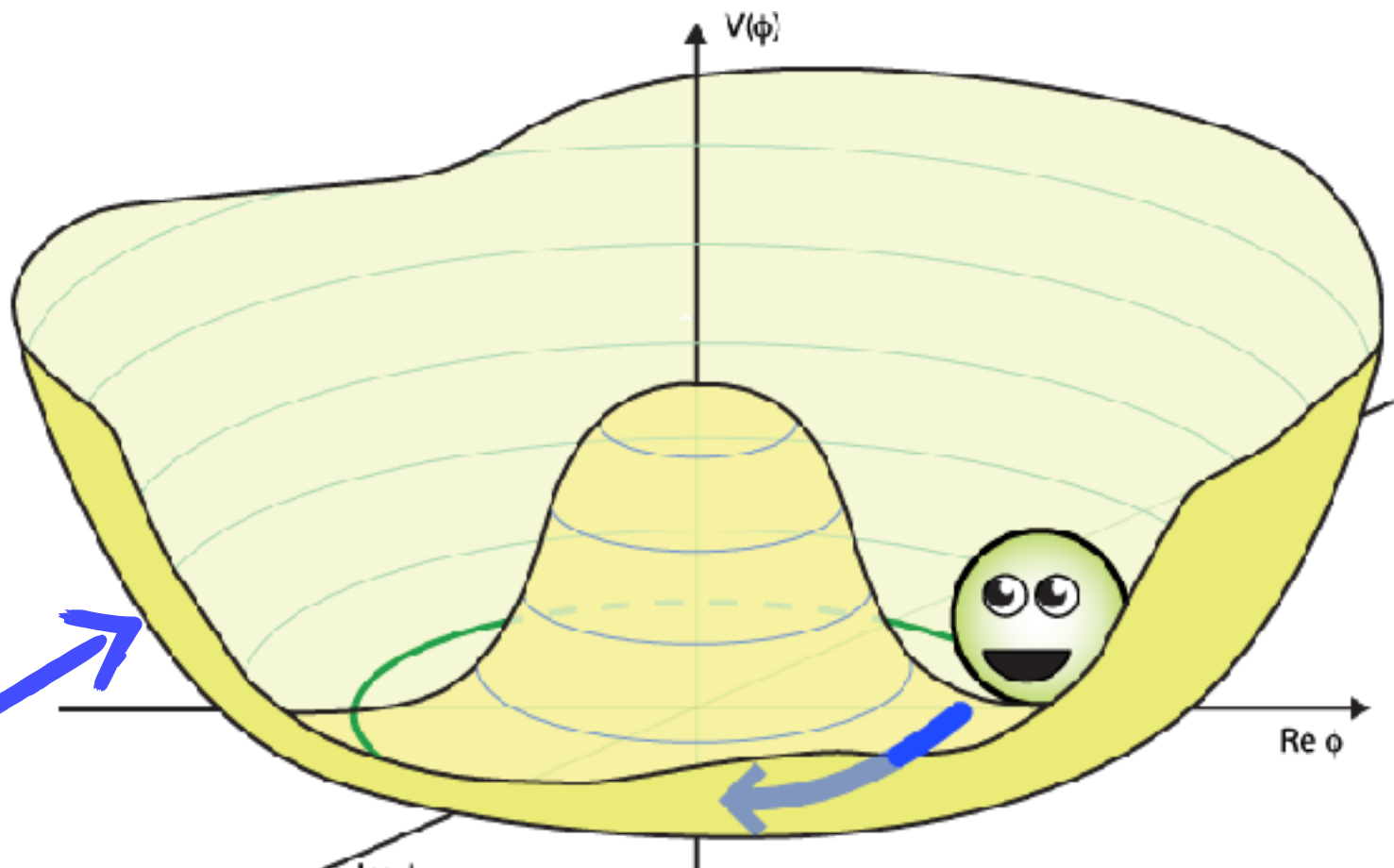
HH AS A SM PROBE

From G. Salam

$$\mathcal{L} = -\frac{1}{4} F_{\mu\nu} F^{\mu\nu} + i \cancel{F} \cancel{D} \cancel{\phi} + Y_i Y_{ij} Y_j \phi + h.c. + |\partial_\mu \phi|^2 - V(\phi)$$

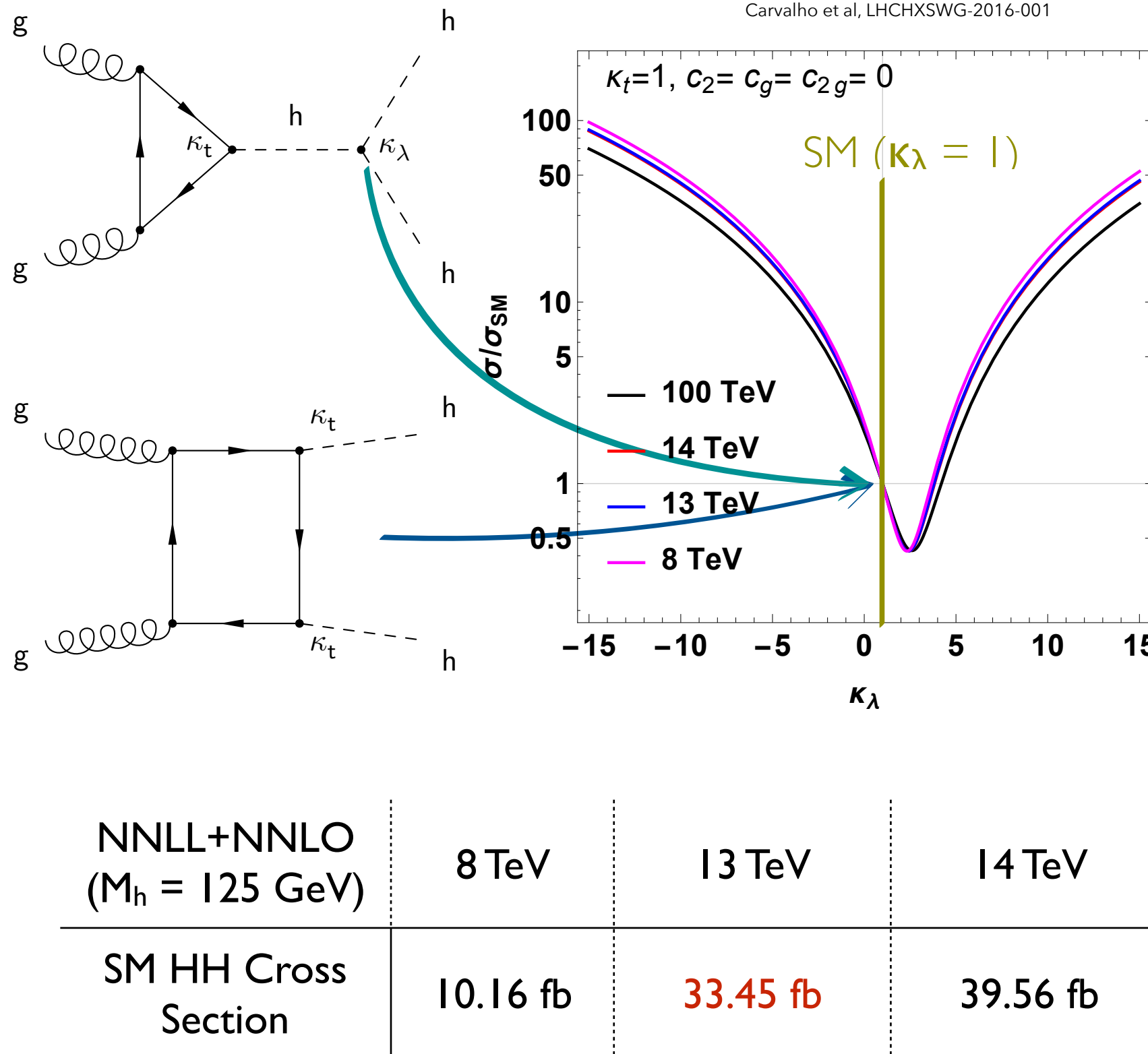
ASSUMPTION KNOWLEDGE

HH: only direct probe to Higgs Self-Coupling!



Higgs Mass Higgs Self-Coupling

SM HH PRODUCTION



Destructive interference between HH diagrams almost maximal for SM

Not expected to be sensitive to SM HH @ LHC

But:

(1) BSM can increase $\sigma(\text{HH})$ [$\kappa_\lambda = 10 \rightarrow \sigma_{\text{BSM}} > 10 \times \sigma_{\text{SM}}$]

(2) Important to test the reach of current analysis for projecting HL-LHC sensitivity

NNLL+NNLO
($M_h = 125 \text{ GeV}$)

8 TeV

13 TeV

14 TeV

SM HH Cross Section

10.16 fb

33.45 fb

39.56 fb

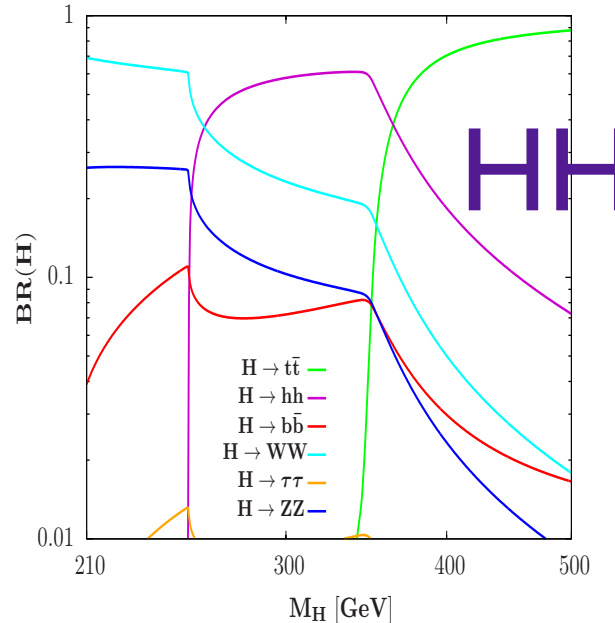
LHCHXSWG YR4

HH RESONANT

Many different BSM models predict HH resonances Experimental solution:
model independent results on narrow width resonances

Low $\tan\beta$ MSSM

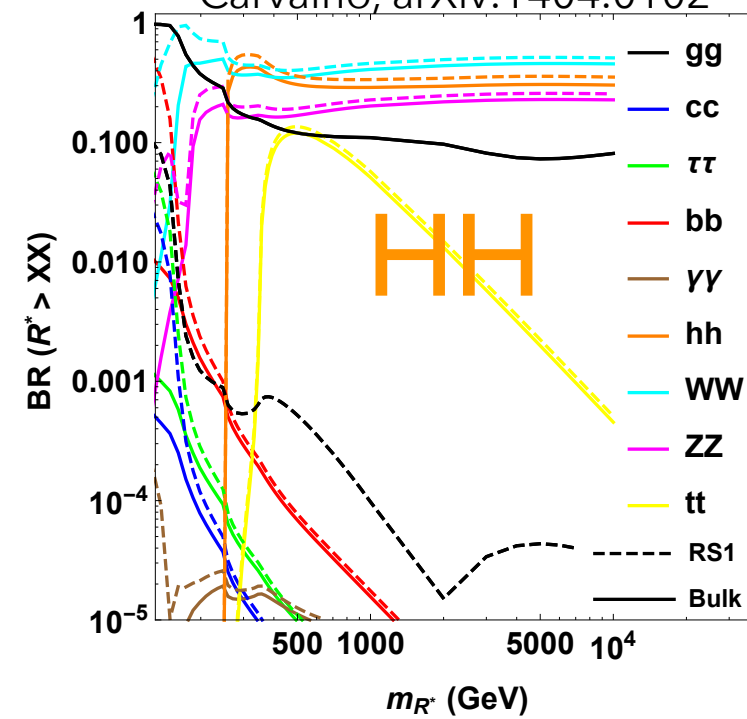
Djouadi & Quevillon, arXiv:1304.1787



Benchmark model
Radion (spin-0), and Graviton (spin-2)

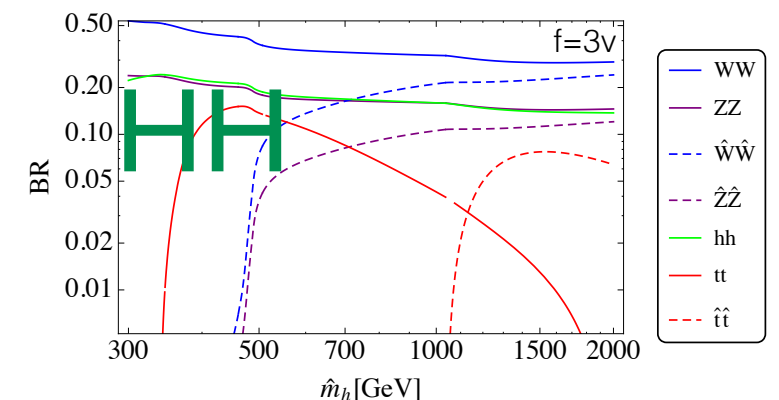
Warped Extra Dimensions

Carvalho, arXiv:1404.0102



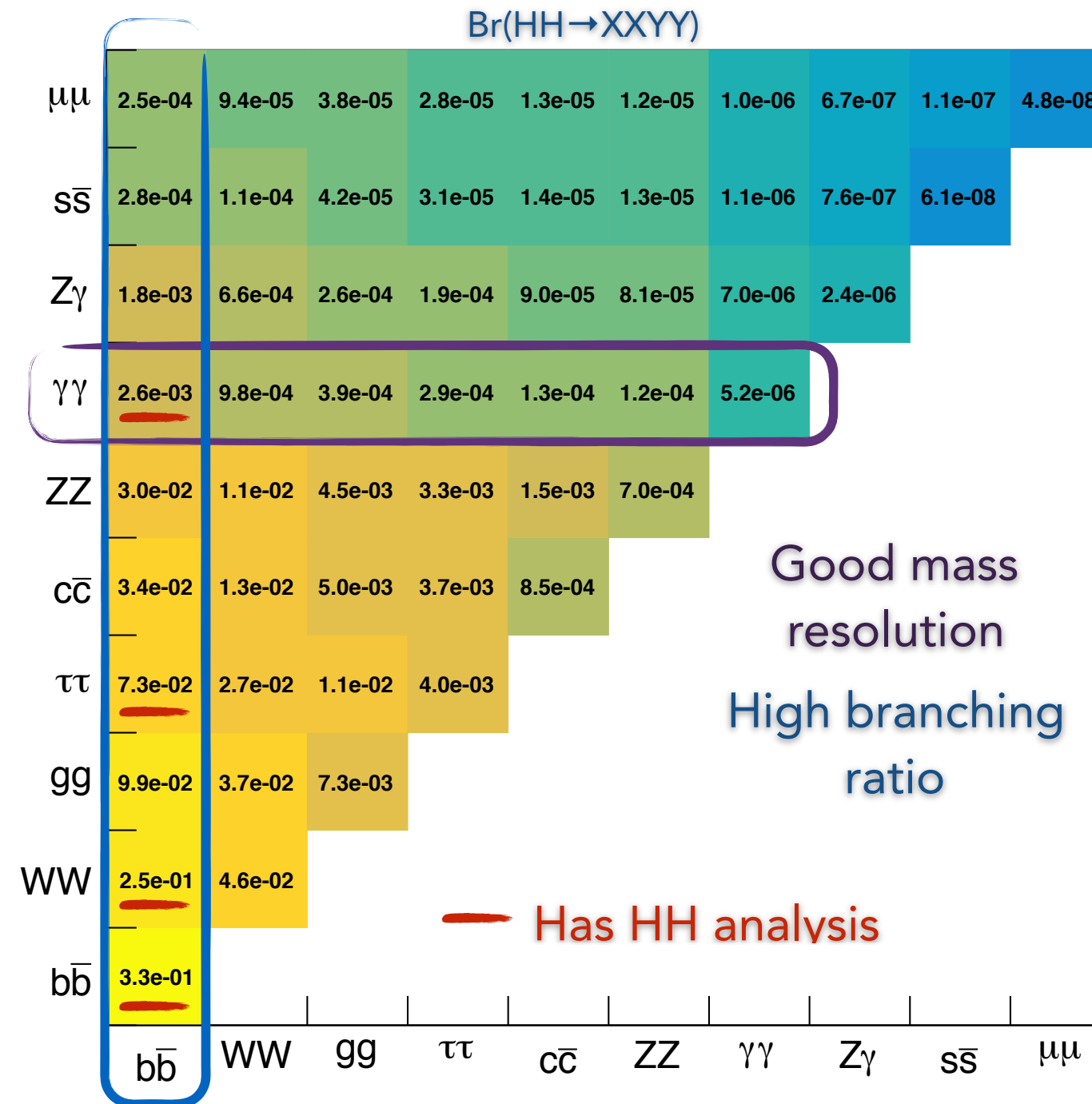
Neutral Naturalness

N. Craig's talk on HCouplings



FINAL STATE

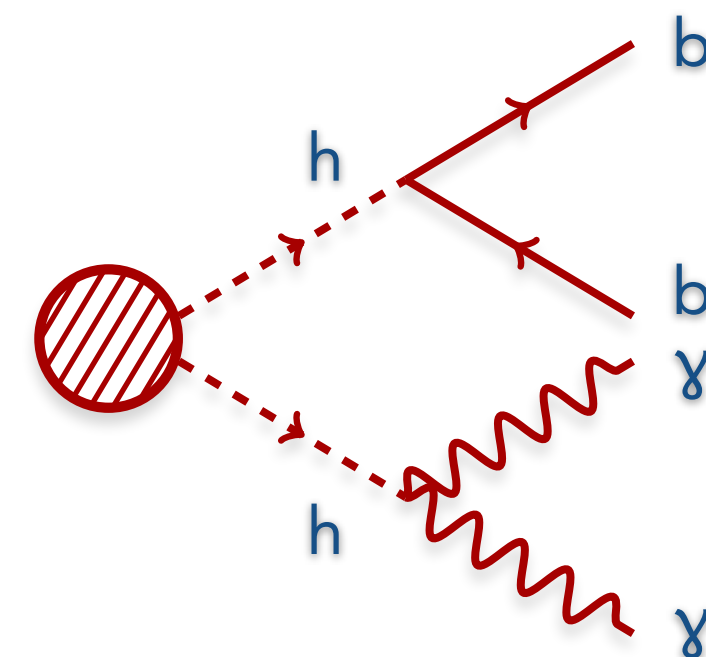
$\text{HH} \rightarrow b\bar{b}\gamma\gamma$ [Br(HH $\rightarrow b\bar{b}\gamma\gamma$) = 0.26%]: Low background + All objects are reconstructed



$H \rightarrow b\bar{b}$: High branching ratio + b-tagging information provides good S/ \sqrt{B} handle

$H \rightarrow \gamma\gamma$: High trigger and selection efficiency + Good energy resolution

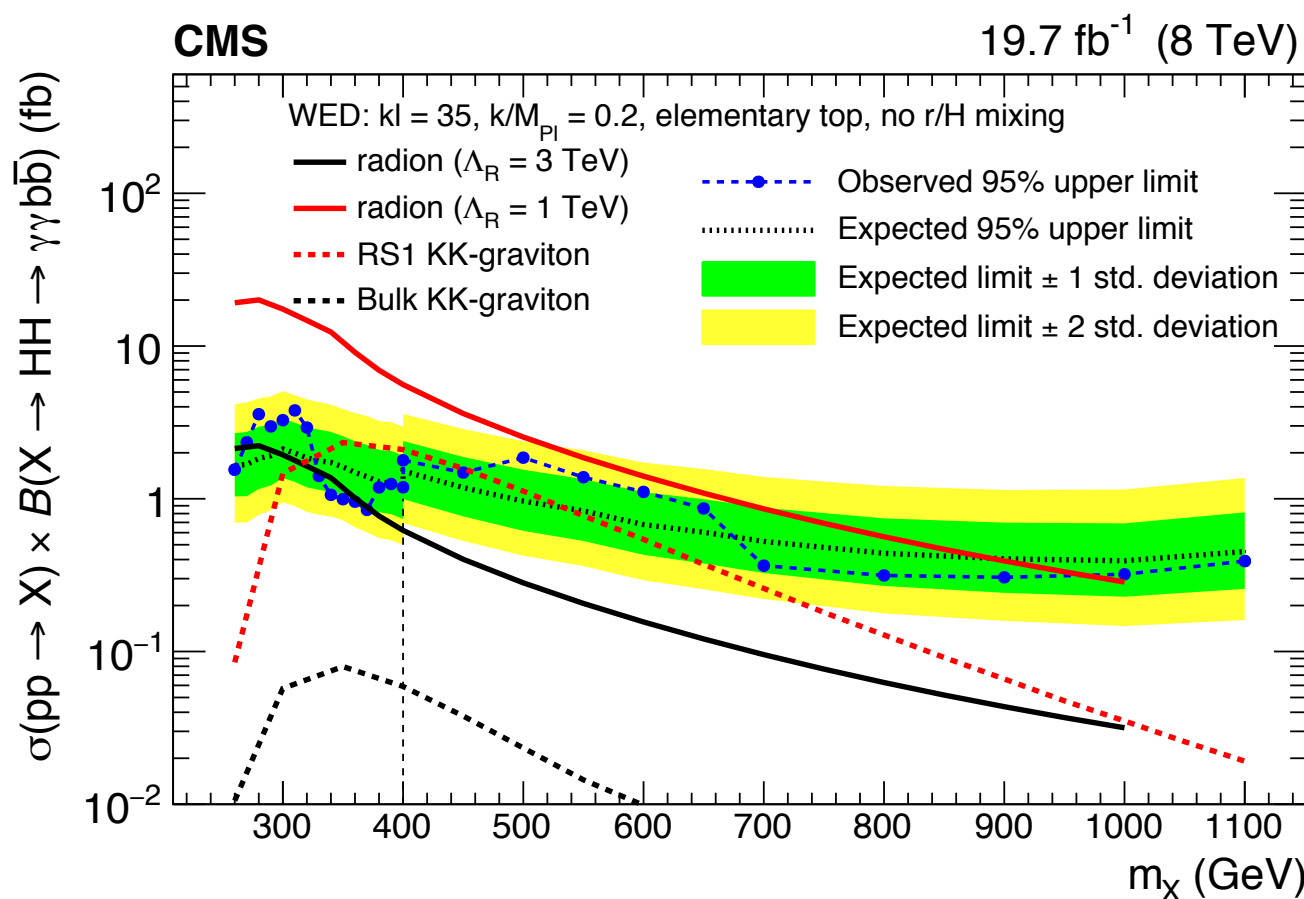
Expected to be the most sensitive channel to non-resonant SM HH production



PREVIOUS RESULTS

Run I

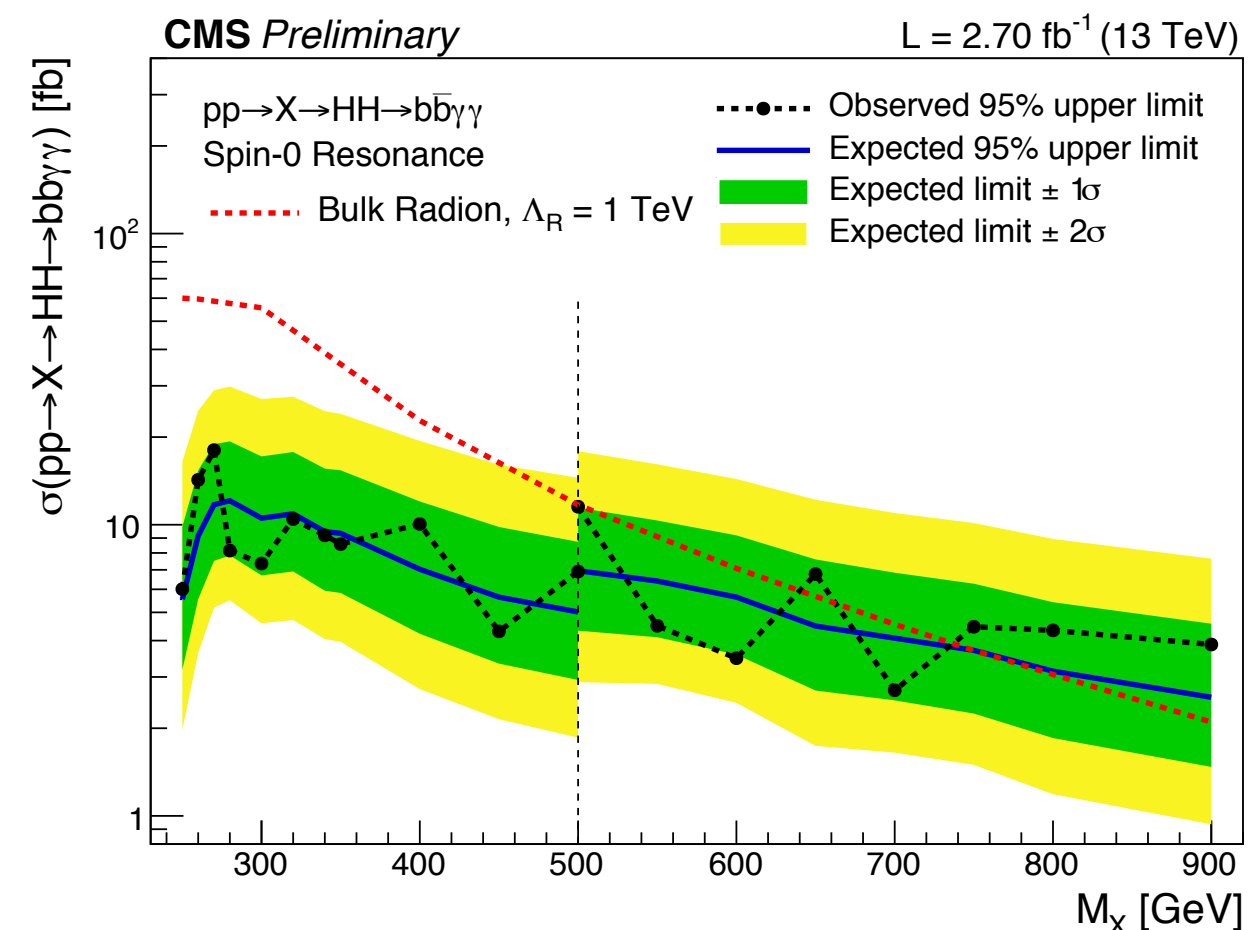
- Limit on SM-like non-resonant production:
 - $\sim 74 \times \text{SM}$ (62) observed (expected)



Phys. Rev. D 94 (2016) 052012

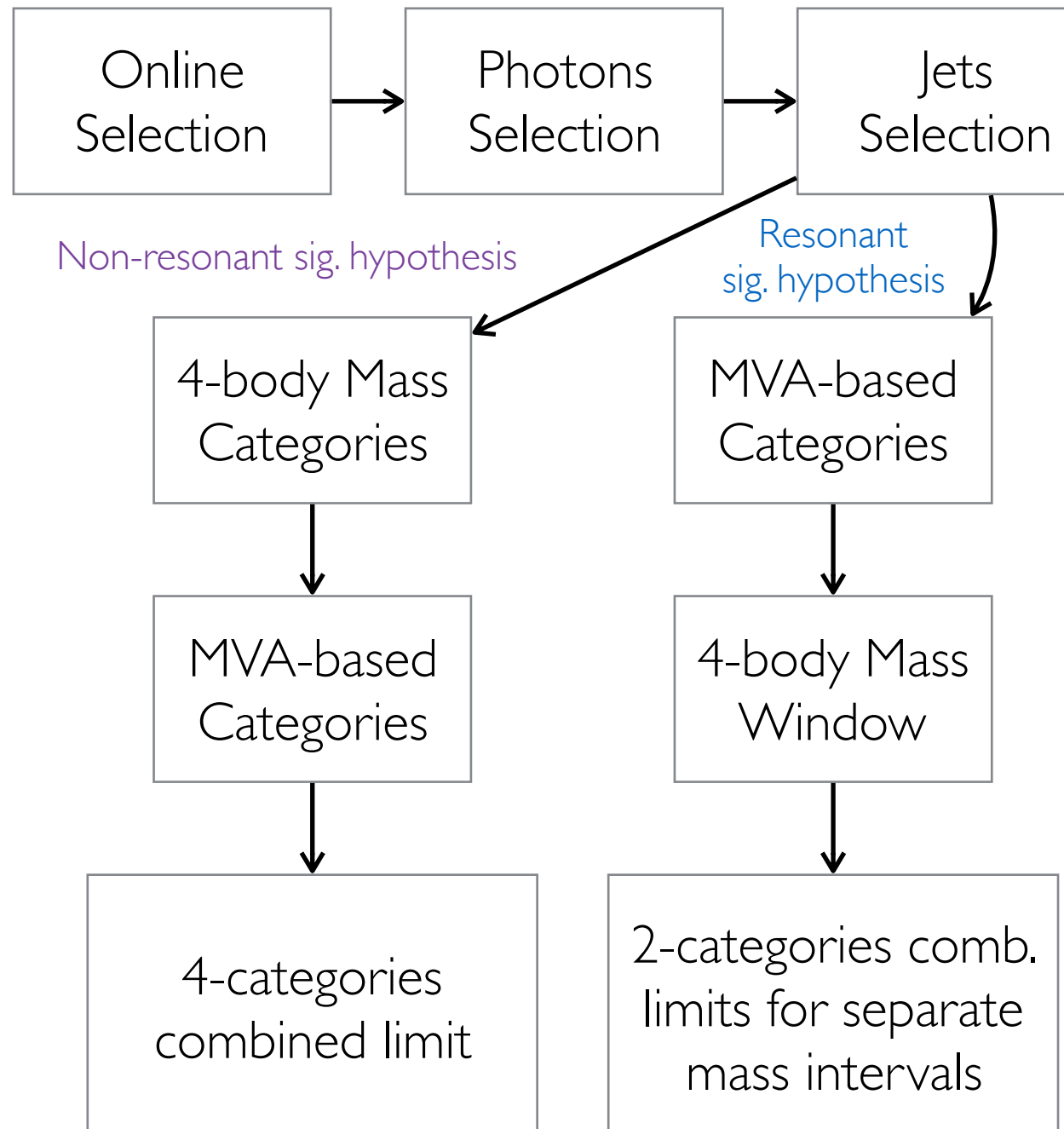
Run 2 (2015 data)

- Limit on SM-like non-resonant production:
 - $\sim 90 \times \text{SM}$ observed and expected



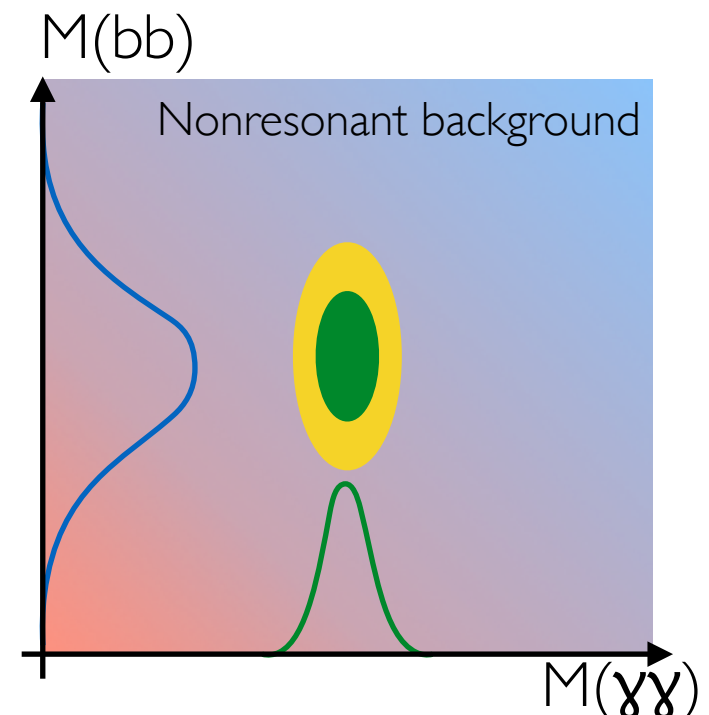
[CMS PAS HIG-16-032](#)

ANALYSIS STRATEGY

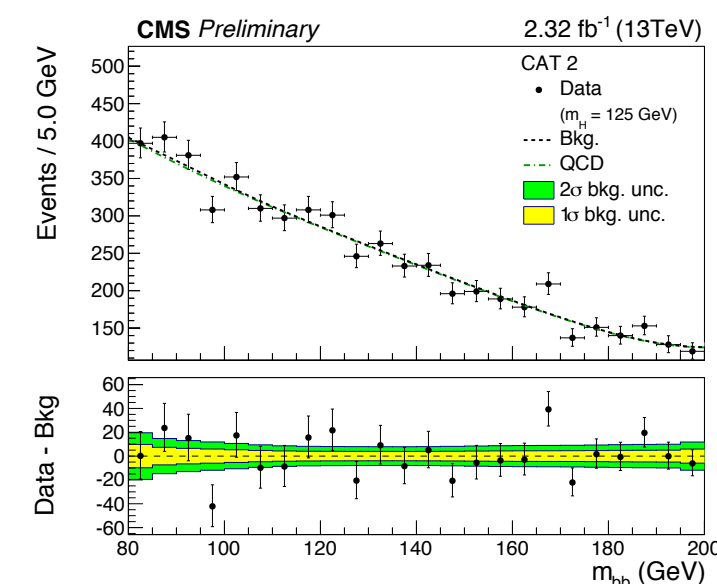
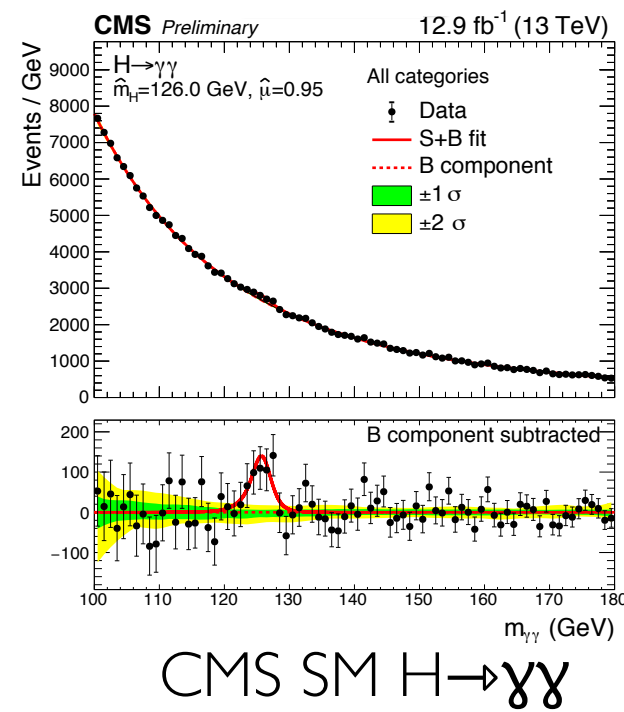


Signal extraction via parametric fit on 2D plane $M(jj):M(\gamma\gamma)$

$M(jj)$ and $M(\gamma\gamma) =$ 1D parametric signal shapes



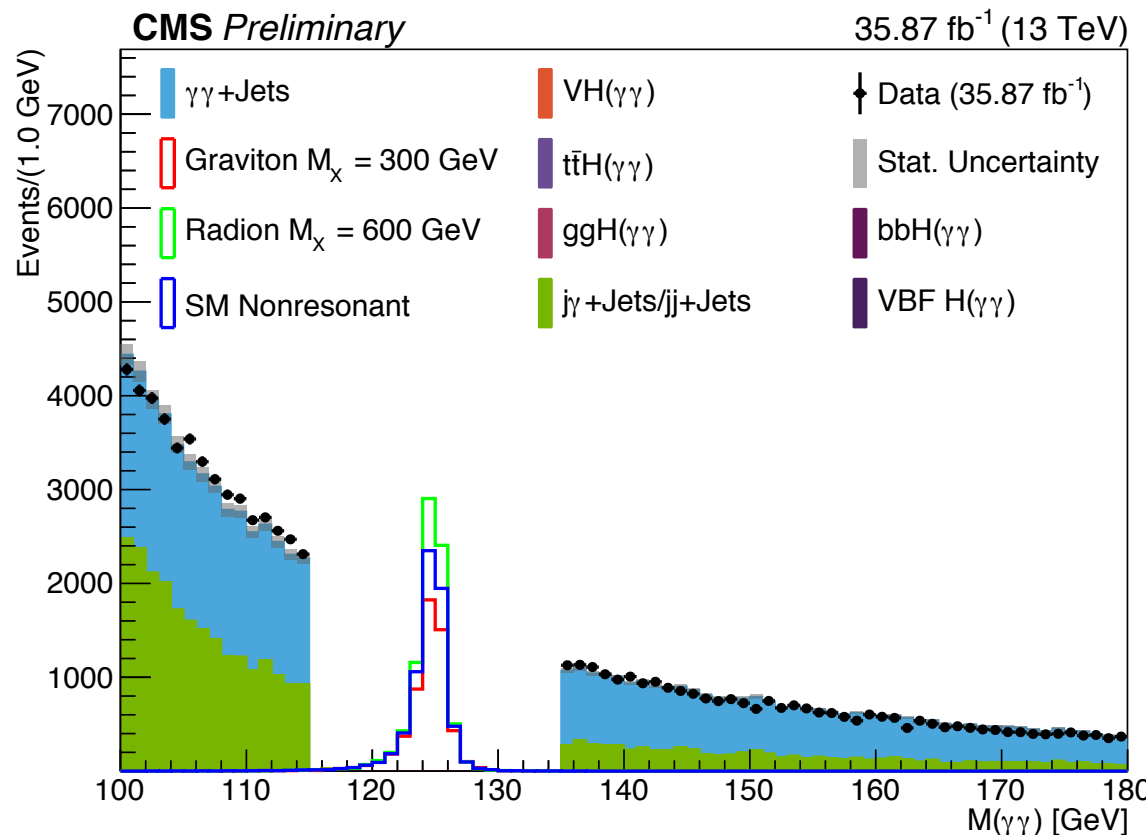
Analysis backgrounds:
non-resonant photons produced via QCD
Single Higgs



PHOTONS & JETS

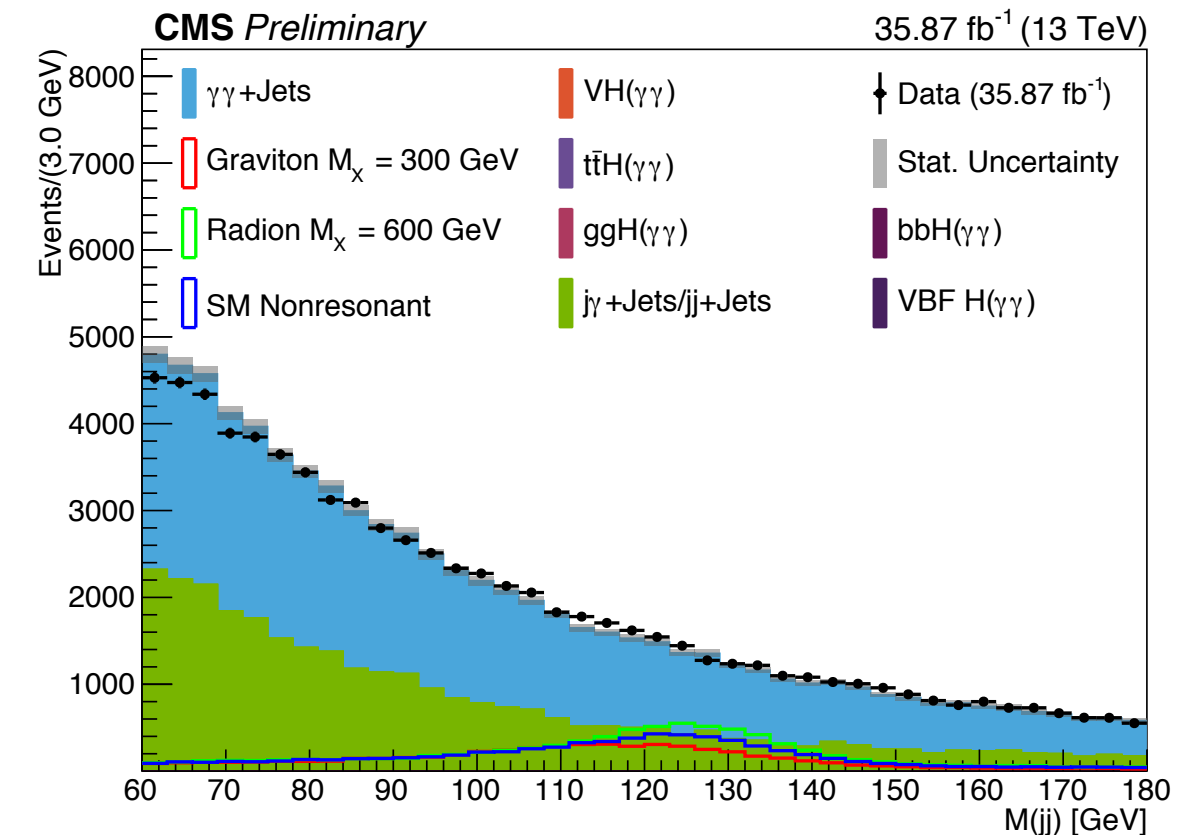
Photons selection

- Online and offline kinematic selection based on high quality $\gamma\gamma$ candidates
- MVA-based photon quality criteria applied with a $\sim 90\%$ signal efficiency
- Vertex chosen based $\gamma\gamma$ candidate-vertex matching MVA ($\sim 100\%$ signal efficient)



Jets selection

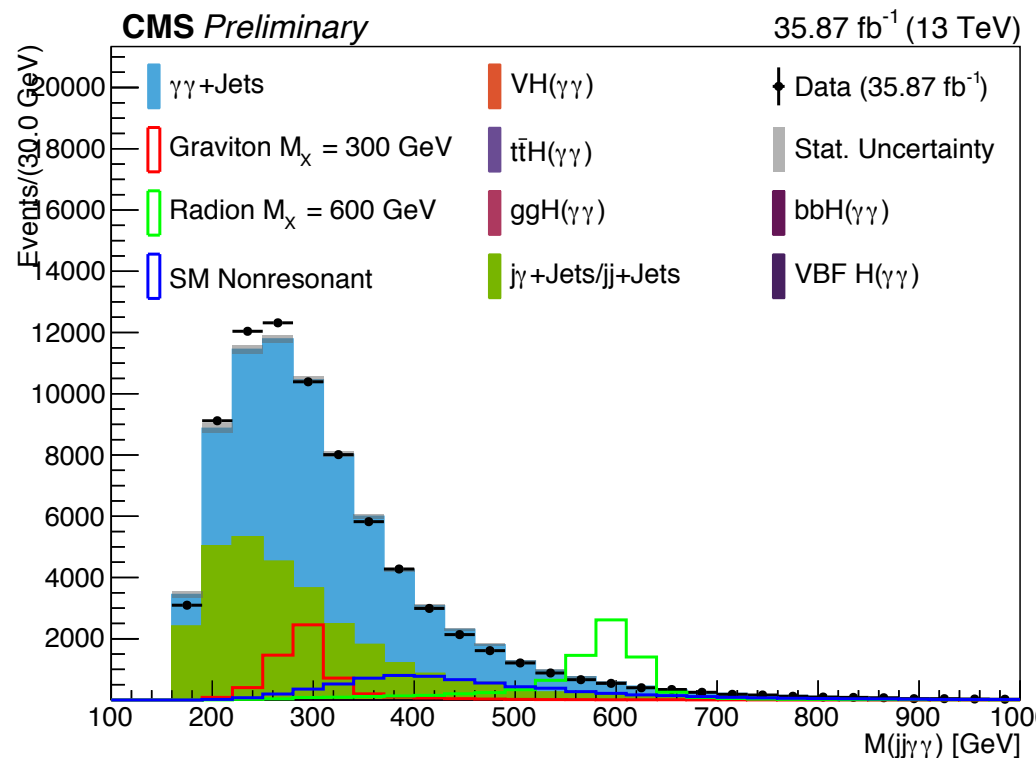
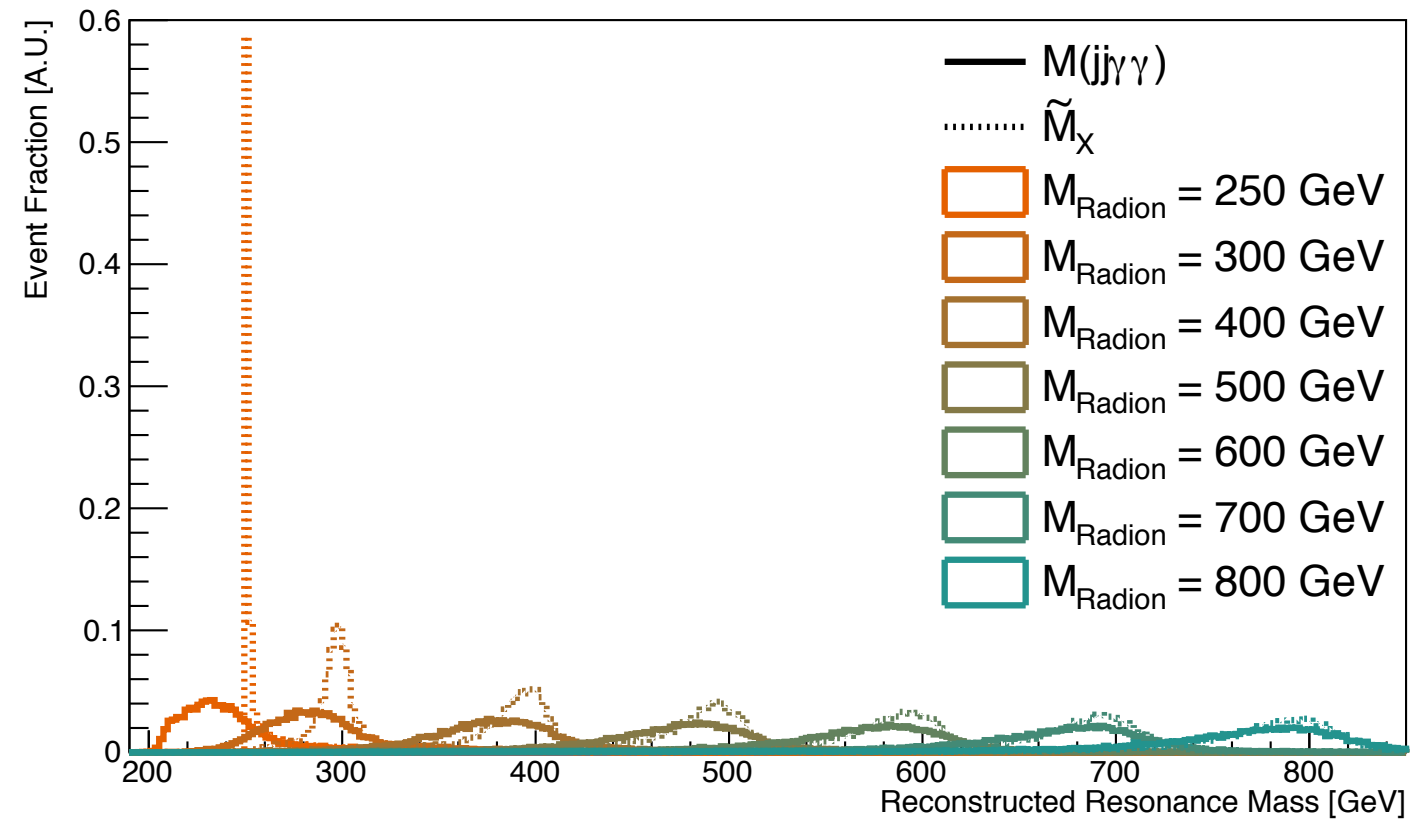
- $\Delta R(\text{jet}, \gamma\text{'s}) > 0.4, p_T(\text{jets}) > 25 \text{ GeV}, |\eta(\text{jets})| < 2.4$
- $60 < M(jj) < 180 \text{ GeV}$
- jj candidate: two jets with highest b-tagging score



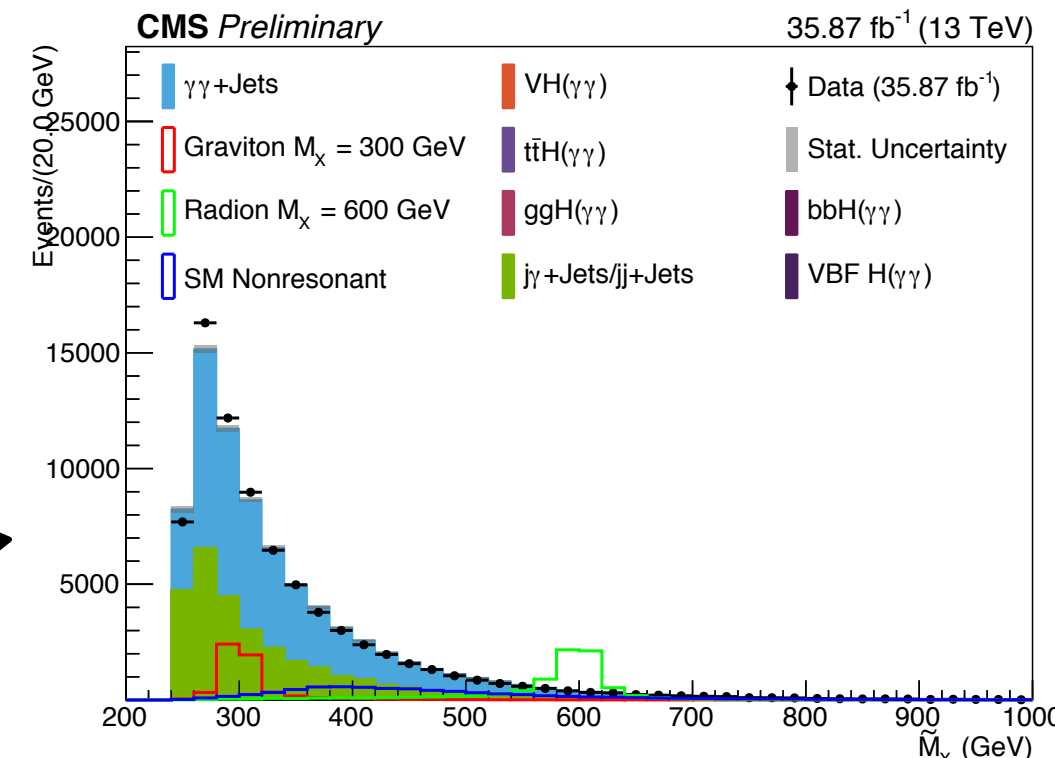
EFFECTIVE MASS

$$\tilde{M}_x = M(jj\gamma\gamma) - M(jj) - M(\gamma\gamma) + 250$$

- Minimizes dependency on photon and jet energy scale while avoiding kinematic biases when selecting mass windows
- Significantly reduces 4-body invariant mass width
- Resonant mass window:
 - Interval in \tilde{M}_x that covers 60% of signal shape

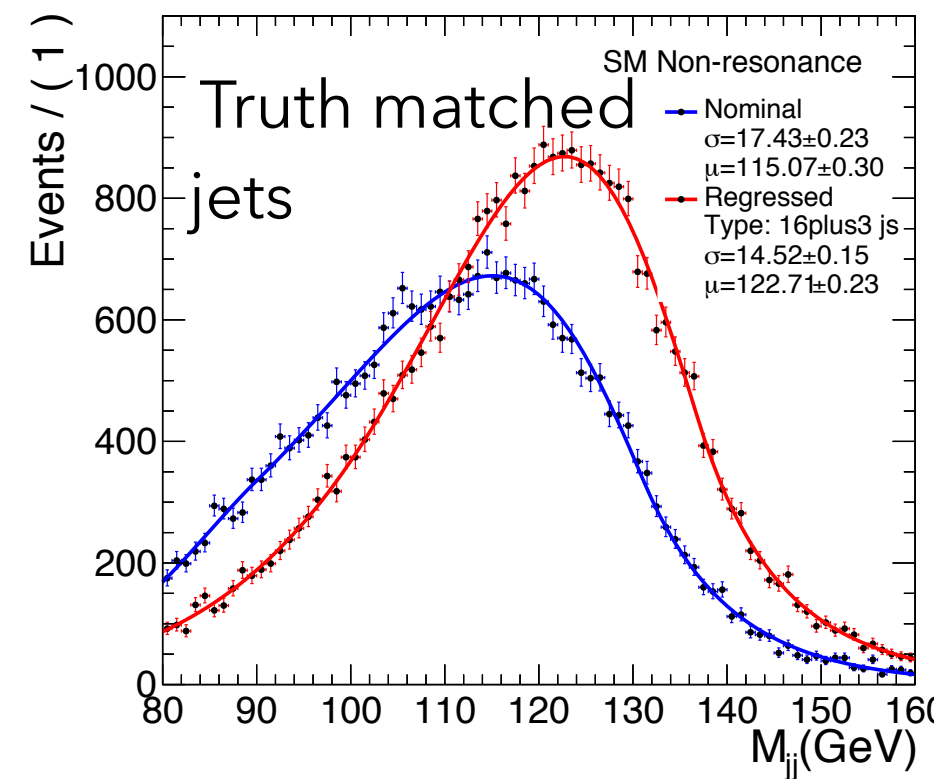


\tilde{M}_x improves the S/B of the mass window selection without shaping the background

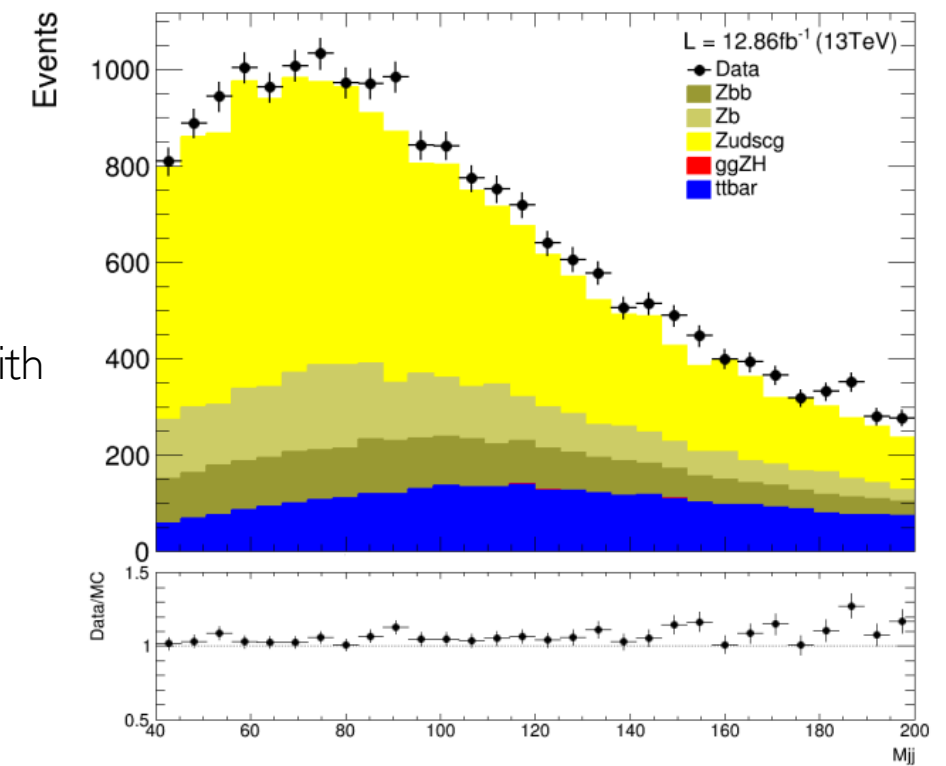


FLAVOR-SPECIFIC JET ENERGY CORRECTIONS

- CMS does not provide flavor-specific jet corrections
- But we know that b-jets have specific features that we can exploit to perform these corrections
- **Procedure: regression** obtained via a boosted regression tree, and trained specifically for our analysis
- **Improvement on $M(jj)$ width of up to 25%,** depending on kinematic region
- Method validated on control sample of $Z(l\bar{l})bb$ events

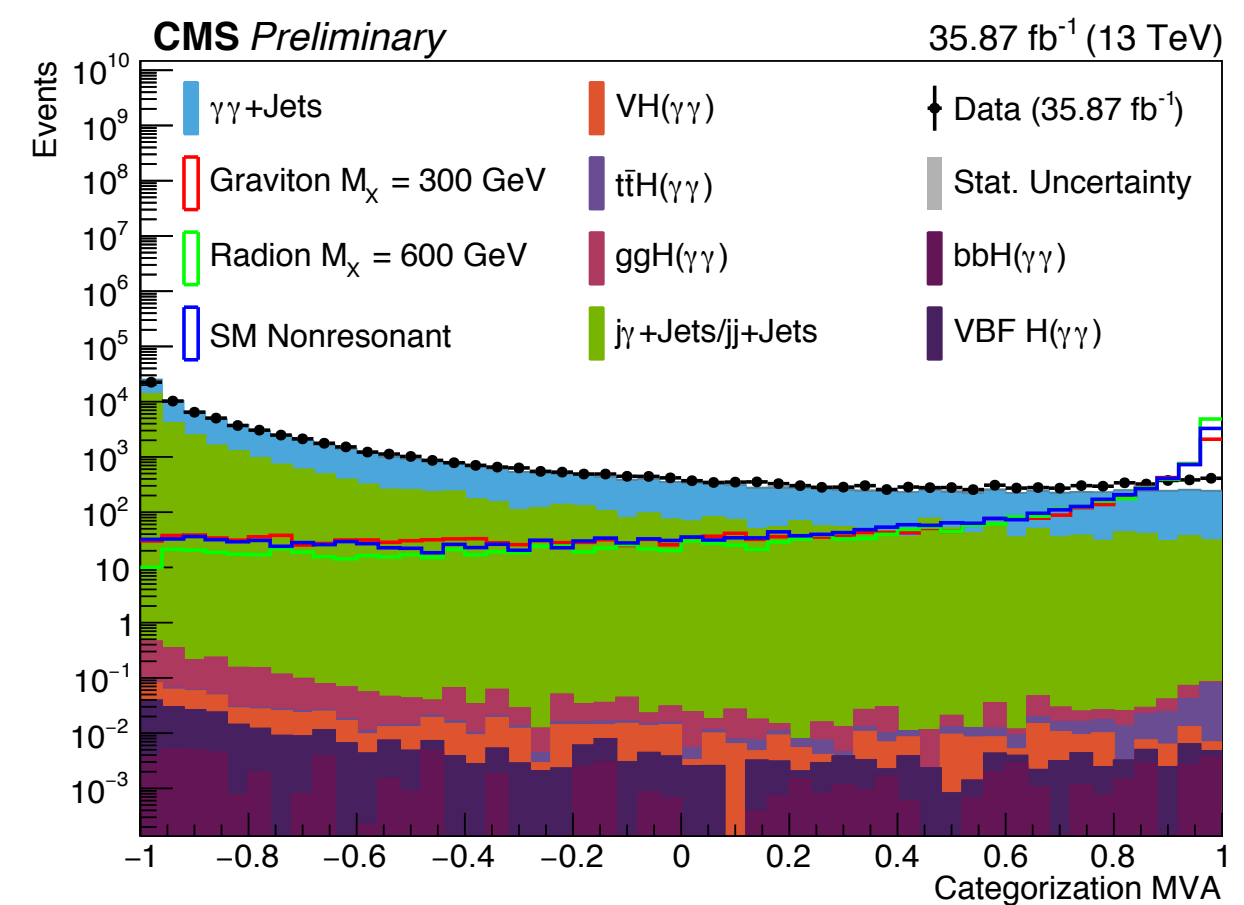
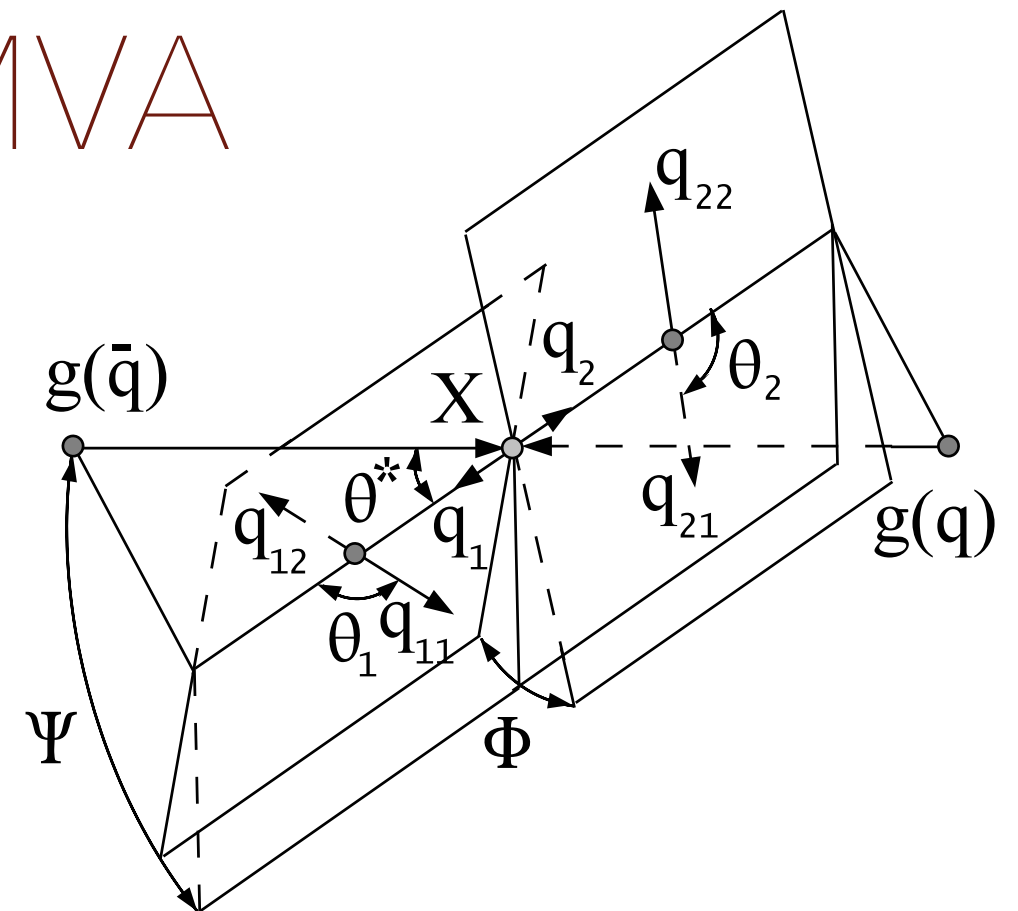


$M(jj)$ resolution improved by $\sim 18\%$
 $M(jj)$ scale now closer to 125 GeV (signal hypothesis)

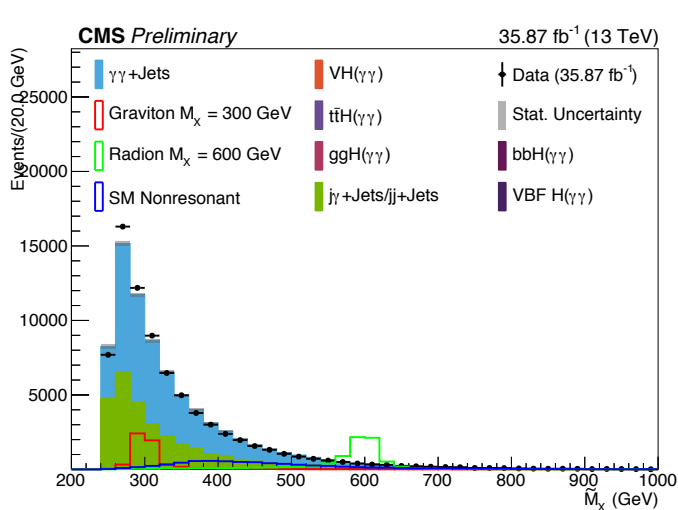
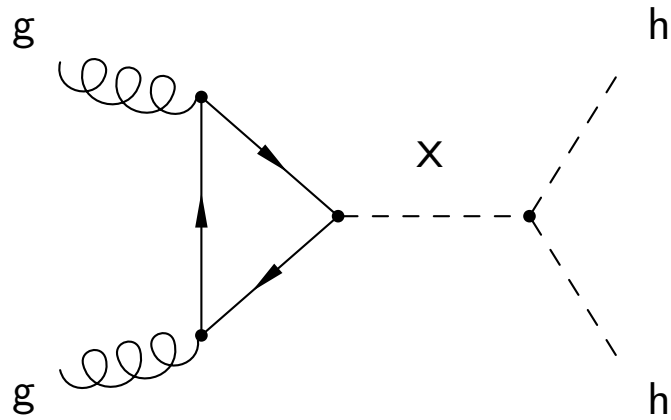
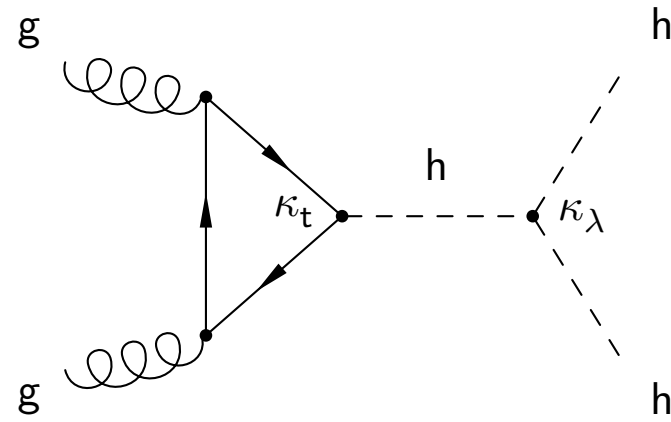


CATEGORIZATION MVA

- Different bits of information can be combined for a better performing categorization procedure
- In this analysis, we take advantage of the **jets b-tagging scores and the helicity angles** from the four reconstructed final state particles
- A boosted decision tree is used to combine all discriminating variables
- Training is performed for resonant and non-resonant signals
- Two categories are defined based on BDT output: **Medium Purity and High Purity categories**
- About **15% improvement of SM HH limit** with respect to simple b-tagging-only categorization



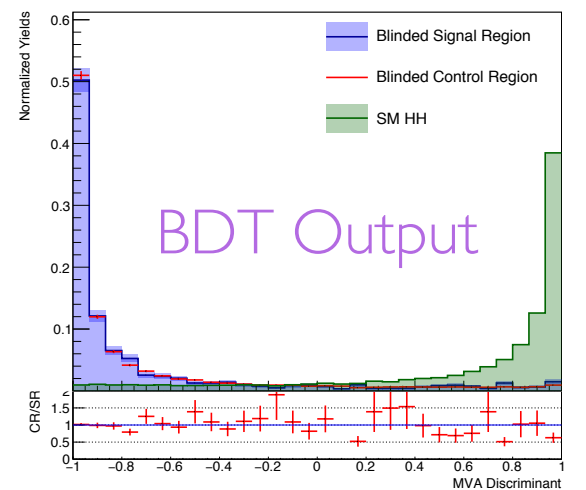
STRATEGIES SUMMARY



\tilde{M}_x Usage

Two categories defined:
 $\tilde{M}_x < 350 \text{ GeV}$ and
 $\tilde{M}_x > 350 \text{ GeV}$

Mass window requirement dependent on resonance mass hypothesis
 Analysis optimized in two regions: Low mass ($< 500 \text{ GeV}$) and High mass ($> 500 \text{ GeV}$)



Categorization BDT

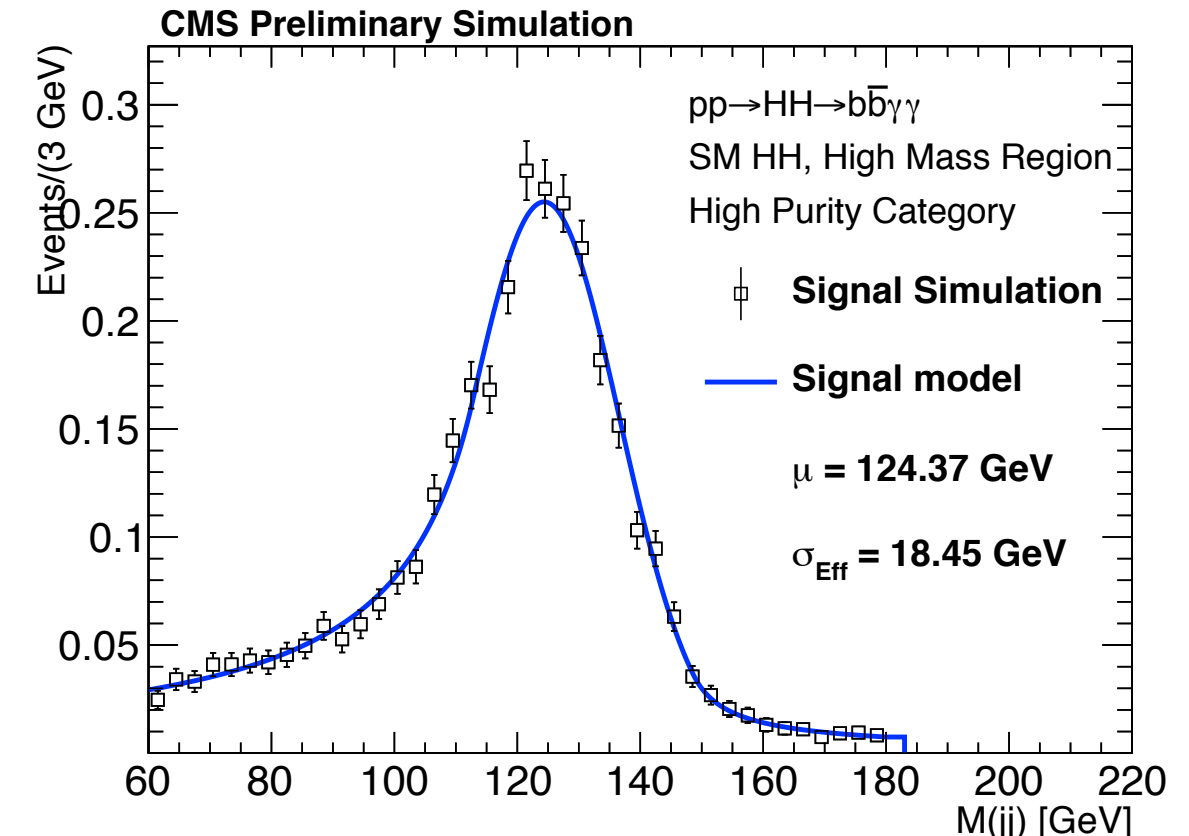
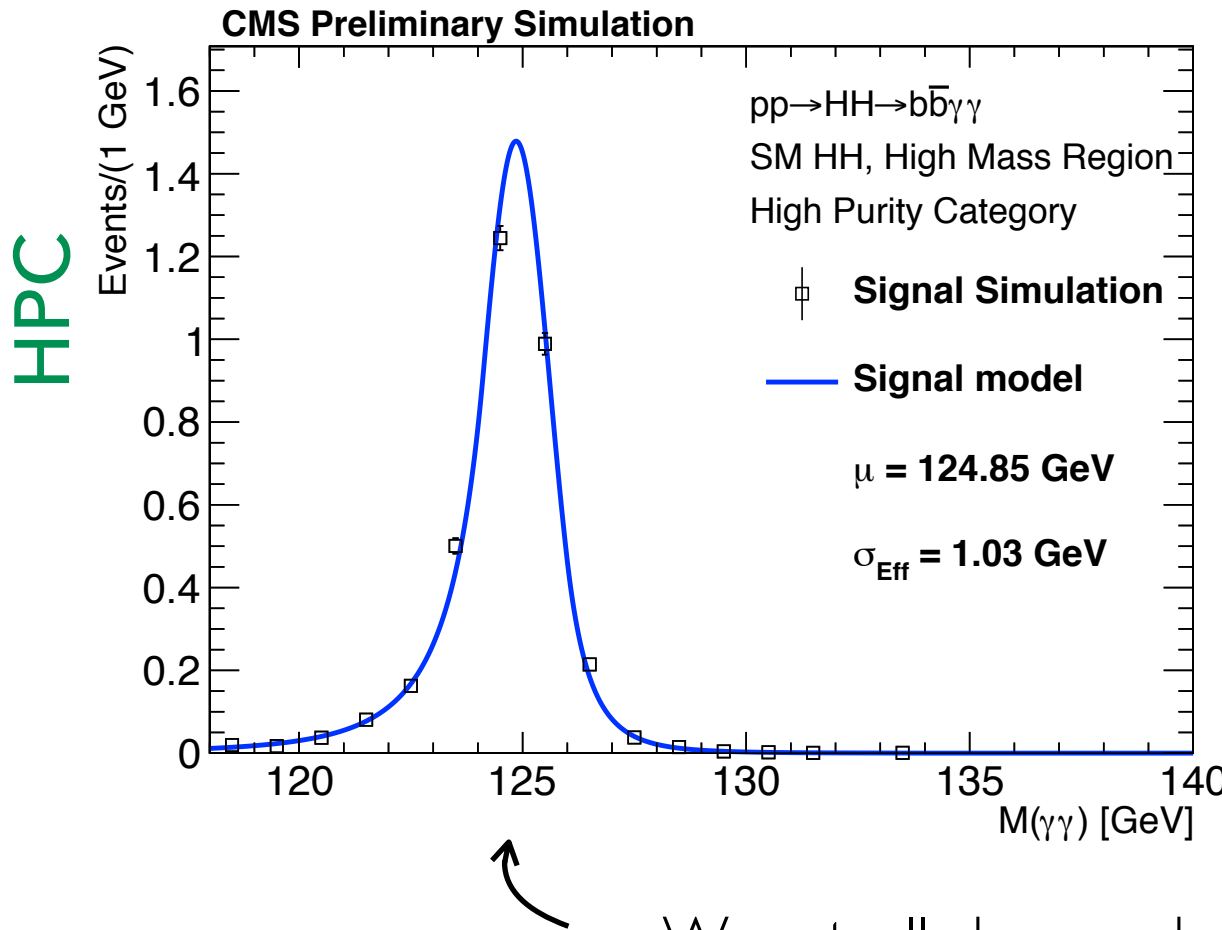
Two categories defined based on BDT output: High Purity and Medium Purity

Two categories defined based on BDT output: High Purity and Medium Purity

THE SIGNAL

Example!

The analysis is a two-dimensional bump search!



We actually know where the bumps should be!

Taking advantage of the good resolution in reconstructing the $M(\gamma\gamma)$ peak

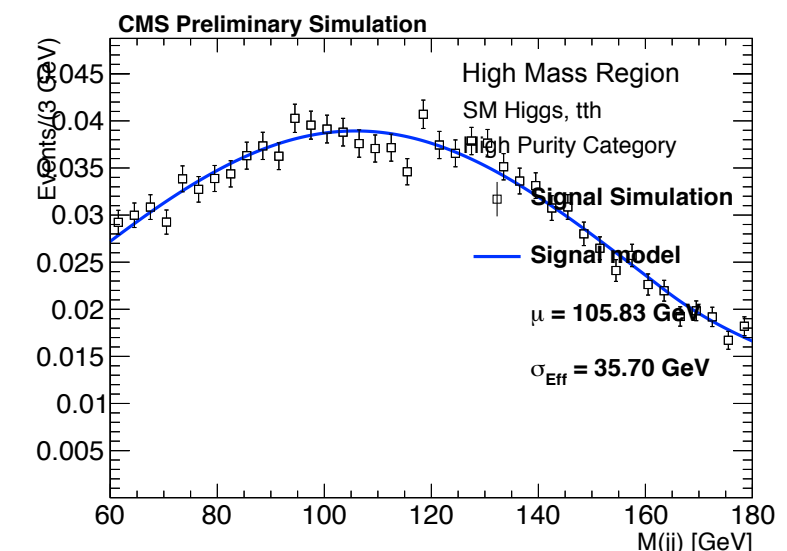
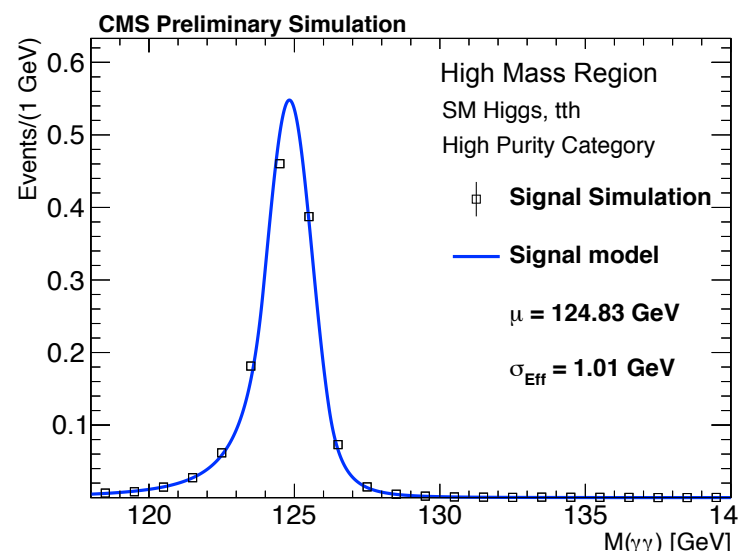
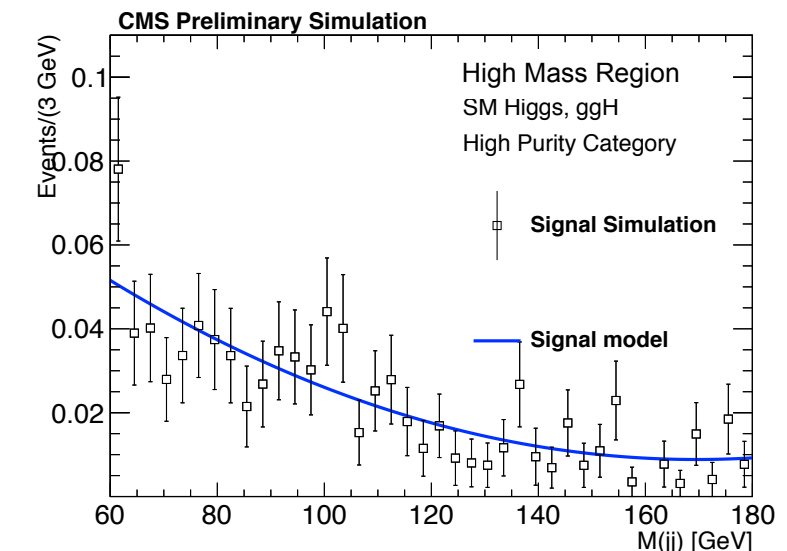
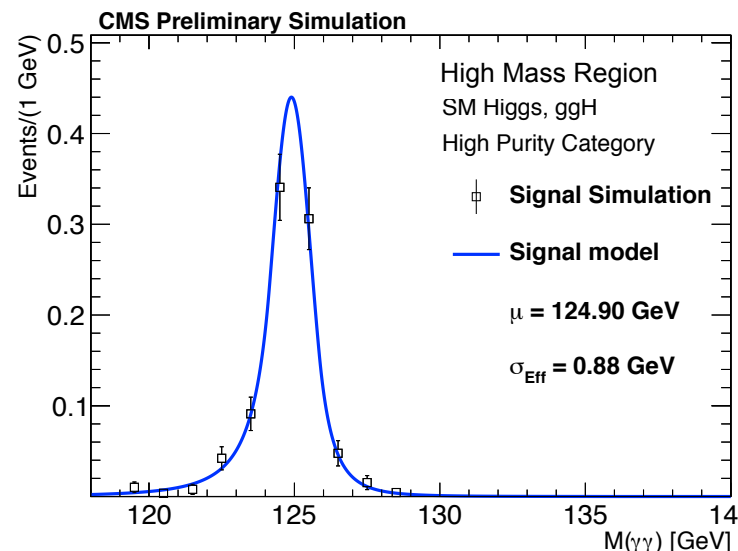
$M(jj)$ fit impact on final result is enhanced by b-jet energy regression procedure

Each 1D observable modeled independently with a parametric form

HIGGS MODELING

Example!

- With the full 2016 dataset, the single Higgs background contamination in the non-resonant search is non-negligible
- The mass window requirement mitigates this contamination on the resonant analysis
- Production mechanisms accounted for are: ggH, VBF, VH, ttH and bbH
- The impact on the final limits is limited by the non-resonant $M(jj)$ shapes



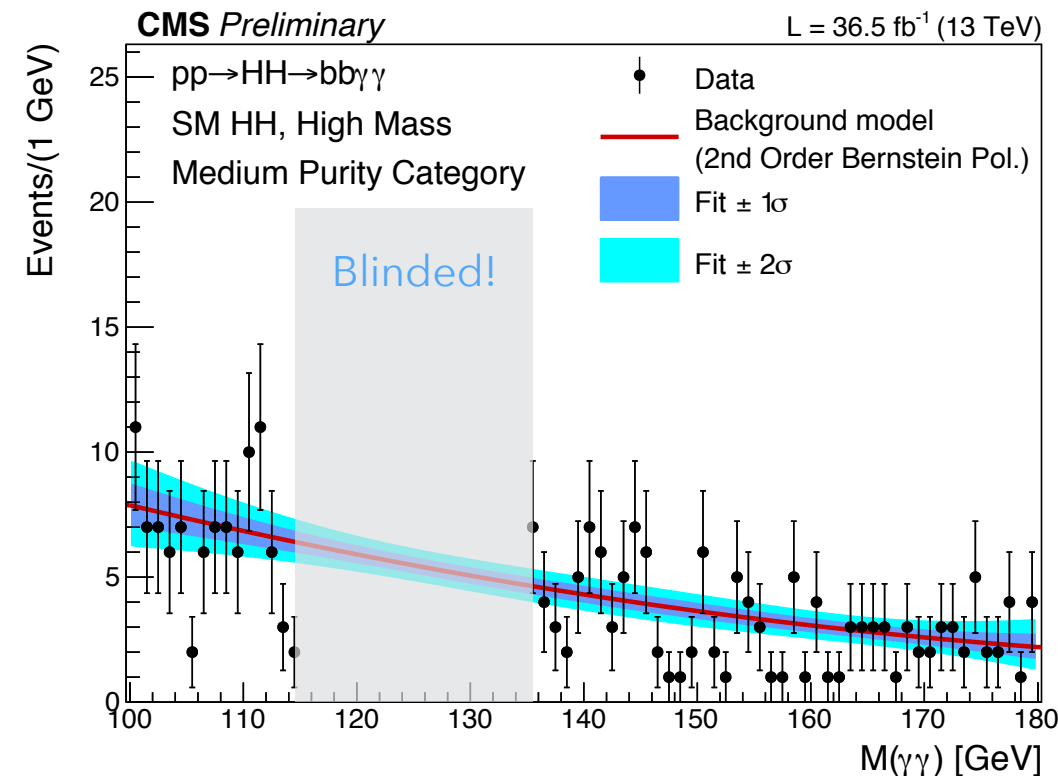
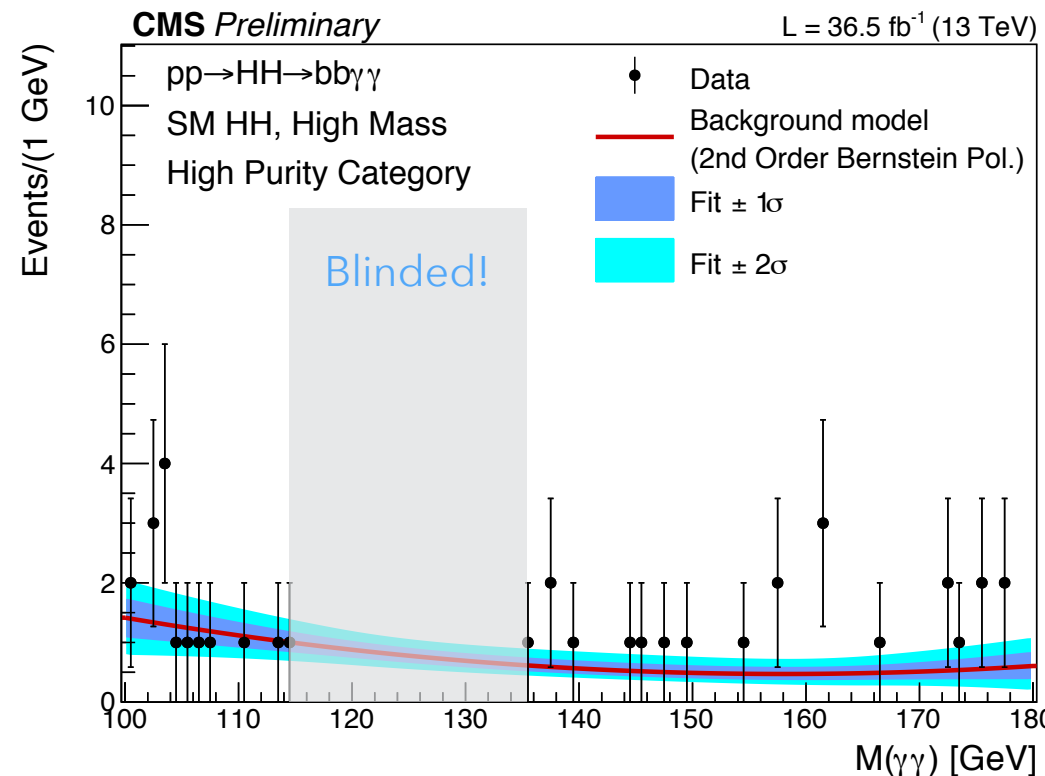
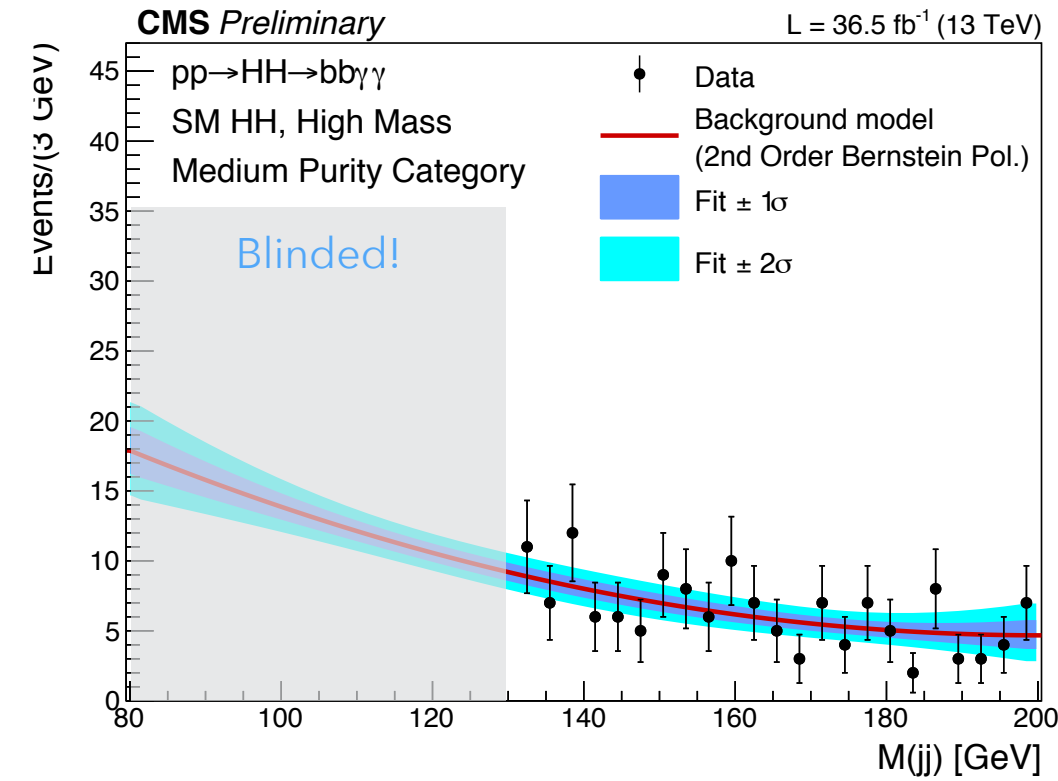
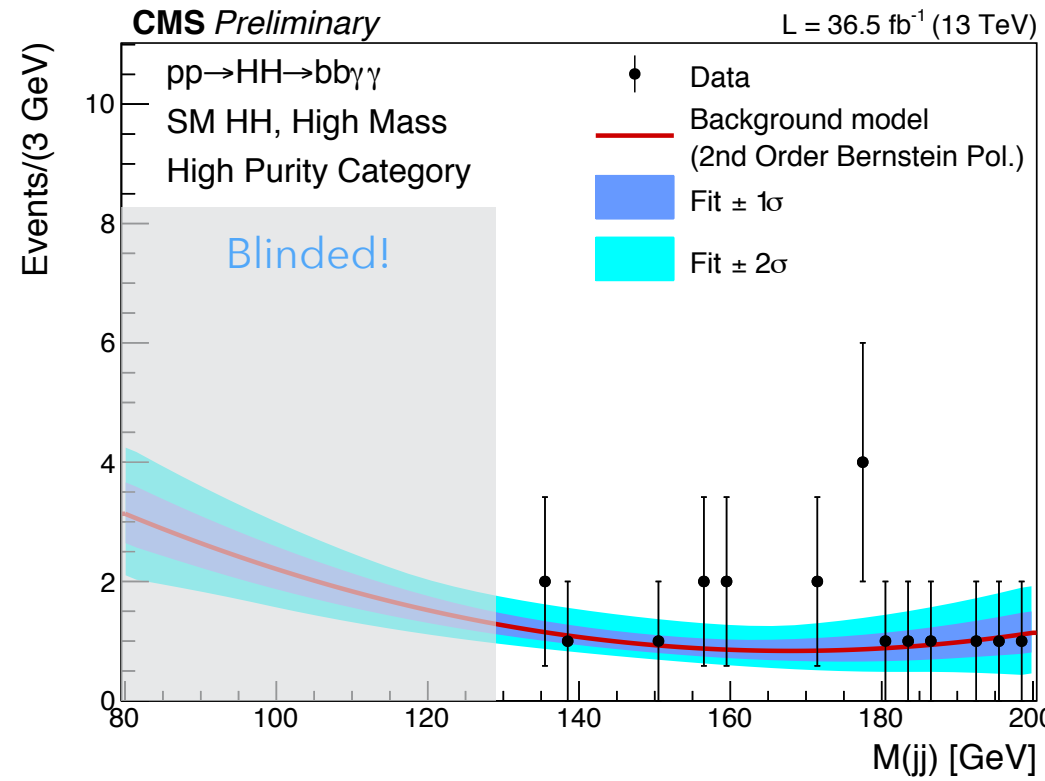
SM HH, High Mass

SM HH, High Mass

Each 1D observable modeled independently with a parametric form

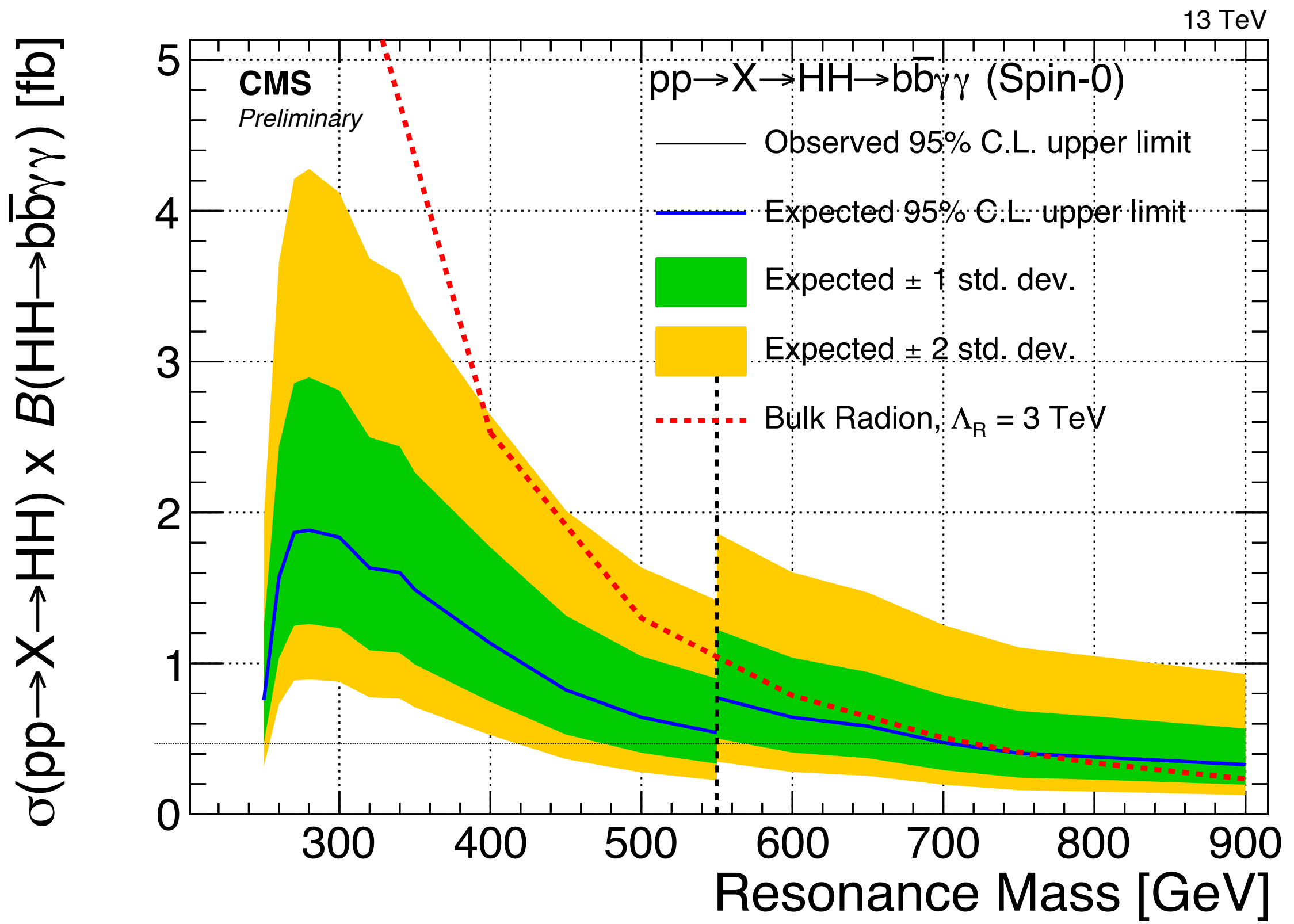
BLINDED BACKGROUND FITS

Smoothly falling $M(\gamma\gamma)$ and $M(jj)$ are modeled parametrically



RESONANT RESULTS

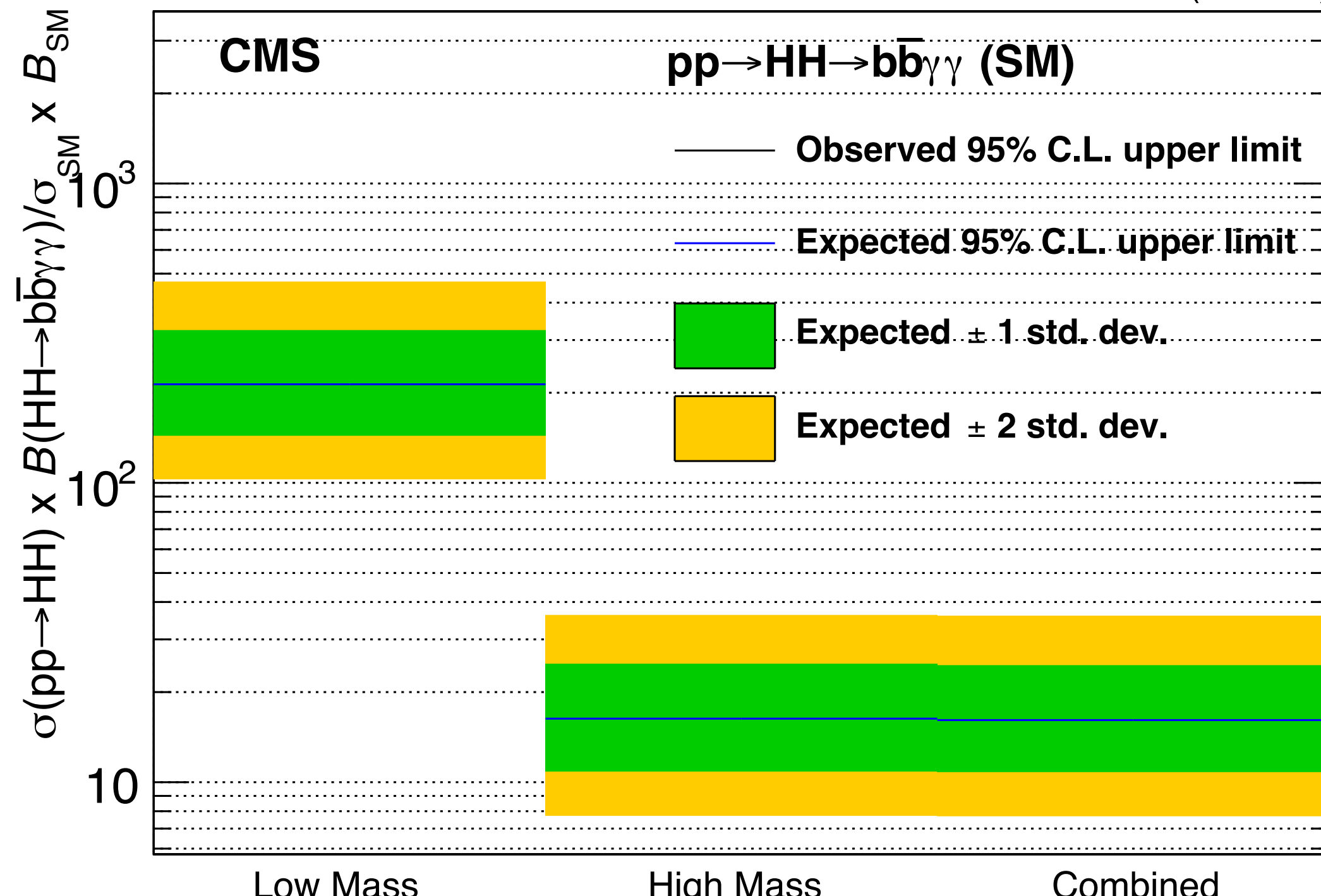
Blinded!



SM NON-RESONANT RESULTS

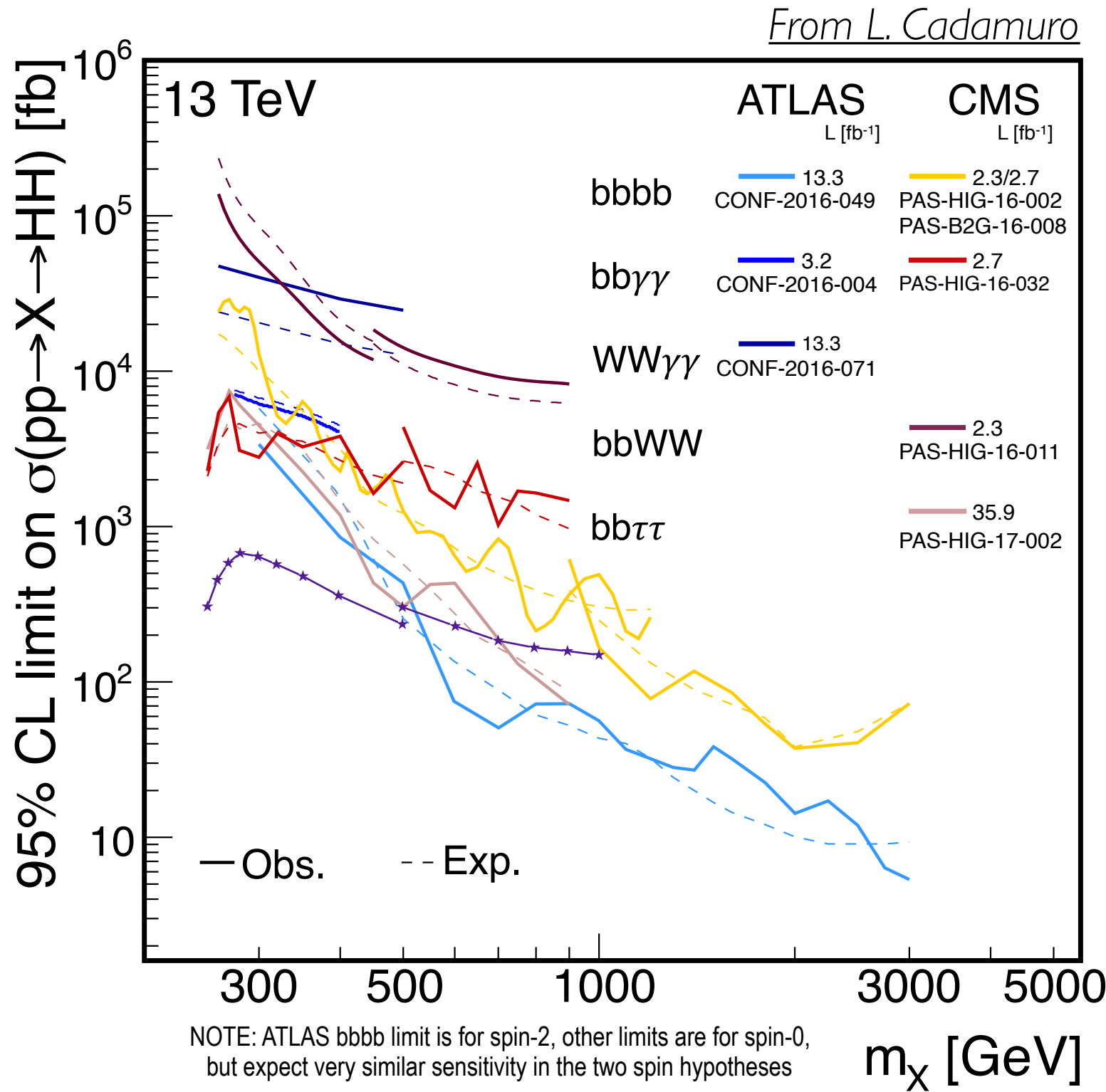
Blinded!

35.87 fb⁻¹ (13 TeV)



Expected combined limit at $\sim 16.7 \times SM$

HH SUMMARY



Chan.	Obs. (exp.) 95% C.L. limit on σ/σ_{SM}		
	ATLAS	CMS	
bbbb	29 (38)	342 (308)	
bbWW	-	410 (227)	
bb $\tau\tau$	-	28 (25)	
bb $\gamma\gamma$	117 (161)	91 (90)	
WW $\gamma\gamma$	747 (386)	-	
	2.3-3.2 fb ⁻¹	13.3 fb ⁻¹	35.9 fb ⁻¹

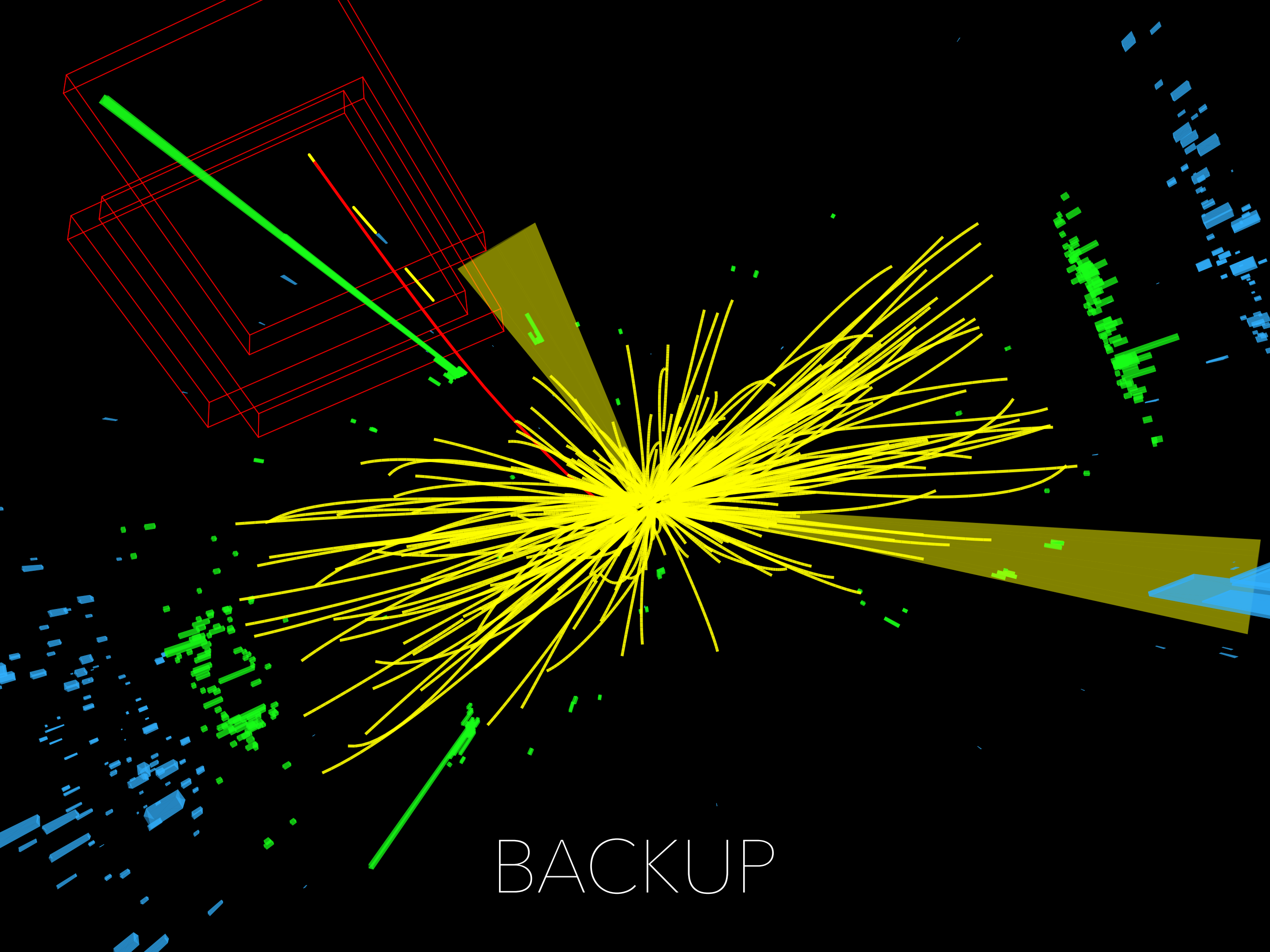
■ : Test of anomalous HH couplings

**New bb $\gamma\gamma$ (35.9 fb⁻¹):
17xSM**

SUMMARY

- | Nature has provided a new tool to look for new physics: The Higgs boson
- | **H → γ's+MET**: good example of using the Higgs as a tool to constrain specific BSM physics phase spaces
 - These type of searches will greatly benefit from the incoming LHC dataset, and will be sensitive to branching ratios well below the experimentally allowed range
- | Understanding the intricacies of the Higgs sector with **HH** production is a flagship analysis:
 - Highly sensitive to a multitude of new physics models
 - Important to understand the physics reach of the HL-LHC
 - **bb̄γγ**: currently the most sensitive channel at CMS (17xSM expected)
- | The performance of the analyses presented is heavily dependent on the good online and offline performance of the **CMS ECAL**, which has been achieved so far during Run 2

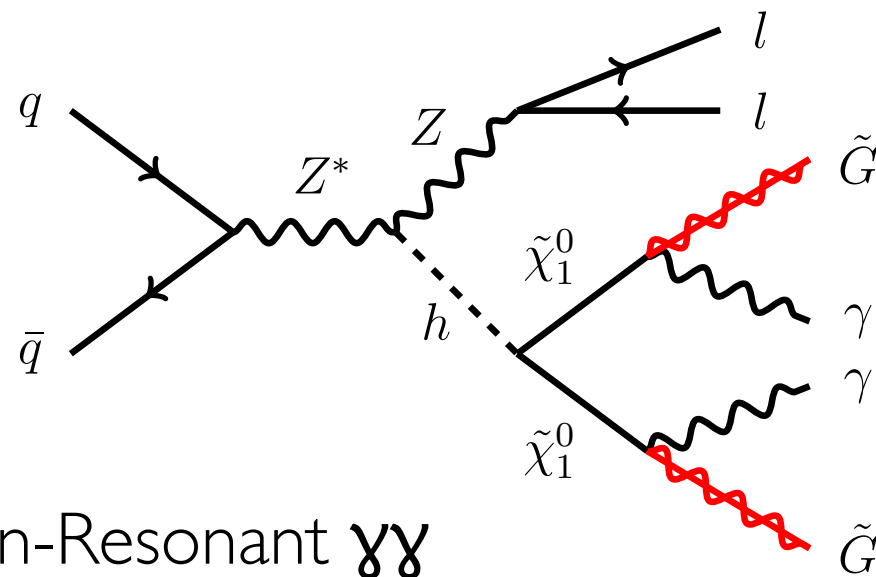
THANKS!



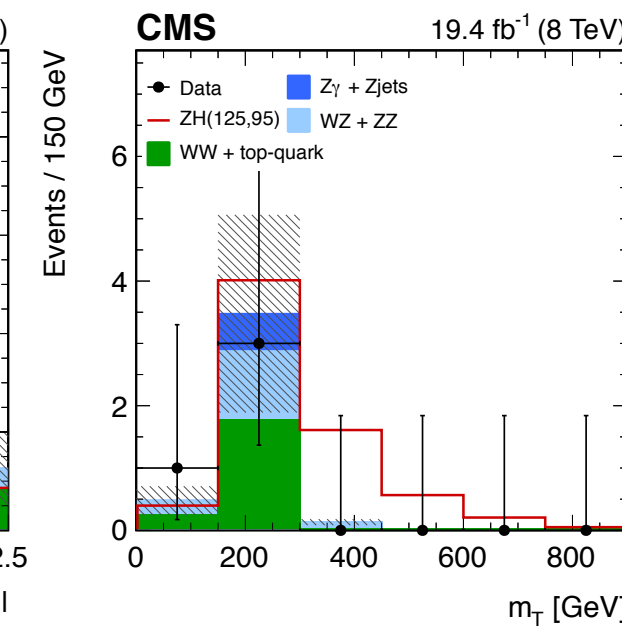
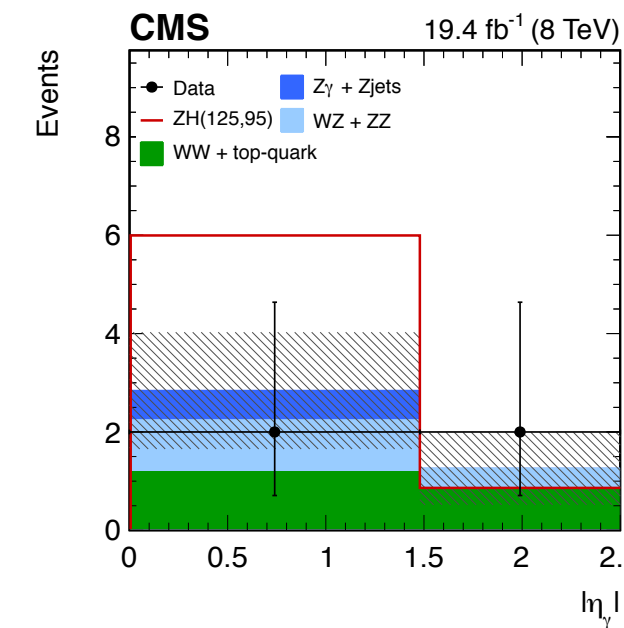
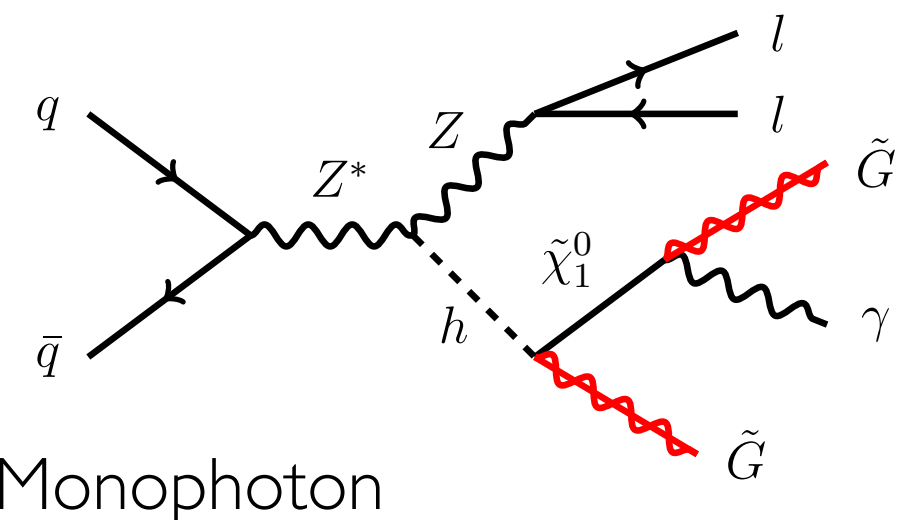
BACKUP

CMS ZH LL+PHOTONS+MET (1)

Phys.Lett. B753 (2016) 363-388



- Searches for $Z(\text{II})H$ production of non-resonant topologies
 - Selection requirements only on one photon
- Straightforward triggering on $Z \rightarrow \text{II}$ (muons and electrons)
 - Lower cross section, but also lower backgrounds



FROM PULSES TO OBJECTS (1)

Energy
reconstruction
for photons
and electrons

$$E_{e,y} = \sum_i [A_i \times S_i(t) \times C_i] \times G(\eta) \times F_{e,y}$$

Pulse Amplitude

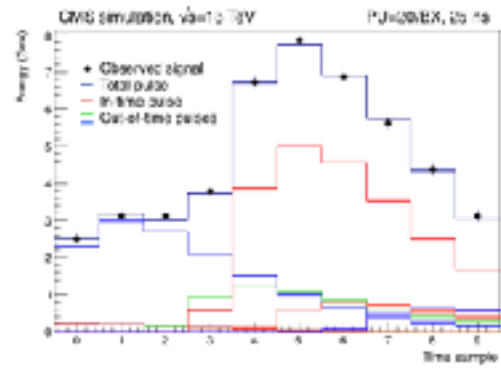
Laser Monitoring

Intercalibration

Global Scale

Cluster
Corrections

Multifit Amplitude Reconstruction

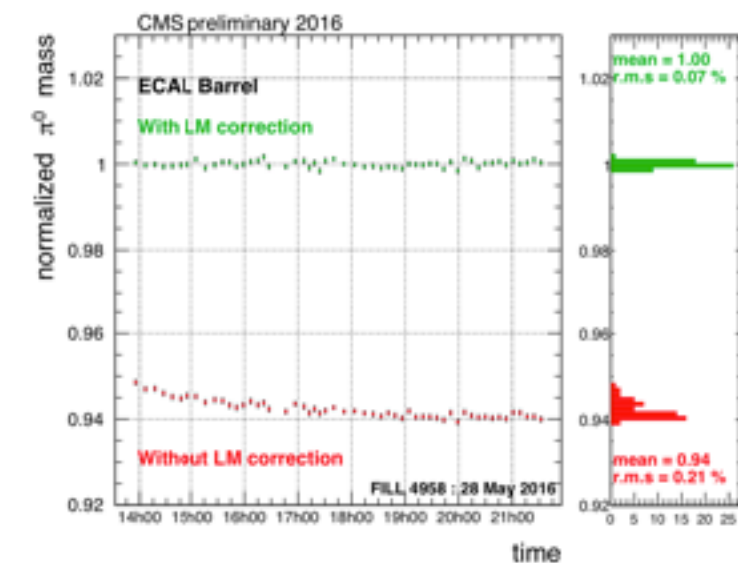
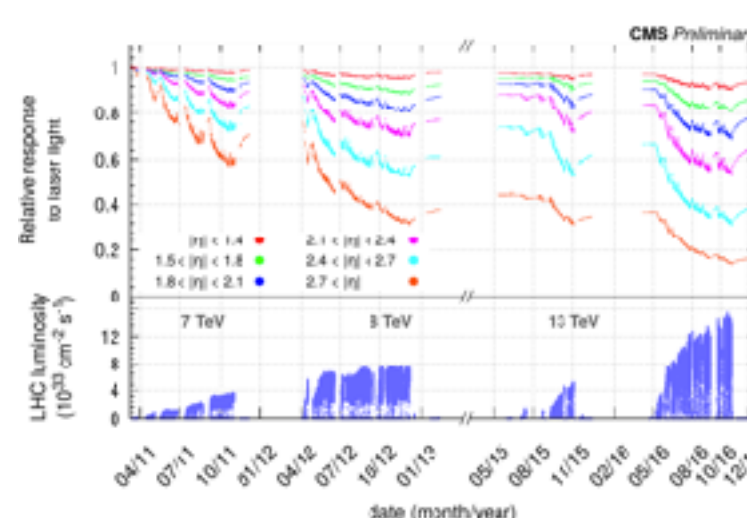


Time samples

Different pulses contributions

$$\chi^2 = \sum_{i=1}^{10} \frac{\left(\sum_{j=1}^M A_j \times p_{ij} - S_i \right)^2}{\sigma_{S_i}^2}$$

Laser Monitoring for Changes in Response



FROM PULSES TO OBJECTS (2)

Energy
reconstruction
for photons
and electrons

$$E_{e,y} = \sum_i [A_i \times S_i(t) \times C_i] \times G(\eta) \times F_{e,y}$$

Pulse Amplitude

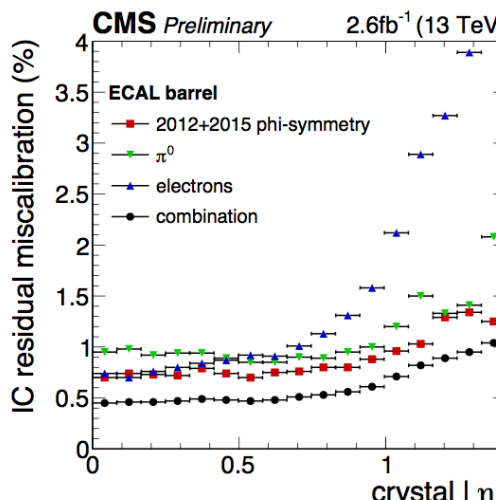
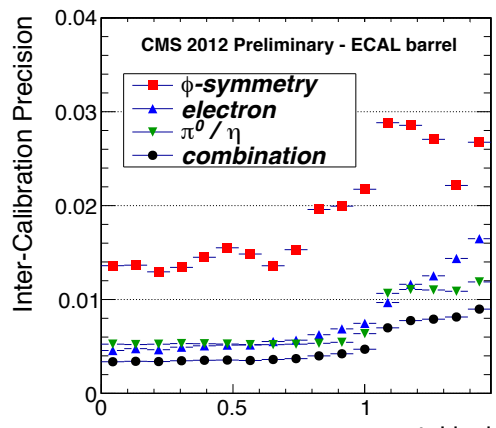
Laser Monitoring

Intercalibration

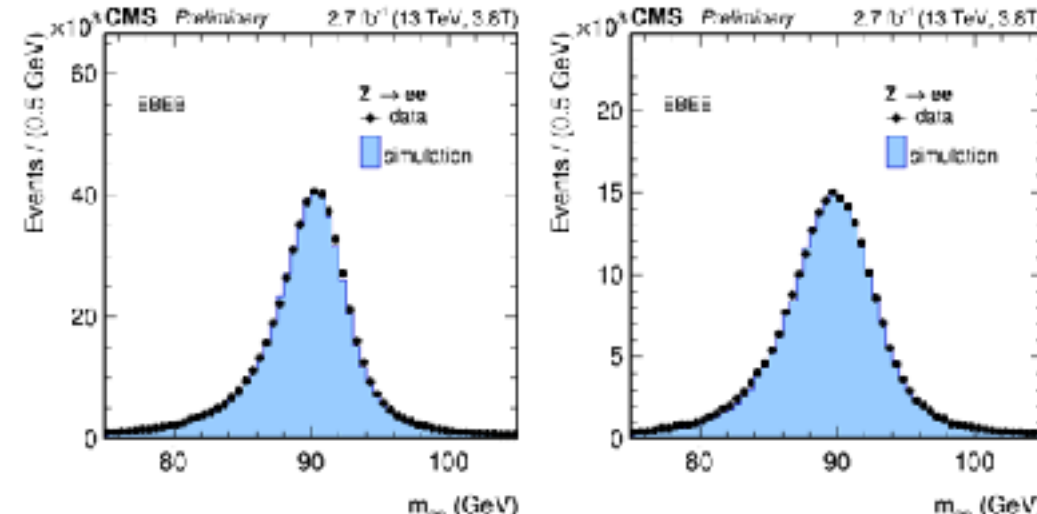
Global Scale

Cluster
Corrections

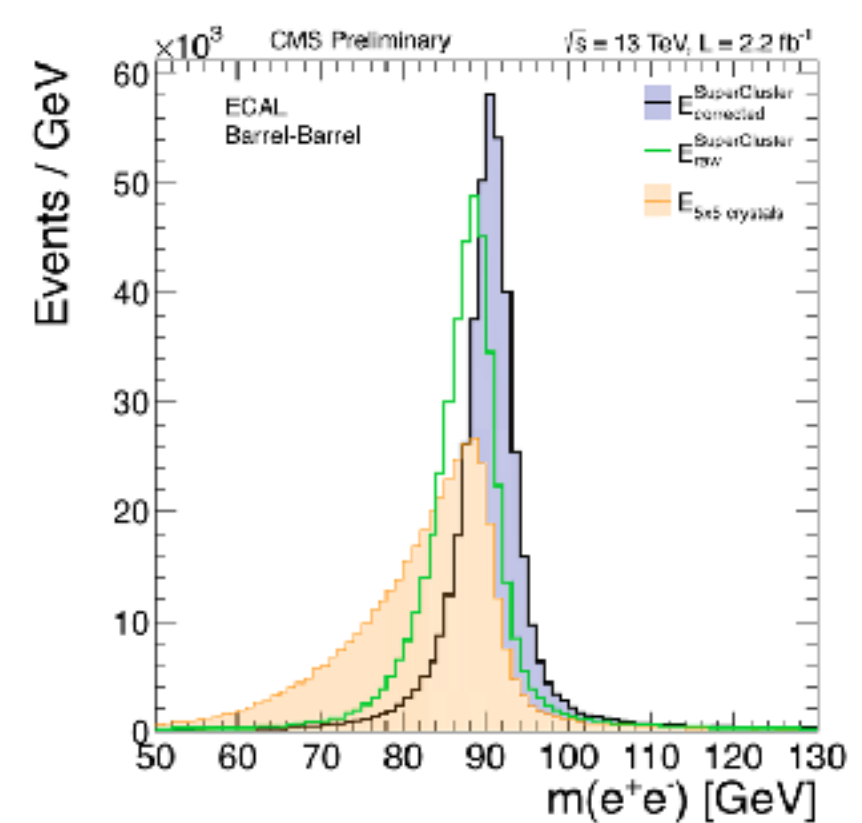
Single-Channel Inter-Calibration



Global Scale Setting with $Z \rightarrow ee$

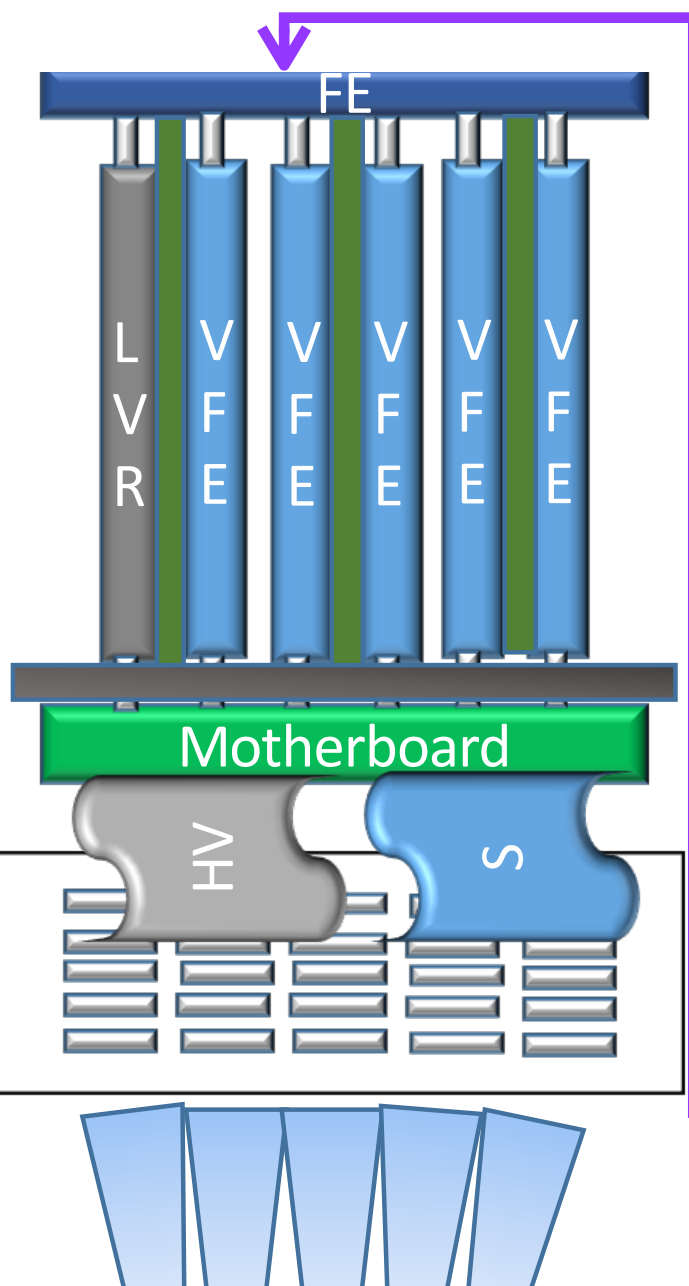


Cluster Corrections (Energy Regression)



THE ECAL PHASE II TRIGGER PRIMITIVES

New very front end (VFE) and front end (FE) electronics



ECAL@LHC: Trigger primitives (TP) calculated on FE based on 5x5 crystal matrix (trigger tower), individual crystal information sent if accepted at L1

ECAL@HL-LHC: Full crystal information sent to off-detector electronics, where trigger primitive is calculated

